DISS. ETH NO. 25418

Requirements for cardioprotective GRK2 inhibition in vitro and in vivo

A thesis submitted to attain the degree of

DOCTOR OF SCIENCES of ETH ZURICH

(Dr. sc. ETH Zurich)

presented by

STEFAN WOLF

Mag. pharm., Karl-Franzens-University Graz

born on 17.07.1987

citizen of Austria

accepted on the recommendation of

Prof. Dr. Ursula Quitterer

Prof. Dr. Jonathan Hall

2018

Table of contents

1. SUMMARY

In the family of G protein-coupled receptor kinases (GRKs), GRK2 and GRK5 are the predominant members expressed in the heart. Both kinases are up-regulated in the failing heart. To date, a major pathophysiological role is established for GRK2 while the impact of GRK5 for heart failure pathogenesis is still under investigation. Although it is widely accepted that GRK2 inhibition is cardioprotective, mechanisms underlying cardioprotection are incompletely understood. Therefore, the major goal of my thesis was the identification of mechanisms required for cardioprotective GRK2-inhibition.

In the first part of my thesis, I compared activities of different GRK2 inhibitors in vitro and in vivo. GRK2 was inhibited by three different approaches: (i) the dual-specific GRK2 and Raf/Erk axis inhibitor RKIP (raf kinase inhibitor protein), (ii) the small molecule paroxetine, which was previously established as a cardioprotective ATP-site GRK2 inhibitor by drug repurposing, and (iii) the dominant-negative GRK2-inhibitory mutant, GRK2-K220R.

In order to compare substrate specificities of the GRK2 inhibitors, RKIP and paroxetine, I established an in vitro kinase assay. The test system used recombinant GRK2 purified from Sf9 (Spodoptera frugiperda) cells, which were infected with a recombinant GRK2-encoding baculovirus. The GRK2 substrates, phosducin and SRSF1 (serine/arginine-rich splicing factor 1), and the GRK2 inhibitor RKIP were purified from E. coli BL21-DE3 bacteria with T7 RNA polymerase-directed expression of recombinant proteins applying the pET expression system. The in vitro phosphorylation assay detected different modes of GRK2 inhibition by RKIP compared to paroxetine. RKIP only inhibited the GRK2-mediated phosphorylation of phosducin with an IC50 value of 950 nM whereas GRK2-mediated SRSF1 phosphorylation was not significantly decreased by RKIP up to 30 microM. In contrast, the ATP-site inhibitor paroxetine inhibited the phosphorylation of phosducin and SRSF1 with comparable IC_{50} values in the micromolar range. These different substrate specificities of the GRK2 inhibitors paroxetine and RKIP could be of major relevance in vivo, because paroxetine showed cardioprotection against myocardial infarction-induced heart failure whereas the in vivo function of RKIP is still under investigation.

For the investigation of the in vivo role of RKIP, I used transgenic mice with myocardium-specific expression of RKIP under control of the alpha-MHC promoter, which were previously generated by our group. RKIP-expressing mice were compared with transgenic mice with myocardium-specific expression of the dominant-negative GRK2-K220R mutant. Our results showed that a moderately increased RKIP level of 2.8-3.2-fold over the non-transgenic control was sufficient to trigger severe signs of heart failure at an age of 8 months in the FVB and B6 background as evidenced by cardiac

dysfunction, cardiac hypertrophy with dilation and cardiac lipid overload. RKIP led to activation of the adipogenic and heart failure-promoting transcription factor Pparg (peroxisome proliferator-activated receptor-gamma) by inhibition of the Raf-Erk axis-mediated serine-273 phosphorylation of Pparg. Whole genome microarray gene expression profiling showed up-regulation of heart failure-related Pparg target genes in RKIP-transgenic hearts with signs of heart failure. In contrast, GRK2 inhibition by transgenic expression of the dominant-negative GRK2-K220R mutant did not activate Pparg. In addition, GRK2-K220R retarded the development of chronic pressure overload-induced cardiac dysfunction imposed by abdominal aortic constriction. From these data it is concluded that an intact Raf-Erk axis is required for cardioprotective GRK2 inhibition.

In the second part of my thesis, I investigated the role of GRK5, which could contribute to effects induced by GRK2 inhibition because GRK5 is reportedly up-regulated by GRK2 inhibition. However, the role of GRK5 is still under investigation. To analyse the in vivo role of GRK5, we generated GRK5-transgenic mice with a 2-fold upregulation of GRK5 in heart tissue, which reproduces the GRK5 up-regulation induced by GRK2 inhibition. The phenotype of 6-month-old Tg-GRK5 mice was determined. GRK5-transgenic mice appeared normal. Tg-GRK5 mice did not show any signs of cardiac hypertrophy, i.e. the heart weight to body weight ratio was not significantly different from non-transgenic controls. Histology analysis of hematoxylin-eosin-stained heart sections further documented that moderate GRK5 overexpression did not cause any cardiac abnormalities. Thus, my data show that moderate GRK5 expression had no adverse cardiac effect. With the newly established GRK5-transgenic model, future studies will have to investigate the role of GRK5 under pathophysiological conditions.

In summary, my thesis with RKIP-transgenic mice found that an intact Raf-ERK axis is required for cardioprotective GRK2 inhibition. In addition, a new transgenic model was established, which allows to study the impact of compensatory GRK5 up-regulation under conditions of GRK2 inhibition.

2. ZUSAMMENFASSUNG

In der Familie von G-gekoppelten Rezeptorkinasen (GRKs) sind GRK2 und GRK5 die vorherrschenden exprimierten Isoformen im Herzen. Im Stadium der Herzinsuffizienz sind beide Isoformen hochreguliert. Während die pathophysiologische Relevanz von GRK2 als erwiesen gilt, ist der Einfluss von GRK5 auf die Pathophysiologie von Herzinsuffizienz noch unklar. Auch wenn die kardioprotektiven Eigenschaften einer GRK2 Hemmung weitestgehend akzeptiert sind, sind jedoch die zugrundliegenden Mechanismen noch nicht vollständig geklärt. Das Ziel dieser Doktorarbeit ist deshalb die Identifizierung von Mechanismen welche für eine kardioprotektive GRK2 Hemmung benötigt werden.

Im ersten Teil meiner Arbeit vergleiche ich verschiedene GRK2 Inhibitoren in vitro und in vivo. Dabei wurde GRK2 auf drei verschiedenen Wegen gehemmt: (i) mit dem dualen Inhibitor RKIP (raf kinase inhibitor protein), der den Raf/Erk Signalweg und GRK2 hemmt, (ii) durch Hemmung der ATP Bindungsstelle mit Paroxetin, das im Zuge von „Drug repurposing“ als kardioprotektive Substanz entdeckt wurde und (iii) die dominant-negative GRK2 hemmende Mutante, GRK2-K220R.

Um die Substratspezifität von GRK2 Inhibitoren, RKIP und Paroxetin zu vergleichen, habe ich ein in vitro Kinase Assay etabliert. Für das Testsystem wurde GRK2 in Sf9 (Spodoptera frugiperda) Zellen exprimiert, welche mit rekombinanten, GRK2 kodierenden, Baculoviren infiziert wurden. Die GRK2 Substrate Phosducin und SRSF1 (serine/arginine-rich splicing factor 1) sowie der GRK2 Inhibitor RKIP wurden in E.coli BL21-DE3 Bakterien unter Kontrolle T7-RNA-Polymerase und unter Verwendung des pET-Expressionssystems exprimiert. Anschließend wurden die rekombinanten Proteine aufgereinigt. Das in vitro Phosphorylierungs-Assay zeigte zwei unterschiedliche Arten der GRK2 Hemmung durch RKIP und Paroxetin. RKIP inhibierte nur die GRK2-vermittelte Phosphorylierung von Phosducin mit einem IC_{50}-Wert von 950 nM, wohingegen die GRK2-vermittelte SRSF1-Phosphorylierung durch RKIP bis zu 30 microM nicht signifikant verringert wurde. Im Gegensatz dazu inhibierte der ATP-Inhibitor Paroxetin die Phosphorylierung von Phosducin und SRSF1 mit vergleichbaren IC_{50}-Werten im mikromolaren Bereich. Diese unterschiedlichen Substratspezifitäten der GRK2-Inhibitoren Paroxetin und RKIP könnten in vivo von großer Relevanz sein. Während Paroxetin bei Herzinfarkt-induzierter Herzinsuffizienz kardioprotektiv wirkt, wird die in vivo Funktion von RKIP noch kontrovers diskutiert.

Um die Rolle von RKIP in vivo zu untersuchen verwendete ich ein transgenes Mausmodell, das RKIP unter Kontrolle des alpha-MHC-Promotors spezifisch im Herzmuskel exprimiert. Dieses Mausmodell wurde zuvor von unserer Gruppe generiert. RKIP-exprimierende Mäuse wurden mit transgenen Mäusen verglichen, die spezifisch im Herzen die dominant-negative GRK2-K220R-Mutante

exprimieren. Unsere Ergebnisse zeigen, dass eine 2,8-3,2 fache Erhöhung des RKIP-Spiegels in 8 Monate alten FVB- und B6-Mäusen schwere Zeichen einer Herzinsuffizienz, im Vergleich zur nicht-transgenen Kontrolle, auslösten. Dies äusserte sich durch kardiale Dysfunktion, Hypertrophie mit Dilatation und Verfettung des Herzgewebes. RKIP führte zur Aktivierung des adipogenen und Herzinsuffizienz-fördernden Transkriptionsfaktors Pparg (peroxisome proliferator-activated receptor-gamma). Dabei hemmt RKIP die Raf/Erk-Achsen-vermittelte Serin-273-Phosphorylierung von Pparg. Eine Gesamtgenom-Microarraygenexpressionsanalyse zeigte in RKIP-transgenen Herzen mit Anzeichen von Herzinsuffizienz eine Hochregulierung von Pparg-Genen. Im Gegensatz dazu wurde Pparg durch die GRK2-Hemmung durch transgene Expression der dominant-negativen GRK2-K220R-Mutante nicht aktiviert. Darüber hinaus verzögerte GRK2-K220R das Auftreten von Herzinsuffizienzanzeichen in einer durch chronische Hypertonie erzeugten kardialen Hypertrophie. Aus diesen Daten kann geschlossen werden, dass eine intakte Raf/Erk-Achse für die kardioprotektive GRK2-Hemmung erforderlich ist.

Im zweiten Teil meiner Dissertation untersuchte ich die Rolle von GRK5, die durch GRK2-Inhibition hochreguliert wird. Damit könnte GRK5 zu Effekten beitragen, welche durch GRK2 Inhibition induziert werden. Die Rolle von GRK5 ist jedoch noch unklar. Um die in vivo Rolle von GRK5 zu analysieren, haben wir GRK5-transgene Mäuse mit einer 2-fachen Hochregulation von GRK5 im Myokard generiert, was der GRK5-Hochregulation unter GRK2-Hemmung entspricht. Anschließend wurde der Phänotyp von 6 Monate alten Tg-GRK5-Mäusen bestimmt. GRK5-transgene Mäuse erschienen normal und zeigten keine Anzeichen von Herzhypertrophie, denn das Verhältnis von Herzgewicht zu Körpergewicht unterschied sich nicht signifikant von nicht-transgenen Kontrollen. Die histologische Analyse von Hämatoxylin-Eosin-gefärbten Herzquerschnitten zeigte ferner, dass eine moderate GRK5-Überexpression keine Herzanomalien verursachte. Somit zeigen meine Daten, dass eine moderate GRK5-Expression keinen nachteiligen Einfluss auf das Herzen hat. Mit dem neu etablierten GRK5-transgenen Modell müssen zukünftige Studien die Rolle von GRK5 unter pathophysiologischen Bedingungen untersuchen.

Zusammenfassend ergab meine Arbeit mit RKIP-transgenen Mäusen, dass eine intakte Raf/ERK-Achse für die kardioprotektive GRK2-Inhibition benötigt wird. Darüber hinaus wurde ein neues transgenes Modell etabliert, das ermöglicht den Einfluss einer kompensatorischen GRK5-Hochregulation unter GRK2-Hemmung zu untersuchen.

3. ABBREVIATIONS

6xHis	hexahistidine-tag
A	adenine
AAC	abdominal aortic constriction
AC	adenylate cyclase
A. dest	distilled water
AGC	family of protein kinase A,G, and C
Akt	protein kinase B
ARRB	β-arrestin
AT1R	angiotensin II type-1 receptor
ATP	adenosine triphosphate
B6	C57BL/6 mouse
β-AR	β-adrenergic receptor
βARKct	amino acids 495-689 of GRK2
BSA	bovine serum albumin
C	cysteine
CD	carboxyl terminal domain
Ca^{2+}	calcium
cAMP	3',5'-cyclic adenosine monophosphate
CaMKII	Ca^{2+}/calmodulin-dependent kinase II
CMV	human cytomegalovirus promoter
CVD	cardiovascular disease
DAG	diacylglycerol
DNA	deoxyribonucleic acid
EDTA	ethylenediaminetetraacetic acid
ELISA	enzyme-linked immunosorbent assay
eNOS	endothelial nitric oxide synthase

ERK1/2	extracellular signal-regulated kinase 1/2
FASN	fatty acid synthase
FVB	friend virus B mice
G	guanine
G protein	guanine nucleotide-binding protein
Gα	α-subunit of the heterotrimeric G protein
Gβ	β-subunit of the heterotrimeric G protein
Gγ	γ-subunit of the heterotrimeric G protein
Gβγ	βγ-complex of the heterotrimeric G protein
GDP	guanosine diphosphate
GIRK	inwardly-rectifying potassium channel
GPCR	G protein-coupled receptor
GRK	G protein coupled receptor kinase
GTP	guanosine triphosphate
HDAC	nuclear class II histone deacetylase
HF	heart failure
IP_3	inositol 1,4,5-triphosphate
IPTG	isopropyl β-D-1-thiogalactopyranoside
IκBα	nuclear factor of kappa light polypeptide gene enhancer in B-cells inhibitor, α
kDa	kilo Dalton
KD	kinase domain
LB	lysogeny broth
MAPK	mitogen-activated protein kinase
MEK	mitogen-activated protein kinase kinase
MHC	myosin heavy chain
min	minute(s)
MOI	multiplicity of infection
MOPS	3-(N-morpholino)propanesulfic acid

ND	amino terminal domain
NES	nuclear export signal
NFκB	nuclear factor 'kappa-light-chain-enhancer' of activated B-cells
Ni-NTA	nickel-nitrilotriacetic acid
NLS	nuclear localization sequence
NO	nitric oxide
OD	optical density
PAGE	polyacrylamide gel electrophoresis
PBS	phosphate buffered saline
PBST	PBS-Tween
PCR	polymerase chain reaction
PDC	phosducin
PEG	polyethylene glycol
PH	pleckstrin homology
PIP_2	phosphatidylinositol 4,5-biphosphate
PKA	cAMP dependent protein kinase
PKC	protein kinase C
PKG	cGMP-dependent protein kinase
PLB	phospholamban
PLCß	ß-isoform of phospholipase C
PMSF	phenylmethylsulfonyl fluoride
PPARG	peroxisome proliferator-activated receptor gamma
PVDF	polyvinylidene difluoride
RGS	regulator of G protein signalling
RH	regulator of G protein signalling homology
RNA	ribonucleic acid
RhoGEF	rho guanine nucleotide exchange factor
RKIP	raf-1 kinase inhibitor protein

RT	room temperature (25 °C)
SDS	sodium dodecyl sulphate
SD	standard deviation
Sf9	spodoptera frugiperda clone 9
SOB	super optimal broth
SOC	super optimal broth with catabolite repression
SRSF1	serine/arginine-rich splicing factor 1
SSRI	selective serotonin reuptake inhibitor
T	thymine
TAE	tris, acetic acid, EDTA
TAG	triactylglycerol
Taq	thermus aquaticus
TBE	tris, boric acid, EDTA
TBS	tris-buffered saline
TBST	TBS-Tween
TE	tris, EDTA
TEMED	tetramethylethylenediamine
Tg	transgenic
Tris	tris(hydroxymethyl) amino methane
Ucp1	uncoupling protein 1
x-gal	5-bromo-4-chloro-3-indolyl-β-D-galactopyranoside

4. INTRODUCTION

4.1. G protein-coupled receptor signalling

4.1.1. Characteristics of G protein-coupled receptors

The family of G protein-coupled receptors (GPCRs) are ubiquitously expressed and regulate almost all known physiological processes, ranging from glucose metabolism to blood pressure regulation to neurotransmission. Dysregulation of GPCR signalling can cause pathophysiological processes and diseases. As a result, GPCRs are drug targets accounting for more than half of all prescriptions worldwide. (*1, 2*)

GPCRs are the largest and most diverse group of membrane receptors in eukaryotes (*3*). Around 350 out of 826 human GPCRs are considered to be potential drug targets. (*4, 5*) They are also known as seven-membrane receptors, because of their characteristic motif of seven membrane-spanning α-helices. Based on their sequence homology they could be classified according to the GRAFS classification system into five families: glutamate, rhodopsin, adhesion, frizzled/taste2, secretin (*4, 6*). Extracellular signals such as light energy, peptides, lipids, sugar and proteins are relayed by GPCRs across lipid bilayers inside the cell. Due to the variety of different ligands GPCRs have a structurally diverse amino terminal, extracellular, domain, while they share the highly conserved characteristic arrangement of seven membrane-spanning domains (*7*). In an agonist-dependent manner these receptors interact with at least three families of intracellular proteins:

- heterotrimeric G proteins
- arrestins
- G protein-coupled receptor kinases (GRKs)

4.1.2. Classical heterotrimeric G protein signalling

The most well-known function of GPCRs is the interaction with the heterotrimeric G proteins and the subsequent activation of intracellular second messengers (*8*). Upon ligand binding a conformational change in the GPCR occurs and the ionic interaction between the third cytoplasmic loop and the sixth transmembrane segment is disrupted, which makes the binding with the heterotrimeric G protein

possible (*9-14*). The heterotrimeric G proteins are composed of Gα-, Gß-, and Gγ-subunits. The activated receptor acts as a guanine nucleotide exchange factor (GEF) and catalyses the exchange of GDP, which is bound to the Gα-subunit, for GTP. Upon nucleotide exchange, Gα-GTP dissociates from the Gßγ dimer and both are free to interact with different downstream effectors. The signal is inactivated through hydrolysis of GTP on the Gα-subunit. Binding of regulator of G protein signalling (RGS) protein to Gα subunit is promoting the GTPase activity (*15*) and thereby allowing the re-association with Gßγ-subunits. Thus, the heterotrimeric G protein is prepared for a new cycle of activation (*16*). (Figure 1)

4.1.2.1. Gα – protein family

The Gα-subunit, the guanine-nucleotide-binding protein, is name giver for the heterotrimeric G protein. In humans, there are 20 different Gα subunits (39 – 52 kDa) encoded by 16 genes (*17*). They are divided into four main classes based on sequence similarity: Gαs (s,olf), Gαi/o (i1, i2, i3, oA, oB, t1, t2, z) Gαq (11,14,15,16,q) and Gα12/13 (12, 13) (*18*). Each class regulates key effectors and the generation of second messengers that in turn trigger signalling cascades (*19*).

Selectivity of GPCR-Gα binding

Although there is a staggering number of 826 GPCRs in humans, they primarily couple to only four major Gα families. As a result, several GPCRs are able to couple to the same Gα subtype. Receptors are also able to bind more than one Gα protein. For example, the β_2 adrenergic receptor (β_2-AR) in smooth muscle cells couples primarily to Gαs, resulting in relaxation, but can also bind $G\alpha_i$ for inhibition of this response (*20*). Although binding selectivity could be regulated by altered cell-type-specific expression levels, many different receptors and Gα proteins are expressed simultaneously. The determinants of selectivity are still unclear. Recently, it was revealed, that on each Gα protein exists a pattern of amino acids (barcode) which are recognized by a distinct region on the receptor. A conserved core in the barcode allows common GPCR-Gα binding, where different receptors recognize distinct positions in the bar code of the same Gα protein, like multiple keys (receptors) can open the same lock (Gα protein) using non-identical cuts (*21*).

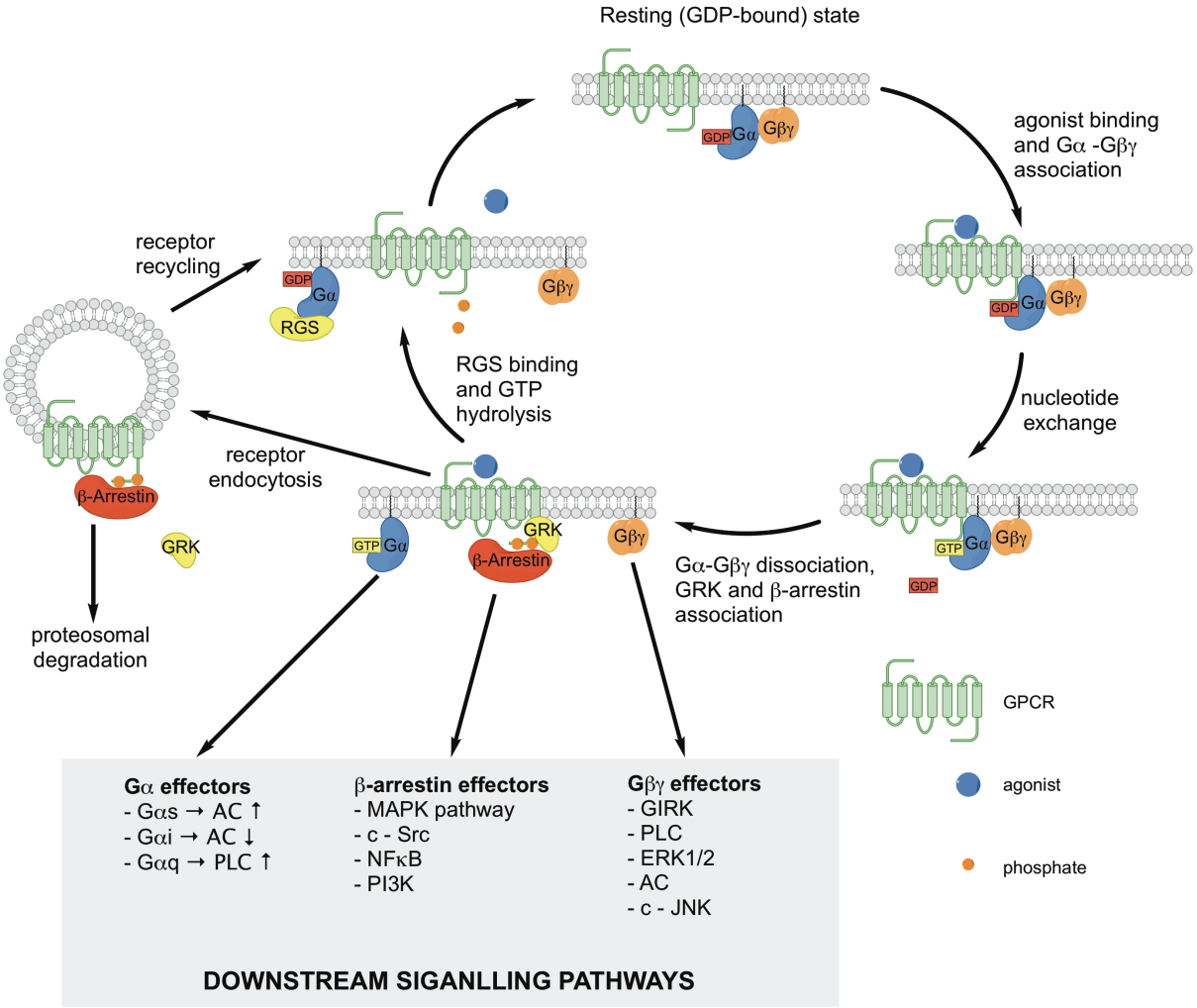

Figure 1: G Protein-coupled receptor activation, reactivation and signalling.

At rest, the heterotrimeric G protein is bound to GDP and not associated with a receptor. After agonist binding, Gαßγ couples to the receptor followed by a GDP-GTP exchange. Gα and Gßγ dissociate from each other and the receptor, leading to downstream signalling. The active GPCR is phosphorylated by GRKs leading to ß-arrestin binding. ß-arrestin-bound receptors are then primed for endocytosis and sorted for proteosomal degradation or recycling. RGS leads to Gα-GTP hydrolysis and Gα returns to Gα-GDP, the initial resting state (adapted from (*22*)).

Effectors of $G\alpha_s$

The $G\alpha_s$ protein binds directly to the adenylate cyclase (AC) and stimulates the conversion of adenosine triphosphate (ATP) to the second messenger 3',5' - cyclic monophosphate (cAMP) (*23*). cAMP activates the serine/threonine kinase cAMP-dependent protein kinase A (PKA), which belongs to the group of AGC kinases. The group of AGC kinases are named after PKA, PKC and PKG and consists of 63 evolutionary related serine/threonine kinases including the GRK family (*24*). PKA phosphorylates a broad array of substrates, which regulate a variety of physiological functions and gene expression (*25, 26*).

Effectors of $G\alpha_{i/o}$

The $G\alpha_{i/o}$ class was named for the ability to inhibit the cAMP production of AC by a direct interaction of these proteins (*27*).

Effectors of $G\alpha_{q/11}$

In 1990, Taylor et al identified and characterized $G\alpha_q$ and $G\alpha_{11}$ as an activator of the ß-isoform of the phospholipase C (PLCß) (*28*). PLCß hydrolyses phosphatidylinositol 4,5-biphosphate (PIP_2) into the second messengers, diacylglycerol (DAG) and inositol 1,4,5-triphosphate (IP_3). Both have far-reaching regulatory and metabolic roles. IP_3 is freely diffusible and leads to an intracellular calcium release. DAG remains membrane bound and activates protein kinase C. (*29*) These events regulate many physiological processes such as contraction (*30, 31*), chemotaxis (*32, 33*), opioid sensitivity (*34-36*), cell proliferation and survival (*37, 38*).

Effectors of $G\alpha_{12/13}$

$G\alpha_{12/13}$ is the most recently discovered class of Gα subunits and was identified based on the nucleotide sequence of $G\alpha_{12}$ and $G\alpha_{13}$ (*39*). $G\alpha_{12/13}$ activates all four members of the RhoGEF family (*40, 41*). RhoGEF activates the small monomeric GTPase RhoA by catalysing the exchange of GDP to GTP of RhoA (*42*).

4.1.2.2. The Gßγ complex

In humans, five different ß- (Gß, 36 kDa) and 12 γ-subunits (Gγ, 7-8 kDa) have been described (*17*). The Gßγ complex is a tightly bound dimer, consisting of one Gß- and one Gγ-subunit. All 5 Gß isoforms have a seven-bladed ß-propeller structure and are composed of seven WD (tryptophan-aspartate) sequence repeats (*43*). The Gßγ dimer is attached to the plasma membrane through isoprenylation at a C-terminal cysteine residue of the Gγ subunit(*44*).

Gß1-4 share a greater than 80% sequence identity and Gß5 is the outliner with just 50% sequence identity. Amongst the Gγ subunits there is a significant lower identity. Most Gß-subunits can interact with most Gγ-subunits, but not all 60 possible dimers occur (*45*). The functional significance of the individual Gßγ combination is not well understood.

Effectors of the Gßγ dimer

In addition to its classical role, where Gßγ-subunits are needed for GPCR-Gα-subunit interaction, Gßγ-subunits mediate signalling on its own. The first effector of Gßγ-subunits discovered was an inwardly-rectifying potassium channel (GIRK) in arterial myocytes (*46*). Upon acetylcholine stimulation, Gßγ-subunits are the main mediators of channel activation through direct binding (*47*).

The process of receptor desensitization is also regulated by Gßγ-subunits via GRK2/3 activation. Gßγ-subunits provide a binding site for the cytosolic GRK2/3 and promotes its membrane recruitment. Subsequent receptor phosphorylation leads to desensitization and downregulation (*48*).

The activity of membrane bound PLCß is increased by direct binding to Gßγ subunits (*49*). Various adenylate cyclase isoforms are activated or inhibited by Gßγ subunits (*50-52*). In addition, Gßγ-subunits regulate neuronal N- and P/Q-type Ca^{2+} channels (*53, 54*).

It is known, that the extracellular signal-regulated kinase 1/2 (ERK1/2) pathway is stimulated by $G\alpha_i$-coupled GPCRs and that this ERK1/2 activation is Gßγ-subunits mediated (*55, 56*). Similar studies showed a Gßγ-dependent activation of the c-Jun N-terminal kinase and p38 pathway (*57, 58*).

4.1.3. Role of arrestins in GPCR signalling and desensitization

The family of arrestins was originally described for their role in desensitization and intracellular trafficking of GPCRs. These 48 kDa proteins are named arrestins because of their ability to “arrest”

(*59*) GPCR signalling after GRK phosphorylation. Arrestins have emerged as key regulators of multiple signalling pathways (*60, 61*).

The arrestin family can be divided into two groups: visual arrestins (arrestin 1 and arrestin 4), which are expressed in the retina, and non-visual arrestins. Non-visual arrestins are also called ß-arrestins, ß-arrestin 1 (=ARRB1 or arrestin 2) and ß-arrestin 2 (= ARRB2 or arrestin 3), which are ubiquitously expressed. They are termed ß-arrestins, because of their functional regulation of the $ß_2$-adrenergic receptor following agonist stimulation (*62, 63*).

Canonical role of ß-arrestins

Cells have a desensitization mechanism to terminate G protein signals. This mechanism includes phosphorylation of the ligand-bound GPCR by GRKs and subsequent recruitment of ß-arrestin to the receptor. ß-arrestin binds to the phosphorylated C-tail and transmembrane core of the GPCR, thus sterically hinders G protein coupling and thereby terminates signalling (*64-66*). The GPCR/arrestin-complex is targeted to clathrin-coated pits (CCP). Arrestin serves as an adapter between the receptor and elements of the endocytotic machinery, such as the main components of clathrin-coated pits: clathrin (*67*) and clathrin adaptor AP2 (*68*). After internalization GPCRs are sorted to degradation (*69*) or recycled back to the plasma membrane (resensitization) (*68, 70*).

Initially it was believed, that arrestin and heterotrimeric G protein binding are mutually exclusive. But some GPCRs are able to sustain G protein-dependent signalling after undergoing arrestin-dependent internalization (*71-75*). Recent data show that some GPCRs can assemble to a “megaplex”, composed of receptor, G protein and arrestin (*76*). In this setting, arrestin binds to the C-tail, but fails to envelop the receptor intracellular domains, which would hinder the G protein to access the receptor. This complex continues to generate G protein-mediated signalling, while undergoing arrestin-dependent redistribution.

4.1.3.1. Effectors of ß-arrestin signalling

Studies over the past 20 years have shown that the function of ß-arrestins go well beyond this canonical role and mediate signalling on its own (*77*). The first signalling pathway to be discovered was the ß-arrestin mediated activation of c-Src downstream of the $ß_2$AR (*78*). ß-arrestin 1 functions as an adaptor protein recruiting c-Src to the activated GPCR. This effect leads to activation of downstream ERK1 and 2. One of the best understood arrestin functions is scaffolding of the mitogen-activated protein kinases (MAPK) complex of the ERK cascade (*79, 80*), p38 (*81*), and Jnk2 and 3

(*82*). In addition, ß-arrestin 1 and 2 both bind to the NFκB inhibitor, IκBα and decrease basal NFκB signalling (*83*).

4.1.3.2. ß-arrestin-biased signalling

Most GPCR-targeting drugs are thought as a balanced agonist, which regulates both downstream signalling pathways in a similar way to that of the endogenous reference agonist. These agonists display equivalent potencies for two different pathways such as G protein and ß-arrestin. Antagonist are thought to inhibit all second messengers activated by these agonists (*84*). However, over the last two decades, several "biased" or "functionally selective" ligands have been discovered, which activate ß-arrestins while inhibiting G proteins or vice versa. A ligand induces and stabilizes a unique receptor conformation, which favours one pathway. Also, conformational changes in ß-arrestin occur after receptor-ß-arrestin interaction and persist longer than the direct receptor binding (*85*). The conformational signature of arrestin correlates with the predicted signal and trafficking functions (*86*). One example for a biased ligand is the ß-blocker carvedilol, which inhibits G protein-dependent signalling, while stimulating ß-arrestin mediated signalling (*87*).

Post-translational modifications such as phosphorylation of GPCRs, which modify the conformational architecture of the receptor, can bias signalling (*88*). Different members of the GRK family have distinct phosphorylation patterns or receptor barcodes, which lead to receptor conformations that differentially couple to signal transducers (*89*).

4.2. GRK signalling

G protein-coupled receptor kinases (GRKs) belong to the family of AGC serine/threonine kinases (*90*) and are well known for terminating GPCR signalling. The seven members of the GRK family can be divided into 3 subfamilies based on sequence similarities: visual or rhodopsin-kinases subfamily (consisting of GRK1 and GRK7), ß-AR kinase subfamily (consisting of GRK2 and GRK3) and the GRK4 subfamily (consisting of GRK4, GRK5 and GRK6) (*91*). While GRK2 (*90, 92*), GRK3 (*93*), GRK5 (*94*) and GRK6 (*95, 96*) are ubiquitously expressed (*97*), GRK1 and GRK7 expression is restricted to the retina. GRK1 and GRK7 are particularly in cones expressed, where they primarily target rhodopsin (*98, 99*) and GRK4 is highly expressed in testes (*100*).

4.2.1. Structural organization of GRKs

The members of the GRK family (62 kDa – 80 kDa) are multi-domain proteins, which share structural and functional hallmarks. All GRKs have an amino-terminal domain (N-terminal domain or ND), which is unique to the GRK family and the first 20-25 amino acids are essential for GPCR binding (*101*). It is followed by a regulator of G protein signalling (RGS) homology domain (RH), which is interrupted by a serine/threonine protein kinase domain (KD) (*102*). The KD contains the enzymatically active site and is tailed by an AGC kinase consensus sequence. This 500-520 amino acid assembly is shared by all GRKs and AGC kinases. The carboxyl-terminal domain (C-terminal domain or CD) is the most diverse region and contains the structural elements responsible for cellular localization and membrane association (*103, 104*).

4.2.1.1. Unique features of the visual GRK subfamily

The visual GRK subfamily requires prenylation on the C-terminal domain for membrane association. GRK1 has a characteristic CAAX-motif for farnesylation (*105*), whereas GRK7 is geranylgeranylated (*99*).

4.2.1.2. Unique features of the β-adrenergic receptor kinase subfamily

GRK2/3 are cytosolic proteins and the C-terminus contains a pleckstrin homology (PH) domains, that interacts with Gßγ subunits and the phospholipid PIP2 (*48, 106, 107*). Recently, a second Gßγ-binding site has been described in the N-terminal domain of GRK2 (*108*). These specific interactions help to target GRK2 to the membrane.

4.2.1.3. Unique features of the GRK4 subfamily

Members of GRK4/5/6 subfamily use a different mechanism for membrane targeting. The C-terminal domain includes an amphipathic helix with a patch of hydrophobic amino acids surrounded by basic residues (*109, 110*). The N-terminal domain contains patches of basic residues, which bind to PIP2 and thereby catalytic activity is increased (*111, 112*). GRK4 and GRK6 carry in addition C-terminal palmitoylation sites for enhanced lipid binding (*100, 113*). All members of the GRK4 subfamily contain a nuclear localization sequence (NLS) (*110, 114, 115*) and a nuclear export signal (NES) (*115*).

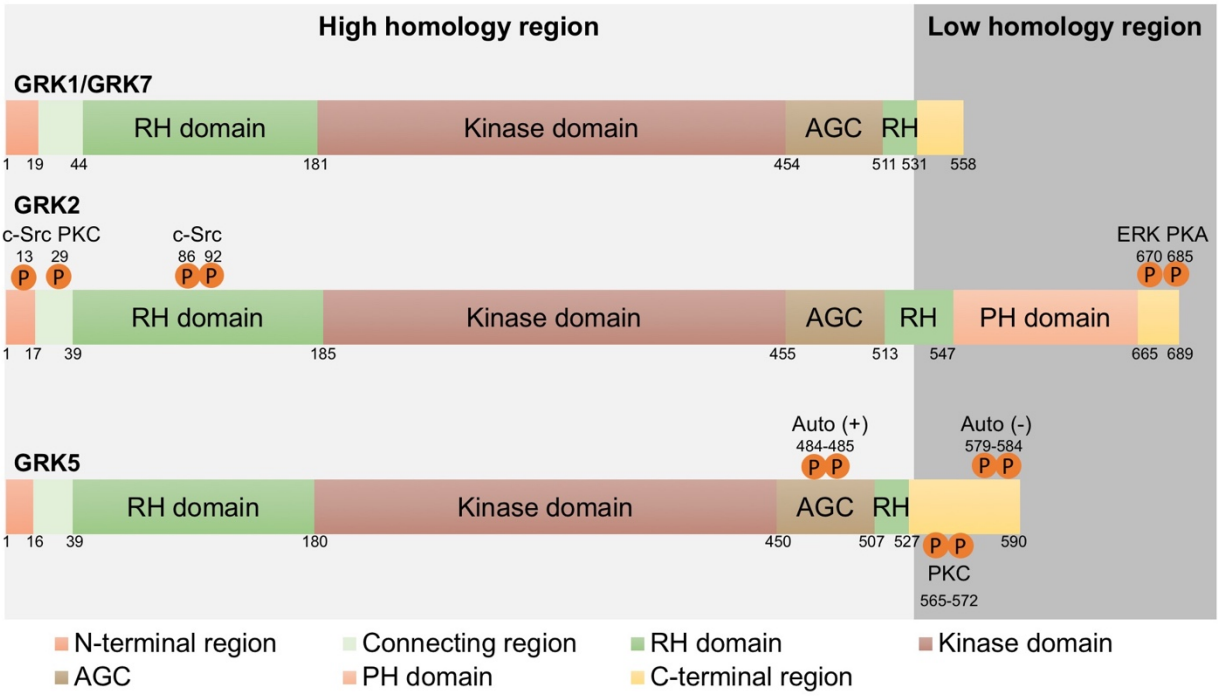

Figure 2: Major domains and homology of GRK subfamily.

Numbers below the structures indicate amino acid residues in human GRKs (adapted from (*116*)).

4.2.2. Molecular functions of GRKs

The ability to phosphorylate active GPCRs was the first GRK function to be discovered, but over the last years various non-receptor substrates were documented. In addition, GRKs are able to regulate signalling via direct binding to other proteins, independent of their enzymatic activity.

4.2.2.1. Receptor substrates

GRKs specifically recognize and phosphorylate serine/threonine residues on the third intracellular loop and the cytosolic tail of the agonist-activated GPCRs. Phosphorylation facilitates high affinity binding of arrestin, which sterically blocks further signalling by GPCRs to heterotrimeric G proteins (*117*) and serves to desensitize receptors (*118*). A unique feature of GRKs is the ability to phosphorylate only agonist-activated GPCRs. Other second messenger-dependent kinases such as PKA and PKC do not differentiate between inactive and active receptors and promote heterologous

desensitization (*119, 120*). In contrast to PKA and PKC, GRKs do not have a consensus phosphorylation site. GRK2/3 phosphorylates different serines/threonines than GRK4/5/6, as shown for some GPCRs like the β_2-AR (*89*) or the neurotensin receptor (*121*). These distinct phosphorylation patterns establish a "receptor barcode" that imparts distinct conformations to the recruited β-arrestin. β_2-AR phosphorylation by GRK2 is important for desensitization of the receptor's cAMP signalling. However, just phosphorylation by GRK6 activates the β-arrestin-mediated ERK1/2 signalling (*89*). A similar effect has been shown for other GPCRs such as the angiotensin II type-1 receptor (AT1R): receptor endocytosis is primarily mediated by GRK2/3, whereas GRK5/6 promote ERK activation (*122*).

4.2.2.2. Non-receptor substrates

GRKs participate not only in desensitisation, but also phosphorylate a growing number of non-receptor substrates. The list of non-GPCR substrates includes single transmembrane domain receptor kinases, toll-like receptors, death receptors, transcription factors, cytoskeletal proteins and adapter proteins. These interactions extend the repertoire of pathways whose signalling is controlled by GRKs (*123*).

In 1998, tubulin was the first non-GPCR target to be discovered (*118, 124, 125*). GRK2 and GRK5 phosphorylates tubulin with a preference for β-tubulin (*118*). GRK2 is able to phosphorylate two other membrane-cytoskeleton linkers of the ezrin/radixin/moesin family: ezrin (*126*) and radixin (*127*). Phosphorylation of tubulin or ezrin could facilitate clathrin–mediated endocytosis and cytoskeletal rearrangements (*104*). In addition, GRK5 phosphorylates moesin on threonine 66 and thereby promotes tumor growth, invasion and metastasis (*128*). Synucleins are another class of GRK substrates. GRK2 phosphorylates α- and β-synuclein very efficiently, whereas GRK5 prefers α-synuclein (*129*). Phosducin is a soluble phosphoprotein predominantly expressed in the retina, that complexes with Gβγ and inhibits competitively all Gβγ-mediated effects of GRK2 (*130*). But phosducin is also a GRK2 substrate and its phosphorylation reduces Gβγ binding ability (*131*). Moreover, GRK5 is able to phosphorylate β-arrestin 1 on serine 412. Phosphorylated β-arrestin 1 in turn prevents activation of Src by serotonin 5-HT4 receptors (*132*).

GRKs are able to regulate nuclear proteins and multiple transcription factors. GRK5, which has a nuclear localization sequence (*114*), phosphorylates nuclear class II histone deacetylases (HDACs) (*133*). GRK2, which lacks a nuclear localization sequence and is excluded from the nucleus, is implicated in the phosphorylation of transcription factors in the cytoplasm, whereupon they

translocate to the nucleus (*134*). GRK2/5 mediate TNFα (tumor necrosis factor α) induced NFκB (nuclear factor κB)-signalling in macrophages by phosphorylation of IκBα (inhibitory κB) (*135*).

Non-GPCR membrane receptors, such as platelet-derived growth factor receptor-β (PDGFRβ), can be phosphorylated and desensitized by GRK2 (*136*) and GRK5 (*137*).

4.2.2.3. Non-enzymatic functions of GRKs

GRKs regulate several signalling proteins via direct interaction, independently from their kinase activity. All GRKs contain a RH-domain in their N-terminal domain, but only the RH-domains of GRK2 and GRK3 have been shown to bind $G\alpha_q$ and inhibit subsequently $G\alpha_q$-mediated PLCβ activation (*138, 139*). Even within the $G\alpha_q$-subfamily the GRK2 RH-domain $G\alpha_q$ interaction is fairly selective: it binds $G\alpha_q$, $G\alpha_{11}$ and $G\alpha_{14}$, but not $G\alpha_{16}$ (*138, 140*). Mutagenesis studies identified eight residues in the RH domain of GRK2 essential for $G\alpha_q$ binding, six of which are present in GRK3, but not in other GRKs (*139*).

Originally, binding of GRK2/3 C-terminal PH domain to Gβγ was believed to just recruit GRK2/3 to the membrane (*106, 141*). Recently, a different function of Gβγ binding has been discovered: GRK2 is involved in the fast desensitization of GIRK channels, which are activated by Gβγ. Upon GPCR activation GRK2 translocates to the membrane and quenches the channel activity by titrating Gβγ away from the channel (*142*).

GRK-interacting proteins (GITs) were the first proteins discovered that bind to GRKs and serve as effectors, without being phosphorylated (*143*). GITs are multidomain scaffolding proteins that interact with various partners, including ADP ribosylation factors, small GTPases and many kinases (*144*). GRK2 directly binds to clathrin via its C-terminal domain *(145).*

4.2.3. Regulation of GRKs

Regulation of GRK2

GRKs are regulated by phosphorylation and protein-protein interactions. Gβγ stimulates GRK2/3 activity 10-12 fold (*146, 147*), due to enhanced recruitment of the kinase to an activated GPCR (*48, 147, 148*). In addition, Gβγ-binding changes the conformation of the kinase domain allosterically

(*149*). Also, anionic phospholipids such as phosphoinositides enhance GRK2/3 activity (*107, 148, 150, 151*). Furthermore, GRK2 is controlled by various phosphorylation sites within the N- and C-terminal domains (Figure 2). cSrc-mediated phosphorylation of GRK2 enhances kinase activity and increases $G\alpha_q$ binding (*152, 153*). PKA phosphorylation of GRK2 at serine 685 increases kinase activity via $G\beta\gamma$ association (*154*), whereas MAPK-mediated phosphorylation at serine 670 reduces $G\beta\gamma$-binding and thereby inhibits GRK2 activity (*155*). PKC-mediated phosphorylation of the carboxyl terminal domain of GRK2 increased the catalytical activity towards receptors (*156*). In addition, PKC phosphorylates GRK2 on Serine 29, which relieves calmodulin-induced inhibition of GRK2 (*157*).

Regulation of GRK5

In contrast to GRK2/3, GRK5 is activated by phospholipids such as PIP_2 (*111*). Upon activation of $G\alpha_q$-coupled receptors GRK5 can translocate to the nucleus. This nuclear accumulation is dependent on CaM binding to a specific site on the N-terminal domain (*158*). GRK5 is also regulated through various phosphorylation sites on its C-terminal region (*159*). GRK5 activity is inhibited by PKC phosphorylation (*160*) and CaM binding, which promotes GRK5 autophosphorylation (*161*). Both, the autophosphorylated residues as well as residues phosphorylated by PKC are located within the same 28-amino acid region (residues 563-590). This region appears to function as an autoinhibitory domain (*159*). In contrast to these findings, rapid phospholipid-stimulated autophosphorylation at serine 484 and threonine 485 enhances GPCR phosphorylation (*162*).

4.2.4. Physiological and pathophysiological functions of GRKs

Multiple GRK subtypes are expressed virtually in every cell with their extensive and complex signal regulation. Insufficient or extensive GRK activity is associated with a variety of human disorders.

4.2.4.1. Function of GRKs in the cardiovascular system

GPCRs are essential regulators in cardiovascular physiology. β-ARs, which control cardiac contractility (*163*) and the AT1 receptor are prominent GPCRs in cardiac growth (*164*). There is enormous potential for therapies targeting these GPCRs in cardiac diseases, either directly via interaction with the GPCR (e.g. β-AR-blocker) or via their signalling proteins, such as β-arrestins or

GRKs. β-ARs are activated by circulating catecholamines. Any kind of injury or stress on the heart is followed by a release of high levels of these hormones, which can induce persistent activation of β-ARs. Continuous β-AR hyperstimulation results in profound desensitization initiated by GRK-phosphorylation. The resulting loss of responsiveness to catecholamines contributes to heart failure (HF) development (*165*). More than 25 years ago, it was discovered that this desensitization is accompanied by GRK2 upregulation (3-4 fold) (*166, 167*). GRK2 overexpression in the heart results in decreased isoproterenol-stimulated contractility and reduced cAMP production (*168*), impaired cardiac function (*169*), and increased apoptosis (*170*). Similar to GRK2, GRK5 is also upregulated in patients with various cardiovascular diseases (*171-173*) and GRK5 overexpression shows marked receptor desensitization, including β_1-AR (*174*).

4.2.4.2. GRK2 and heart failure

As described above, β-AR dysregulation is a hallmark of the failing heart molecular signature. Under healthy conditions, β_1-AR and β_2-AR are the predominant subtypes in the human heart, which are expressed in an approximate 77:23 ratio (*175*). Heart failure is associated with loss of β-AR density which is selective for the β_1-AR (*165, 176*). This down-regulation of β_1-AR subpopulation, with little or no change in β_2 receptors, shifts the ratio towards 50:50 (*176*). In 1993 it was found that GRK2 is involved in β-AR dysregulation (*166*). Several mouse models as well as human studies proofed the upregulation of GRK2 in heart failure (*22*). In addition, GRK2 activity and expression is increased in the adrenal medulla during HF (*177*). As a result, adrenal α_2-AR dysfunction is observed in the adrenal gland, which causes the loss of sympathoinhibitory function of these receptors, and catecholamine secretion is elevated (*177-181*).

In addition to membrane bound localization, GRK2 was detected in mitochondria, where phosphorylation of non-GPCR targets alters mitochondrial biogenesis and cell survival (*182, 183*). In a GRK2-overexpressing mouse model of ischemia/reperfusion, infarction size and apoptosis post-injury is increased, due to reduced induction of the pro survival Akt pathway und NO generation (*170*). Induced by oxidative stress, mitochondrial localisation of GRK2 is dependent on phosphorylation of serine 670 by ERK, resulting in enhanced binding to heat shock protein 90, which chaperons GRK2 to mitochondria (*184, 185*). Mitochondrial-targeted GRK2 is essential for prodeath signalling, while GRK2 inhibition by βARKct leads to cardioprotection (*184*).

Due to the strong correlation between cardiac GRK2 expression and HF, GRK2 inhibition seems to be a promising target. Several studies of GRK2-inhibtion mouse models show a beneficial effect in heart failure. While global homozyqous knock out (KO) GRK2 is lethal (*186*), heterozygous KO GRK2 (GRK2 (+/-) are viable and have 50% less GRK2 expressed. These mice present enhanced cardiac function (*187*). Furthermore, cardioprotective GRK2 inhibition targets dysfunctional cardiac substrate use in late-stage heart failure (*188*).

Taken together, evidence strongly supports that GRK2 inhibitors represent a potential new and powerful drug class that may yield new therapies for cardiovascular disorders.

4.2.4.3. GRK2 and hypertension

β-ARs, which are regulated by GRK2, regulate inotropy and chronotopy in the heart and mediate vasodilatation, which influences systemic vascular resistance. In humans, increased GRK2 levels are correlated with increased blood pressure and inversely correlated with β-adrenergic-mediated adenylyl cyclase activity (*189*). In addition to the impaired β-adrenergic function due to GRK activation in humans, also increased GRK2 levels could be detected in lymphocytes (*190*). In a transgenic mouse model with vascular smooth muscle targeted GRK2 overexpression (2-fold) mean arterial blood pressure was increased by about 20% compared to the control (*191*).

The mechanism how GRK2 regulates blood pressure is not fully understood. Lowering GRK2 levels in endothelia cells increases Akt mediated endothelial nitric oxides synthase (eNOS) activity, which leads to enhanced NO production and vasodilatation (*192*).

4.2.4.4. GRK5 and heart failure

In addition to GRK2, GRK5 is the second predominant GRK isoform in the heart (*172*). Studies in humans suggest that GRK5 may be involved in the development of heart failure and cardiac hypertrophy. In the failing heart, GRK5 levels are increased by 68% in the left ventricle (*172*). Like GRK2, GRK5 is responsible for the termination of GPCR signalling. In a cardiac selective GRK5-expressing mouse model cardiac responsiveness to isoproterenol is diminished, demonstrating that, like GRK2, this kinase can act as a β-AR kinase (*174*) and compromises cardiac functions (*193*). GRK2 and GRK5 overexpressing mice have been shown to regulate GPCRs in different ways: adenosine receptors are targeted by GRK5 but not by GRK2, while angiotensin II receptors are

targeted by GRK2 but not by GRK5 (*174*). Transgenic GRK5 mice showed an exaggerated hypertrophic response and loss of cardiac function following pressure overload via transaortic constriction. The exaggerated hypertrophy was attributed to GRK5 accumulation in the nucleus and non-canonical functions (*133*). In the nucleus GRK5 is able to act as a class II histone deactylase (HDAC) kinase. Phosphorylated HDAC5 is exported from the nucleus and MEF2 is de-repressed. MEF2, free of HDAC repression, induces transcription of hypertrophic genes (*133*). Mice with deletion of GRK5 (*194*) and mice which overexpressed a nuclear deficient mutant of GRK5 (*133*) exhibit protection from the pathology of cardiac hypertrophy and HF following transaortic constriction surgery.

Furthermore, calmodulin binds to GRK5 with an affinity 40-times higher than to GRK2 (*161*). Calmodulin inhibits GRK5-mediated phosphorylation of GPCRs, but not the phosphorylation of cytosolic substrates such as casein (*195*). Recent findings discovered that upon activation of selective $G\alpha_q$ coupled receptors, calmodulin binds to GRK5 and leads to translocation in the nucleus (*158*). Stimulation of the angiotensin II and α_1-adrenergic receptors, which both are not desensitized by GRK5, lead to nuclear accumulation of GRK5. Stimulation of the endothelin receptor, which is also a $G\alpha_q$ coupled receptor, but desensitized by GRK5 does not cause nuclear GRK5 localisation (*158*). In addition, GRK5 acts in the nucleus in a kinase-independent manner. GRK5 has got the ability to bind DNA directly and thereby enhance the activity of the hypertrophic transcription factor NFAT. Deletion of NFAT protects GRK5-transgenic mice from the pathology of pressure overload induced HF (*196*). Beyond the transcriptional regulation of GRK5, it is also involved in the regulation of NFκB signalling. Conflicting reports suggest both GRK5-mediated activation and inhibition of NFκB. The overall impact of GRK5 on the NFκB signalling may depend on stimulus and cell type: in neonatal rat ventricular cardiomyocytes NFκB is activated through upregulation of the p50 and p65 subunits, while in bovine aortic endothelial cells NFκB signalling is inhibited (*197-200*).

In contrast to the data of these different rodent studies, a study in humans paints a different picture of the GRK5 role in the heart. In the coding region of the GRK5 gene is a polymorphism, primarily found in African American population with a prevalence of 40%, which leads to a substitution of glutamine (GRK5-Q41) for leucine (GRK5-L41) at position 41 (*201*). GRK5-L41 shows more enzymatic activity compared to GRK5-Q41, resulting in enhanced β-AR desensitization after isoproterenol stimulation. In this study, patients showed lower mortality from heart failure and prolonged survival. This beneficial effect, due to diminished β-AR signalling, can be interpreted as an effect mimicking β-receptor blockade (*202*). Moreover, GRK5-Q41 and GRK5-L41 show comparable nuclear accumulation and ability to stimulate HDAC5 nuclear export (*201*). In addition, in a prospective cohort

of 2673 acute coronary syndrome patients, GRK5-L41 patients in African-Americans showed an improved outcome (*203*).

An explanation for these controversial results could be, that the rodent experiments were performed under conditions of massive GRK5 overexpression (30-fold). However, also in humans the L41Q polymorphism is associated with left ventricular apical ballooning syndrome (*204*).

4.2.4.5. GRK5 and hypertension

In an animal model of angiotensin II- and norepinephrine-induced hypertension, GRK5 protein level was increased subsequent to hemodynamic stress and hypertension (*205*). Transgenic mice with vascular smooth muscle targeted GRK5 expression develop high blood pressure in a sex-specific way. Male mice had a higher blood pressure elevation than female mice. In contrast to GRK2, where blood pressure is not regulated by a decrease in β-adrenergic receptor dilatation, GRK5 induces hypertension mediated by $G\alpha_i$-signalling. $G\alpha_i$ inhibition by pertussis toxin led to restored blood pressure (*206*).

4.2.4.6. Function of GRKs in metabolic homeostasis

GRKs are multi-organ regulators of systemic insulin resistance. Insulin resistance is the diminished ability of cells to respond to the action of insulin and is strongly associated with metabolic disorder such as type 2 diabetes and obesity (*207*).

4.2.4.7. Diabetes mellitus

GRK2 acts as a regulator which targets both the insulin cascade and GPCRs key to insulin sensitivity and metabolism. In different animal models, GRK2 inhibition ameliorates glucose homeostasis (*208*). A 50 % downregulation of GRK2 protein levels in hemizygous GRK2+/- mice enhances insulin sensitivity in serval cell types (*209*), and induced GRK2 ablation could reverse an established insulin-resistant and obese phenotype (*210*). GRK2 also plays a role in β-adrenergic receptor-induced insulin resistance (*211*). A long-term consequence of type 2 diabetes is manifestation of vascular diseases. GRK2 suppression in the liver markedly improves glucose metabolism and also reduces

endothelial dysfunction by improving the impaired endothelial Akt/eNOS-dependent signalling activation via insulin-stimulated phosphorylation of Akt and eNOS (*212*).

GRK5 -/- knock out mice had impaired glucose tolerance and insulin resistance under high fat diet (*213*). In contrast to these findings, GRK5 was identified to modulate the insulin release in a significant manner and inhibition of GRK5 correlates to a an increase of insulin release (*214*).

4.2.4.8. Obesity

GRK2 is an important modulator of age- and diet-induced adiposity. Aged GRK2 +/- mice show decreased obesity and lower circulating levels of insulin and leptin. These hemizygous animals gained less weight and showed reduced adipocyte size under high fat diet (*209*). Tamoxifen-induced GRK2 deletion prevented further weight gain (*210*). Moreover, GRK5 -/- decreases obesity and adipogenesis with a high fat diet (*215*).

4.2.4.9. Cancer

GRKs are relevant players in cancer progression. Alterations in expression and/or activity of GRKs have been shown in several tumor types (*216*).

GRK2

The role of GRK2 in tumor progression is not clear. Enhanced GRK2 levels trigger tumor growth in both xenograft and orthotopic mice models (*217*). In breast cancer, GRK2 protein levels are upregulated, where it shows a tumor-promoting effect. GRK2 phosphorylates and thereby activates histone deacetylase 6, which leads to deacetylation of Propyl Isomerase Pin1, a central modulator of tumor progression (*217*).

In other cancer types GRK2 upregulation showed an antiproliferative effect, such as in thyroid cancer (*218*). In human hepatocellular carcinoma cells, GRK2 overexpression inhibits cell proliferation, via GRK2-mediated cell cycle arrest during G2/M transition (*219*). Inhibition of GRK2 enhances tumor growth, through activation of the mitogen-activated protein kinase pathway (MAPK) (*220*).

GRK5

GRK5 also has a dual role in cancer progression and is able to both inhibit cancer progression and induce tumor growth. In thyroid cancer cells, GRK5 has negative effect on tumor growth, via enhanced TSH-mediated cAMP signalling and has an effect an proliferation and differentiation (*221*). In colon cancer cells, GRK5 induction by tazarotene-induced gene 1 supresses PGE2-stimulated cell proliferation (*222, 223*). GRK5 inhibition reduces migration and invasion of prostate cancer cells via phosphorylation of moesin on T66 (*128*).

Beside the above described inhibitory effect, GRK5 can also promote tumorigenesis. GRK5 is able to inhibit p53 (*224*), a crucial tumor suppressor that induces cell arrest (*225*).

4.2.4.10. Alzheimer's disease

Patients suffering of Alzheimer's disease showed an increased expression of GRK2 protein and mRNA, and the degree of cognitive impairment correlated with the GRK2 level (*226*). In an Alzheimer's disease mouse model, the expression of GRK2, but not GRK5, in the cortex was elevated (*227*). However, aged Tg-GRK5 knockout mice display cognitive deficits and pathological changes in the hippocampal neurons (*228, 229*). Loss of active GRK5 resulted in accelerated accumulation of β-amyloid, as reflected in increased plaque burden in the cortex of Tg-APPsw mice (*230*). GRK5 deficiency also promotes inflammation in Tg-APPsw mice, which is associated with increased microgliosis and astrogliosis (*231*).

4.2.4.11. Parkinson's disease

GRK5 (and GRK 3) is strongly upregulated in Parkinson's disease patients with dementia, but not in cognitively intact patients (*232*). Initially it was found that GRK5 phosphorylates α-synuclein (*129*), the main component of Lewy bodies found in sporadic Parkinson's disease. GRK5-mediated α-synuclein phosphorylation promotes its oligomerization and co-localization with GRK5 in Lewy bodies in the substancia nigra and locus coeruleus in Parkinson's disease patients (*233*). In addition, two nucleotide polymorphisms enhancing promotor activity found in introns of GRK5 enhances the risk of sporadic Parkinson's disease (*233*). In contrast to these findings, later studies fail to reproduce the GRK5 co-localization in Lewy bodies (*234*) or the association of the GRK5 polymorphisms and Parkinson's disease (*235*). However, the role of GRK5 in Parkinson's disease remains unclear.

4.2.5. GRK2 inhibitors for possible treatment of heart failure

The tri-domain structure of GRK2 allows multiple approaches of inhibiting kinase-dependent and kinase-independent effect. Firstly, targeting the ATP-binding site in the central kinase domain is a general way to prevent enzyme activity. Recently the selective serotine reuptake inhibitor paroxetine was found to be a potent GRK2 ATP-site inhibitor. Secondly, compounds interacting with the amino terminal domain can hinder the GRK2-receptor interaction. Thirdly, the carboxyl terminal domain is involved in localization of GRK2 to the plasma membrane by binding Gβγ.

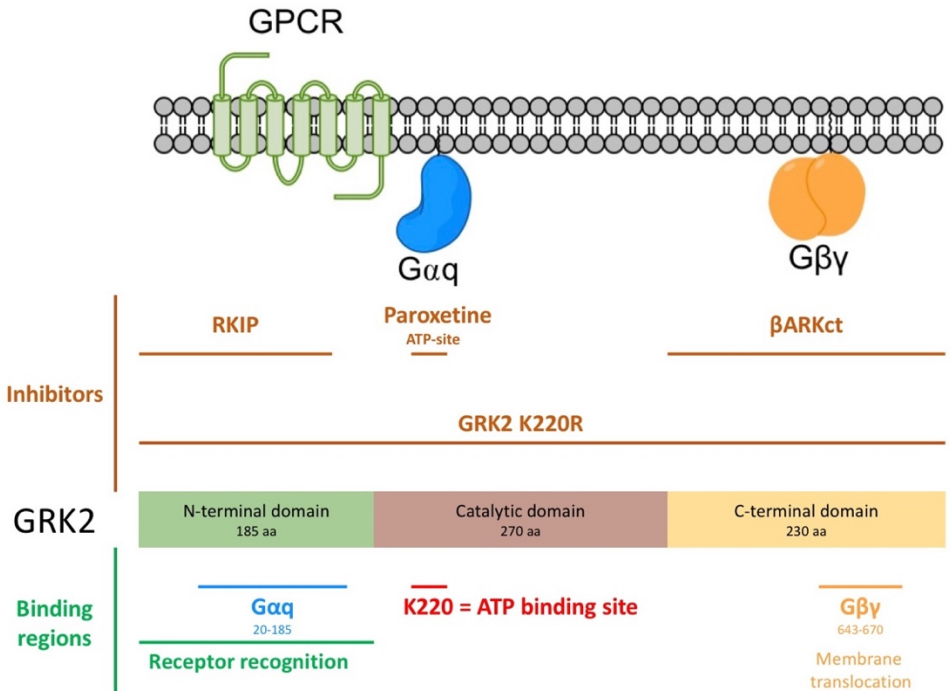

Figure 3: Domain-specific inhibition of GRK2

The tri-domain structure of GRK2 allows for multiple approaches of inhibiting kinase-dependent and -independent effect (adapted from (*104*)).

As discussed in the previous chapter, alterations in GRK2 and GRK5 protein levels are associated with a variety of different human diseases. Over the last 20 years, GRK2/5 research has focused on heart failure, where GRK2 inhibition is a promising therapeutic target.

4.2.5.1. Pathomechanism of heart failure

Heart failure (HF) is a life threatening disease with a prevalence of over 40 million individuals worldwide (*236*), accounting for substantial morbidity and mortality. The prevalence of heart failure is age dependent and with the aging of the population these numbers will increase by 25 % in the next 20 years. HF causes a huge burden for the suffering individual but also for the healthcare systems. Today, 2-3% of the total expenditures of the healthcare systems are attributed just to the treatment of heart failure. By 2030 these costs will be doubled in high income countries (*237*).

Beside the financial burden for society, heart failure is a very serious condition for the individual person in which the heart isn't able to pump sufficient amounts of blood around the body. It is characterised by symptoms such as breathlessness, ankle swelling and fatigue, und signs such as raised jugular venous pressure, pulmonary crackles and peripheral oedema.

The term 'heart failure' describes the final phenotype of several degenerative conditions. In the beginning one or multiple "initial events", either damages the heart muscle or disrupt the ability of the myocardium to generate pumping force. This "initial event" could have an abrupt onset, like after myocardial infarction or a slow onset over many years. One of the most important risk factors are ischemic heart disease and high blood pressure, if not treated (*238*). But heart failure can be assigned to multiple underlying risk factors, which are considerably overlapping. On one hand, there are pathophysiological conditions like lung problems, infections, diabetes, alcohol abuse, HIV/AIDS, obesity, thyroid disorders or radiation which is promoting heart failure.(*239*) On the other hand, sex and age are also important. While the prevalence of people younger than 60 years is less than 2%, it rises up to more than 10 % in the group of people older than 75 years (*240*).

In the early stage of heart failure, the heart is able to adapt and maintain the cardiac homeostasis. A cascade of compensatory mechanisms is activated, such as the adrenergic nervous system, the renin-angiotensin system, cytokines and other mediators. The patient remains asymptomatic for a long period of time. During this period, the heart undergoes "remodelling", the body's reaction of maintaining cardiac function during short term stress. Under constant, long term strain these responses lead to cardiac hypertrophy. With the final loss of function, it moves from early stage to "decompensated" or symptomatic late stage heart failure. Late stage heart failure cannot be cured and the damage of the heart muscle is final.

4.2.5.2. Physiological regulators of GRK2

Raf-1 kinase inhibitory protein (RKIP)

GRKs are tightly regulated by phosphorylation and protein-protein interaction. Raf-1 kinase inhibitor protein (RKIP) belongs to the family of phosphatidylethanolamine-binding proteins (PEBP). RKIP is a dual physiological inhibitor, capable to inhibit both GRK2 (*241*) and the serine/threonine kinase Raf-1, thereby inhibiting the Raf-1/MEK/ERK pathway (*242, 243*). Upon GPCR stimulation, PKC-mediated phosphorylation of RKIP on serine 153 switches the binding affinity from Raf-1 towards GRK2 (*241, 244*). RKIP does not inhibit the enzymatic activity of GRK2, but inhibits the interaction between kinase and receptor, via binding to the N-terminal domain of GRK2 (*241*). Current studies suggest, that the inhibitory mechanism of RKIP is specific towards the GRK2/receptor interaction while cytosolic substrates are not affected (*245*).

RKIP is upregulated in mouse and human heart failure, but its function is discussed controversially. There is some evidence supporting a favourable effect for heart failure patients, due to its ability of GRK2 inhibition (*245*). Taking into account that RKIP is not only a GRK2 inhibitor but also inhibits the cardioprotective and pro survival MAPK-pathway. RKIP, in its unphosphorylated form, could potentially increase cardiomyocyte death. In agreement with this notion, a cardiac-specific RKIP-expressing mouse model showed increased heart dilatation, cardiac dysfunction accompanied by lipid overload and upregulation of cardiac lipid metabolism genes and finally cardiomyocyte death (*188, 220*). Nevertheless, the role of RKIP in heart failure is still an open question.

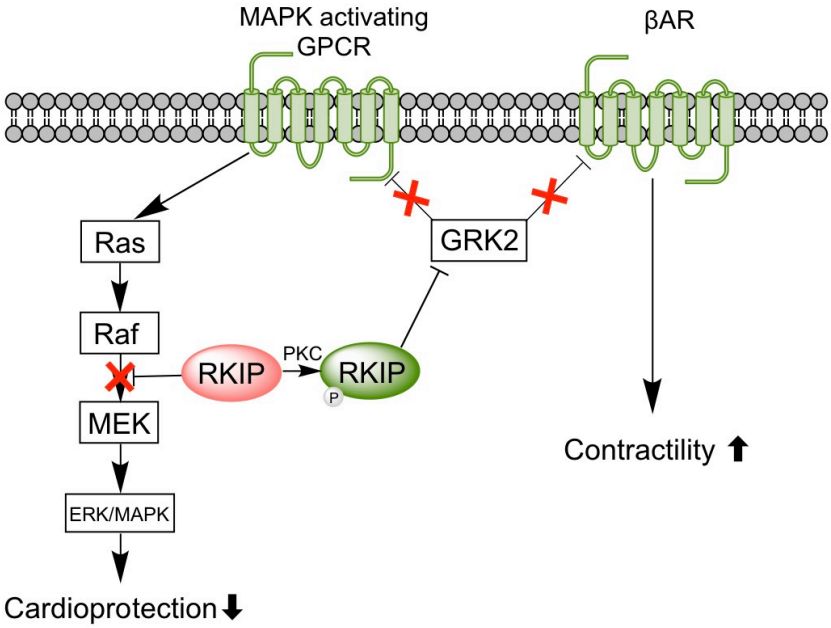

Figure 4: Cardioprotective GRK2 Inhibition requires an intact Raf/ERK axis

RKIP inhibits GRK2 and prevents β-AR desensitisation and internalisation. Thus, this leads increased β-AR signalling, increased cardiac contractility and relaxation. Thereby the development of heart failure is retarded. Inhibition of GRK2 leads via reduced desensitisation of MAPK activating GPCR to an activation of the Raf/ERK axis. The MAPK cascade is contributing to the cardioprotective profile of GRK2 inhibition by counteracting cardiomyocyte death. But RKIP is a dual specific inhibitor of Raf/MAPK, which switches upon PKC phosphorylation from Raf inhibition to GRK2 inhibition. RKIP induces heart failure, cardiac dysfunction and cardiomyocyte death by restraining the RAF/ERK axis.

4.2.5.3. Peptide inhibitors of GRK2

The carboxyl terminal GRK2 inhibitor peptide (βARKct)

About 20 years ago, βARK1ct was the first peptide inhibitor of GRK2 and consists of the C-terminal residues 495-689 of GRK2, which covers the Gβγ-binding site. βARKct prevents the activation and translocation of endogenous GRK2 to the plasma membrane (*168*).

Cardiac-specific expression of βARK1ct in transgenic mice results in prolonged survival and improved cardiac function in a model of acute heart failure, by Gβγ-sequestration as a mechanism of

action (*246*). In a hybrid transgenic mouse model with myocardial expression of both GRK2 (at levels seen in heart failure), and βARKct led to normalization of β-AR signalling (*247*). In addition, upon β-AR activation, βARKct binds to Gβγ proteins to prevent the Gβγ/L-type calcium channel inhibition and thereby improves cardiac contractility by increasing the intracellular calcium levels (*248*).

Currently adenoviral-mediated βARKct gene therapy is under investigation. The effectiveness of this therapy has been demonstrated in several small animal models, but also in clinical relevant larger animal models, such as pig hearts (*249*).

A peptide GRK2 inhibitor derived from the first intracellular loop of β_2-AR

A number of peptides were derived from the intracellular domains of the hamster β_2-AR. The most effective peptide, which compromised the first intracellular loop of the β_2-AR, inhibited the GRK2/receptor interaction with an IC_{50} value of 40μM (*250*). Introduction of charged residues and truncations led to the PepInh: AKFERLQTVTNYFITSE with an increased inhibitory potency by a factor of 40. PepInh showed selectivity towards the GRK family (GRK2: IC_{50} = 0,6μM, GRK3: IC_{50} = 2.6μM and GRK5: IC_{50} = 40μM), but did not interfere with the activity of PKA or PKC (*251*).

The phosducin-derived peptide

Phosducin (PDC) is a cytosolic protein which belongs to the group of Gβγ-binding proteins and occurs in high concentrations in the retina (*252*) and the pineal gland (*253*). A peptide derived from PDC also inhibits GRK2 mediated phosphorylation of rhodopsin (*254*).

4.2.5.4. Small molecule GRK2 inhibitors

Polyanions and Polycations

The first GRK2 inhibitors to be found were polyanionic and polycationic compounds, such as heparin and dextrane sulfate with an IC_{50} value of 0.15 μM (*255*). Heparin and dextrane sulfate are highly charged and insufficient to cross membranes, which impedes their clinical use.

Balanol and Takeda Inhibitors

Balanol is a competitive inhibitor of ATP and targets the kinase domain of various members of the AGC kinase family (*256*). Balanol mimics the structure of ATP and its four rings establish interactions with the ATP binding subsite of GRK2. The natural product balanol is a potent inhibitor of GRK2 (IC_{50} = 42nM). A similar potency was observed against other members of the GRK family (IC_{50} of GRK1 = 340nM, GRK3 = 47nM, GRK4 = 360nM, GRK5 = 160nM, GRK6 = 490nM and GRK7 = 180nM) (*257*). The central catalytic domains of GRKs are approximately 32% identical to the catalytic subunit of PKA, PKG and PKC (*258*). Therefore balanol is also a highly potent inhibitors of other AGC kinase domains too (IC_{50} of PKAα = 3.9nM, PKGα = 1.6nM and PKCα = 6.4nM) (*256*).

Several compounds based on the four-ring structure of balanol were discovered by Takeda Pharmaceutical Company, which exhibit a higher selectivity against GRK2. Takeda103A and Takeda101 showed a >50-fold selectivity over other AGC kinases (*259*), but the oral bioavailability of Takeda compounds is insufficient which precludes their potential use (*260*).

Paroxetine and derivatives

The serotonin-reuptake inhibitor (SSRI), paroxetine, was identified as a potent GRK2 inhibitor, with an IC_{50} of 1.4μM. The crystal structure of GRK2 with paroxetine reveals that paroxetine fits into the enzymatic pocket and stabilizes it in an inactive state. In an in vitro GPCR phosphorylation assay and in living cells paroxetine shows a 60-fold selectivity for GRK2 over other GRK isoform, and a 10-fold selectivity over PKA and a 40-fold selectivity over PKC (*261*).

In vivo studies showed that paroxetine can reverse cardiac dysfunction and remodeling. Two weeks after myocardial infarction mice were treated with paroxetine for 4 weeks. Control mice were treated with fluoxetine, which does not inhibit GRK2, and cardiac function decreased, while the paroxetine group showed improvement of cardiac function (*262*).

Based on the structure of paroxetine different drugs were designed. Ligation of amide moieties to the fluorophenyl ring improved the inhibitory potency, resulting in an IC50 value of 30nM (*263*).

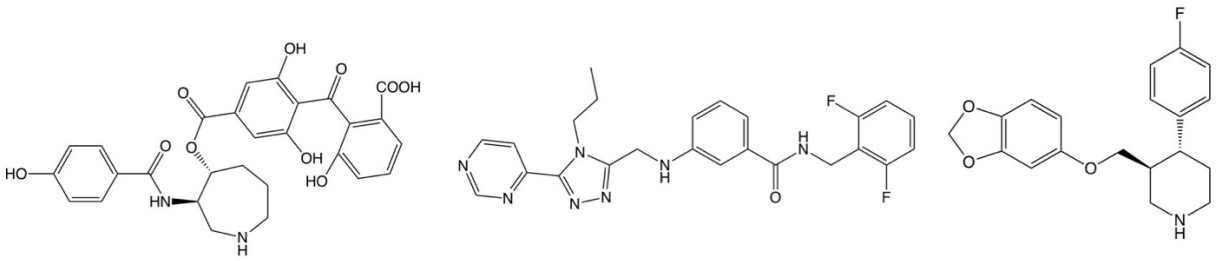

Figure 5: Formula of small molecule GRK2 inhibitor

All three inhibitors are competitive inhibitor of ATP and targets the kinase domain of GRK2. **Balanol** mimics the structure of ATP and its four rings establish interactions with the ATP binding subsite, but lacks selectivity over other AGC kinases (*256, 257*). Based on the structure Balanol the **Takeda compound** was discovered, which displays higher selectivity for GRK2, but insufficient oral bioavailability (*259*). The SSRI **paroxetine** was previously established as a cardioprotective ATP-site GRK2 inhibitor by drug repurposing.

4.2.5.5. RNA Aptamers

A selection process termed SELEX was used to identify a specific RNA inhibitor (C13) that binds and inhibits the GRK2-mediated rhodopsin phosphorylation (*264*). The C13 aptamer binds with high nanomolar affinity to GRK2 and with selectivity over other kinases such as GRK5 (*264*). The crystallographic structures of GRK2 bound to the C13 aptamer revealed that C13 interacts with the catalytic core of the kinase domain of GRK2 and stabilizes it in a unique inactive conformation (*265*). Although the C13 aptamer is not considered to be a viable therapeutic for oral therapy, it can be used in a high-throughput displacement assay to identify specific new small molecule inhibitors for GRK2 (*266*). With such aptamer-displacement assay the FDA-approved drug paroxetine was discovered as a potent GRK2 inhibitor (*261*).

4.3. Aim of thesis

The major goal of my thesis was the identification of mechanisms required for cardioprotective GRK2-inhibition. Although it is widely accepted that GRK2 inhibition is cardioprotective, the underlying mechanisms of cardioprotection are incompletely understood. To this end, I compared activities of different GRK2 inhibitors in vitro and in vivo. Thus, the aims of this project are threefold:

- To establish an in-vitro kinase assay, in order to compare substrate specificities of GRK2 inhibitors, RKIP and paroxetine.
- To compare the unclear role of RKIP with the dominant-negative GRK2-K220R mutant in transgenic mice and characterise the cardiac phenotype.
- To generate GRK5-transgenic mice and study the impact of compensatory GRK5 up-regulation under conditions of GRK2 inhibition.

5. MATERIALS AND METHODS

5.1. Materials

Substance	Origin	
β-glycerophosphate disodium	Sigma-Aldrich	G5422
β-mercaptoethanol	Sigma-Aldrich	63689
[32] γ-ATP	Perkin Elmer Inc.	BLU002001MC
10% Bolt Bis-Tris Plus gel	Invitrogen	NW00107BOX
10x sample reducing agent	Invitrogen	B0004
2-[4-(2-hydroxyethyl)-1-piperazin]ethanesulfonic acid (HEPES)	Biosolve	0008042359BS
2-Propanol	Merck	1.09634.1000
2,2'-azino-bis(3-ethylbenzothiazoline-6-sulphonic acid) (ABTS)	Sigma-Aldrich	A1888
3,3'-diaminobenzidine tetrahydrochloride (DAB)	Sigma Aldrich	D3939
30% Acrylamide/Bis solution	Bio-Rad Laboratories AG	1610158
4x LDS sample buffer	Invitrogen	B0008
Acetic Acid, glacial	Merck	1.00063.1000
Acetone	Merck	1.00014.2500
Adenosine 5′-triphosphate (ATP) disodium salt hydrate	Sigma-Aldrich	A7699
Agarose MP	Cleaver Scientific	9012-36-6
Ammonium persulfate (APS)	Bio-Rad Laboratories AG	1610700
Ampicillin	Carl Roth GmbH + Co. KG	K029.1
Bac-to-BacTM Baculovirus Expression System	Invitrogen	10359016
BactoTM agar	Becton Dickinson AG	214010
BactoTM trypton	Becton Dickinson AG	211705
BactoTM yeast extract	Becton Dickinson AG	212750
BL21(DE3) pLysS Competent Cells, single use	Promega AG	L1195
Boric acid	Merck	1.00165.1000
Bovine Serum Albumin (BSA)	Sigma-Aldrich	A8022
Bromphenol blue sodium salt	Merck	1.11746.0005
Calcium chloride dihydrate (CaCl2x2H2O)	Merck	1.02382.0500
Cellfectin™ II Reagent	Invitrogen	10362-100
Chelex-100	Bio-Rad Laboratories AG	143-2832
Chloroform	Merck	1.02445.1000
Citric acid	Merck	1.00244.1000
Coomassie brilliant blue	Merck	1.12553.0025
D (+)-glucose monohydrate	Merck	1.04074.0500

Desoxyribonucleotide mixture (dNTPs)	New England BioLabs	N0447S
DH10Bac E. coli bacteria	Invitrogen	10361012
di-sodium hydrogenphosphate dihydrate ($Na_2HPO_4x2H_2O$)	Merck	1.06580.0500
Dimethyl sulfoxide (DMSO)	Sigma-Aldrich	D2438
Dimethylformamide	Merck	1.02937.0500
DraIII	New England BioLabs	R3510S
ECL Wester Blotting detection reagent	Amersham	Prime: RPN2232
EndoFree Plasmid Maxi Kit	QIAGEN	12362
Eosin Y solution 0,5% aqueous	Sigma-Aldrich	HT110216
Ethanol	VWR Chemicals	20821.296
Ethidium bromide	Merck	1.11608.0030
Ethylendiamintetraacetic acid (EDTA) solution (0.5M)	Sigma-Aldrich	O3690
Ethylendiamintetraacetic acid tetrasodium hydrate (Na4EDTAxH2O)	Sigma-Aldrich	E5391
Fetal bovine serum (FBS)	Thermo Fisher Scientific AG	hyclone, Lot RZG35920
Formalin solution, neutral buffered, 10%	Sigma-Aldrich	SLBT5369
GeneRuler 1kb DNA ladder 0.5 µg/µL	Thermo Fischer Scientific AG	SM0311
Gentamicin sulfate salt	Sigma-Aldrich	G1264
Glycerol	Merck	1.04092.1000
Glycine	Merck	1.04201.1000
Herculase II fusion DNA polymerase	Agilent Technologies AG	#600675
Herculase II Reaction buffer 5x	Agilent Technologies AG	#600675
Hind III	New England BioLabs	R0104S
human chorionic gonadotropin (hCG)	Sigma-Aldrich	C0434
Hyaluronidase from bovine testes	Sigma-Aldrich	H3884
Hydrogen peroxide (30%)	Merck	1.07209.0250
Hyperfilm	Amersham	28906836
Igepal CA-630 (NP40)	Sigma-Aldrich	I7771
Imidazole	Sigma-Aldrich	I5513
IPTG (isopropyl-β-D-thiogalactopyranose)	Sigma-Aldrich	I5502
Kanamycin	Sigma-Aldrich	K1377
M16 medium	Sigma-Aldrich	M7292
M2 medium	Sigma-Aldrich	M7167
Magnesium chlorid hexahydrate	Merck	1.05833.0250
Magnesium sulfate heptahydrate (MgSO4x7H2O)	Merck	1.05886.0500
Mayer's hemalum solution	Merck	1.09249.0500
Methanol	Merck	1.06009.5000
Mineral oil	Sigma-Aldrich	M5310
MluI	New England BioLabs	R0198S

MOPS SDS running buffer	Invitrogen	B000102
n-Dodecyl β-D-maltoside (DDM)	Sigma-Aldrich	D4641
Non fat dry milk	frema Reform Instant-Magermilchpulver	LIS18902VB
Ni-NTA Agarose	QIAGEN	30210
PageRuler Plus Prestained Protein Ladder	Thermo Fisher Scientific AG	26619
Paroxetine	Sigma-Aldrich	P9623
PBS (Dulbecco's phosphate buffered saline)	Sigma-Aldrich	D8537
PD-10 desalting columns	GE Healthcare GmbH	17-0851-01
Penicillin–Streptomycin Solution Hybri-Max	Sigma-Aldrich	P7539
Penicillin-Streptomycin	Sigma-Aldrich	P0781
pET-3d	Novagen, Merck KGaA	69421-3
pFastBac1	Invitrogen	10360014
Phosphate buffered saline (PBS)	Sigma-Aldrich	D8537
Poly-Mount Xylene	Polyscience	24176
Polyethylene glycol (PEG) 3000	Merck	8.17019.1000
Potassium chloride	Sigma-Aldrich	1.04936.1000
Potassium dihydrogen phosphate	Merck	1.04873.1000
Pregnant mare serum gonatropin (PMSG)	Sigma-Aldrich	G4877
Protease inhibitor cocktail	Sigma-Aldrich	P8340
Proteinase K	Roche	03115879001
PureLink HiPure Plasmid Purification Miniprep Kit	Invitrogen	K2100-02:
PureLink HiPure Plasmid Purification Midiprep Kit	Invitrogen	K210015
PureLink HiPure Plasmid Purification Maxiprep Kit	Invitrogen	K210016
PVDF membrane (Immobilon-P, 0.45 μm)	Merck	IPVH00010
QIAquick Gel Extraction Kit	QIAGEN	28704
RNAlater	QIAGEN	76104
Rneasy Midi kit	QIAGEN	75142
Roti®-Quant	Carl Roth GmbH + Co. KG	K015.02
Sal I	New England BioLabs	R0138T
Sf9 Cells	Sigma-Aldrich	89070101
SOC medium	Invitrogen	15544034
Sodium chloride (NaCl)	Sigma-Aldrich	71380
Sodium desoxycholate	Sigma-Aldrich	D6750
Sodium Dodecyl Sulfate (SDS)	Bio-Rad Laboratories AG	#1610302
Sodium fluoride (NaF)	Merck	1.064490250
Sodium hydroxide (NaOH)	Merck	1.06469.1000
Sodium molybdate	Merck	1.06521.0100
Sodium orthovanadate	Sigma-Aldrich	S6508
T4 DNA Ligase (6 U/μL)	New England BioLabs	M0202
Taq polymerase	Sigma-Aldrich	D1806

TC-100 Insect medium	Sigma-Aldrich	T3160
TE buffer (10 mM TRIS pH 8, 0.1 mM EDTA)	Invitrogen	12090015
TEMED (N,N,N',N'-tetramethylethylenediamine)	Carl Roth GmbH + Co. KG	2367.3
Tetenal Superfix MRP	Tetenal	104462
Tetenal, Roentoroll HC	Tetenal	104450
Tetracycline	Sigma-Aldrich	T7660
Tris(hydroxymethyl)aminomethane (Tris)	Biosolve	0020092391BS
Triton X-100	Merck	1.08603.1000
Trizma® hydrochloride solution (1M)	Sigma-Aldrich	T2194
Tryptan blue	Sigma-Aldrich	T6146
Tween 20	Merck	8.22184.0500
Urea	Merck	1.08487.1000
X-gal (5-bromo-4-chloro-3-indolyl-β-D-galactopyranose)	VWR International GmbH	730-1498
X-ray films (Super R, Fuji Medical x-ray film)	Fuji Medical	
XL1 Blue E. coli bacteria	Stratagene	#200249

Suppliers:

Agilent Technologies AG, Agilent Technologies AG, Basel, Switzerland
Amersham, GE Healthcare GmbH, Glattburg, Switzerland
Becton Dickinson AG, Allschwil, Switzerland
Biosolve, Biosolve BV, Valkenswaard, Netherlands
Bio-Rad Laboratories AG, Cressier, Switzerland
Carl Roth GmbH + Co.KG, Karlsruhe, Germany
Eppendorf AG, Hamburg, Germany
GE Healthcare GmbH, Glattburg, Switzerland
Invitrogen, Thermo Fisher Scientific AG, Reinach, Switzerland
Merck, Merck KGaA, Darmstadt, Germany
New England BioLabs, New England BioLabs GmbH, Frankfurt am Main, Germany
Perkin Elmer Inc., Schwerzenbach, Switzerland
Promega AG, Dübendorf, Switzerland
QIAGEN, QIAGEN GmbH, Hilden, Germany
Roche, Roche Pharma AG, Reinach, Switzerland
Sigma-Aldrich, Sigma-Aldrich Chemie GmbH, Buchs SG, Switzerland
Stratagene, Agilent Technologies AG, Basel, Switzerland
Tetenal, Tetenal Europe GmbH, Norderstedt, Germany
Thermo Fisher Scientific AG, Reinach, Switzerland
VWR International GmbH, Dietikon, Switzerland

5.2. Molecular biology methods

Polymerase chain reaction (PCR)

For the amplification of cDNA fragments, Herculase II fusion DNA polymerase, and for single colony screening of bacterial clones Taq DNA polymerase were used. The polymerase chain reaction was performed in the supplied buffers, with a final primer concentration of 0.4 μM. dNTPs were used at a concentration of 200 μM, and 0.1-1 ng DNA served as a template. DNA amplification was carried out with a standard program using a Thermocycler 3000 (Biometra, Göttingen, Germany).

Step	Temperature	Time	Cycles
1	95°C	2 min	1X
2	95°C	20 s	25-30X
3	55-60°C	20 s	
4	72°C	60 s/1000 bp	
5	72°C	10 min	1X

Table 1: Standard PCR program

Initial melting of the dsDNA (step 1) was followed by 25-30 cycles consisting of melting of dsDNA (step 2) followed by annealing (step 3) and extension (step 4) of primers. PCR was finished with a final elongation step (step 5).

Agarose gel electrophoresis

PCR products were separated by agarose gel electrophoresis. Resolution of DNA is affected by agarose concentration and buffer composition. 2% (w/v) agarose gives the best separation of smaller fragments (0.2-1 kb), while for bigger fragments, 0.8-1.5% (w/v) agarose gels were used. For visualization of the DNA, ethidium bromide in a final concentration of 0.5 μg/ml was used. The gel was prepared with either standard TAE buffer (40 mM Tris, 20 mM glacial acetic acid, 2 mM EDTA) or TBE buffer (89 mM Tris, 89 mM boric acid, 2 mM EDTA) for smaller fragments. For fragment size identification, DNA ladder (GeneRuler 1 kb) was run in parallel to the samples.

DNA gel extraction

For the clean-up of PCR products and removal of primers, enzymes, dyes and salts, PCR samples were separated by agarose gel electrophoresis. DNA was excised under UV-light (365 nm) from the gel and extracted using QIAquick Gel Extraction Kit. Up to 10 μg DNA were purified per column according to the manufacturer's protocol and eluted with 30 μl TE buffer.

Enzyme restriction digestion

For the restriction digest of DNA, suitable enzymes were purchased from New England BioLabs. Supplied buffer were used and reaction conditions were chosen according to the manufacturer's instructions.

Ligation

Digested PCR fragments and digested vector backbone were ligated overnight with T4 DNA ligase in the supplied T4 DNA Ligase Reaction Buffer at 16°C. Vector to insert was used at a molar ratio of 1:4.

Heat shock transformation

For heat shock transformation, 100 μl of competent E. coli XL1 blue bacteria were thawed on ice and subsequently mixed gently with 10 μl of ligation mixture or 1 μl DNA stock solution, and incubated on ice for 20 min. The mixture was heat-pulsed in a 42°C water bath for 45 sec and subsequently incubated on ice for 2 min. SOC medium (900 μl), prewarmed to 37°C, was added followed by incubation in the shaker (200 rpm) at 37°C for 30 min. An aliquot of the DNA-bacteria mixture (10-100 μl) was streaked out on prewarmed LB agar plates containing the appropriate antibiotic for selection of transformed bacteria. After overnight incubation at 37°C single colonies were inoculated in 2 ml LB for 3-4 h at 37°C and 200rpm. Bacteria from 1 ml culture medium were pelleted by centrifugation at 16'000 x g for 1 min, lysed with 100 μl of sterile A. dest. and used for single colony screening.

SOB	
bacto-tryptone	4 g
bacto-yeast extract	1 g
NaCl	0.1 g
dH_2O	Ad 200 ml

SOC	
SOB	48 ml
1 M $MgCl_2$	0.5 ml
1 M $MgSO_4$	0.5 ml
20% (w/v) D (+)-glucose monohydrate	1 ml

LB medium	
bacto-tryptone	50 g
bacto-yeast extract	25 g
NaCl	50 g
dH_2O	Ad 5000 ml

LB agar plates	
LB medium	
bacto-agar	1.5% w/v

Table 2: bacterial growth media

SOB and LB medium components were dissolved and directly autoclaved.

Preparation of competent bacteria

E. coli XL1 blue bacteria were streaked onto LB plates containing tetracycline (20 μg/ml tetracycline in 1:1 ethanol/water) and grown overnight at 37°C. A single colony was cultivated overnight in 5 ml of LB medium and 1 ml of the overnight bacterial suspension was incubated with 119 ml of LB medium the following day and grown to mid-log phase (OD_{600nm}=0.4-0.6). Bacteria were pelleted at 4°C by centrifugation at 3000 x g for 10 min. The bacterial pellet was resuspended in 12 ml of TSB on ice, aliquoted, flash frozen in liquid nitrogen and stored at -80°C.

TSB	
PEG 3000	10 g
DMSO	5 ml
1M $MgSO_4$	2 ml
1M $MgCl_2$	2 ml
LB medium	Ad 100 ml

Table 3: TSB buffer composition

PEG 3000 was dissolved in 40 ml of LB buffer and the pH was adjusted to 6.1. The remaining substances were added and filled up with LB medium to a final volume of 100 ml.

Preparations of plasmid DNA

PureLink HiPure Plasmid Purification Kit was used for Plasmid DNA isolation from bacterial culture. The Midiprep Kit was used for isolation of low copy plasmids from 100 ml of bacterial culture and for preparations of high-copy plasmid DNA, 25 ml culture were used. For the Maxiprep Kit an 8-fold higher amount of bacterial culture was used. All preparations were made according to the manufacturer's protocol (Invitrogen).

Quantification of DNA

dsDNA was quantified by optical density. DNA was diluted in 10 mM Tris-HCl pH7.5 and the absorbance at 260 nm was measured with a BioPhotometer (Eppendorf). Sample purity was determined using the 260/280 nm ratio. A 260/280 ratio of 1.8-2.0 was used as an indicator of DNA purity.

Sequencing

To control for DNA sequence identity, Sanger sequencing was performed by Microsynth AG (Balgach, Switzerland).

Primer

Primer were synthesized by Microsynth AG (Balgach. Switzerland).

5.3. Protein expression systems

5.3.1. Protein expression in bacterial cells

The cDNA of the protein to be overexpressed was cloned into the pET-3d vector backbone. Single use BL21(DE3) pLysS Competent Cells (Promega) were used as a host strain.

pET-3d

The pET expression system has been developed for cloning and expression DNA under control of a T7 promoter (*267*). Expression uses bacterial cells harbouring the lysogenic DE3 prophage, encoding the T7 RNA polymerase, under control of the IPTG (isopropyl-β-D-thiogalactopyranose) inducible *lacUV5* promoter. LacI, which is present in the E. coli genome, forms a tetramer and represses the *lacUV5* promoter encoded by the expression plasmid. IPTG binds and triggers the release of the tetrameric LacI from the *lac* operator (*268, 269*). The *lac* operator triggers transcription and induces protein expression.

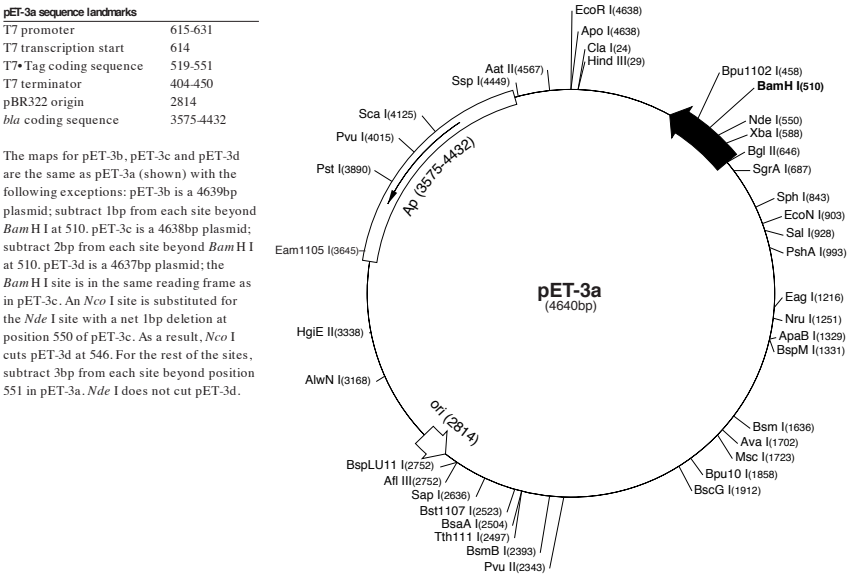

Figure 6:Vector map of pET-3d

The vector map of pET-3d (Novagen) shows the T7 promoter followed by a multiple cloning site and an ampicillin resistance gene.

The pET-3d plasmid with the gene of interest was transformed by heat shock transformation into BL21(DE3) pLysS competent cells and incubated overnight on LB plates containing ampicillin (50 μg/ml). A single colony was cultivated overnight in a rotating incubator (rotation set to 200rpm) at 37°C in 10 ml of LB medium containing ampicillin (50 μg/ml). The next day the overnight culture was diluted to 200 ml and grown to mid-log phase (OD600 = 0.5 - 0.6)

For a time-course analysis of protein expression samples were taken hourly. Bacteria of uninduced 10 ml sample were pelleted at 4000 x g and 4°C for 10 min (Rotanta 460R, Hettich Laborapparate,

Bäch Switzerland). The supernatant was discarded and the pellet was frozen in liquid nitrogen. IPTG was added at a final concentration of 1 mM. During the next 4 hours, samples were taken hourly and treated as above. Finally, the remaining bacterial culture was pelleted as described above and pellets were stored at -80°C.

For protein expression analysis by SDS-PAGE and immunoblotting, samples taken at different time points were thawed on ice, lysed in 200 µl of urea-containing 1 x SDS sample buffer and incubated at room temperature (RT) for 60 min. After the fragmentation of viscous DNA by sonication on ice (HD2200, 2 x 3 impulses with 70% power; UW2200; MS73; BANDELIN electronic GmbH & Co.KG, Berlin Germany) samples were stored at -20°C.

For best expression of target proteins, OD600 at IPTG-induction, IPTG concentration, incubation-temperature and incubation-time were optimized.

5 x SDS sample buffer	
SDS	10 % (w/v)
glycerol	10 % (v/v)
1 M Tris, pH 6.8	25 ml
bromophenol blue	0.05% (w/w)
dH_2O	ad 100 ml

1 x SDS sample buffer containing urea	
5 x SDS sample buffer	10 ml
urea	6 M
β - mercaptoethanol	300 mM
dH_2O	ad 50 ml

Table 4: Composition of SDS sample buffer

5 x SDS sample buffer was stored for daily use at 4°C and for long time storage at -80°C. 1x SDS sample buffer with urea and β - mercaptoethanol were prepared freshly.

Measurement of cell concentration in suspension by optical density

To determine the cell concentration, the turbidity of the cell suspension was measured at a wavelength of 600 nm (OD600) by a Biophotometer (Eppendorf, Germany)

5.3.1. Protein expression in SF9 cells

Insect cell culture is commonly used for recombinant protein production using a baculovirus. Sf9 cells are derived from the pupal ovarian tissue of the fall army worm, *Spodoptera frugiperda (270).*

5.3.1.1. Culture of Sf9 cells

Thawing cells

A frozen aliquot of Sf9 cells was removed from liquid nitrogen and quickly thawed in a 37°C waterbath. The cryovial was decontaminated with ethanol (70%), cells were added drop-wise to prewarmed complete insect medium in a 15 ml centrifuge tube. Cells were counted, viability was checked and $2x10^4$ - $5x10^4$ viable cells/cm^2 were seeded into the appropriately sized flask. Cells were allowed to attach and medium was replaced. Medium was changed daily. Sf9 cells were passaged when cells were 95% confluent. Cell culture flasks with different surface areas were purchased from Sarstedt AG & Co. KG

Complete medium

The complete medium contained TC 100 insect medium supplemented with 10 % (v/v) FBS and 100 U/ml penicillin/100 μg/ml streptomycin.

Cell culture procedures

Adherent Sf9 cells were cultured in complete insect medium under sterile conditions at 27°C without CO_2 regulation under sterile condition in a humidified incubator.

Subculture of adherent cells

Cells were grown until monolayer culture reached 90-95% confluency, which is typically the mid-log phase. At this point, the monolayer was dislodged by the sloughing method. Therefore, medium was removed from the flask and 5 ml new medium was added and streamed across the monolayer. A gentle stream was used to dislodge the cells.

Freezing cells

Once Sf9 cells were doubling regularly, show viability of >90%, and grow in the mid-log phase, they were frozen. Cells were dislodged from the flask, cell density and viability were determined, and cells were centrifuged at 100xg for 5 min. The pellet was resuspended in an appropriate amount of cold freezing medium (9%DMSO, 91% FBS) to achieve a cell density of 3 x 10^6 cells/ml, and 1 ml aliquots were dispensed into cryovials (Nalgene Labware, Fisher Scientific AG). Cells were frozen in a freezing container (Nalgene Labware, Fisher Scientific AG), which decreases the temperature approximately 1°C per minute to -80°C. For long-term storage, cells were kept in liquid nitrogen.

Cell number

For determination of the cell number, a Neubauer hemocytometer (LO-Laboroptik GmbH, Bad Homburg, Germany) was used according to the manufacturer's instruction. An aliquot of the cell suspension was mixed with an equal volume of 0.4% (w/v) Trypan Blue in PBS (Sigma-Aldrich). Ten µl of the 1:1 diluted cell suspension were applied to the hemocytometer and viable cells were counted in all four squares. The cell concentration (cells/ml) was calculated with the following formula:

$$cells/ml = \frac{number\ of\ cells\ \times\ 10\,000}{number\ of\ squares} \times dilution\ factor\ \times\ 100$$

5.3.1.2. Generation of a recombinant baculovirus

The Bac-to-Bac baculovirus expression system

For the generation of a recombinant baculovirus, the Bac-to-Bac® Baculovirus Expression System Kit (Invitrogen) was used. The recombinant baculoviruses were constructed in two steps: the gene of interest was cloned into the pFastBac1 donor plasmid followed by transposition of the pFastBac1 expression construct into a baculovirus shuttle vector (bacmid). The high molecular recombinant bacmid DNA isolated from DH10Bac cells was used to transfect Sf9 cells, in order to generate a baculovirus stock.

Donor plasmid pFastBac1

The gene of interest was cloned in the pFastBac1 donor plasmid. The gene expression is under control of a strong *Autographa californica* multiple nuclear polyhedrosis virus (AcNPV) polyhedron (P_{PH}) promoter. The expression cassette is flanked by the right and left arms of Tn7, and contains a gentamycin resistance gene, and a SV40 polyadenylation signal to form a mini Tn7 (*271*).

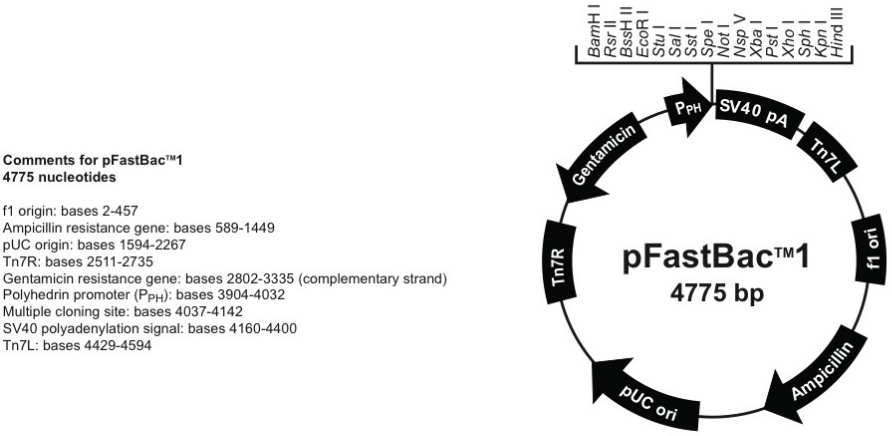

Figure 7: Vector map of pFastBac1 (Invitrogen)

The mini-Tn7 contains a gentamycin resistance gene, an AcNPV polyhedron promoter followed by a multiple cloning site and a SV40 poly(A) signal. The plasmid contains an ampicillin resistance gene to allow for selection in DH10Bac E. coli.

Generation of a recombinant bacmid and baculovirus

For the generation of the bacmid, DH10Bac E. coli bacteria were used as a host for the pFastBac construct. These bacteria contain the baculovirus shuttle vector, consisting of the bMON14272 bacmid DNA (136 kb), and the pMON7124 helper plasmid (*272*). The bacmid contains the low-copy-number mini-F replicon, a kanamycin resistance gene and a segment encoding the LacZα peptide. Inserted into the LacZα gene is the attachment site for the bacterial transposon Tn7 (mini-*att*Tn7), which does not disrupt the LacZα reading frame. The recombinant bacmids were generated by transposing a mini-Tn7 from the pFastBac1to the mini-*att*Tn7 attachment site from the bacmid. The helper plasmid (pMON7124) encodes the transposase and confers resistance to tetracyclin and provides the Tn7 transposition function in trans (*273*). By insertion of mini-Tn7 into the mini-*att*Tn7

site on the bacmid, the expression of LacZα was disrupted and the colonies containing the recombinant bacmid are white in a blue/white screening.

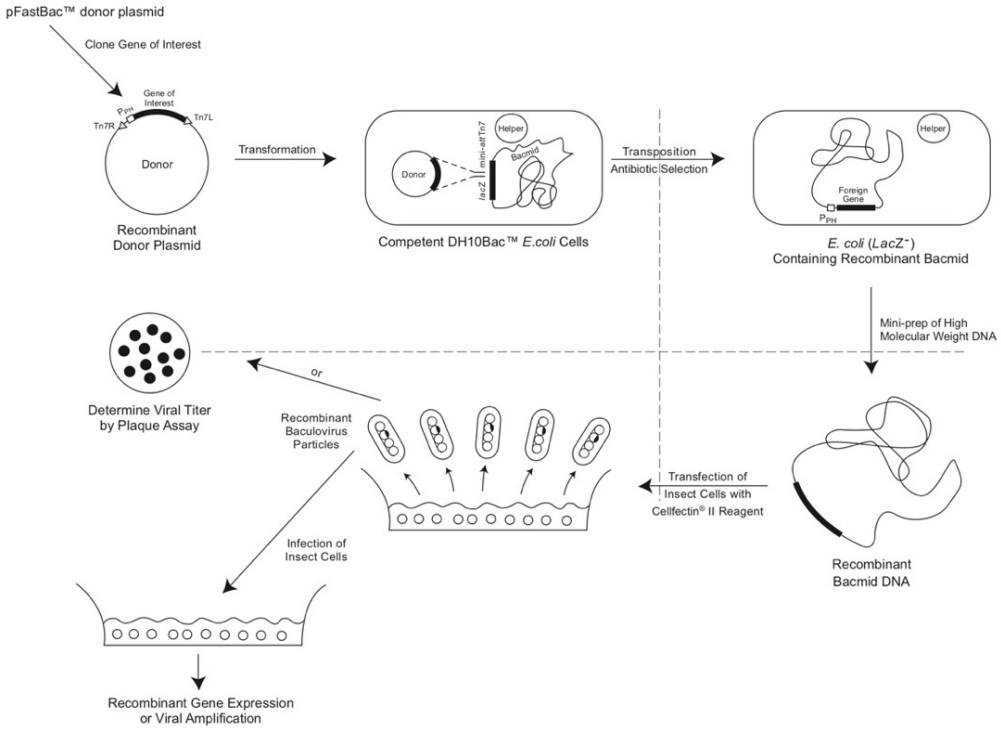

Figure 8: Generation of recombinant baculoviruses and protein expression with the Bac-to-Bac system.

This figure depicts most important steps: the donor plasmid is transformed into DH10Bac™ *E. coli*, where the gene of interest transposes into the bacmid DNA. Insect cells were transfected with the isolated recombinant bacmid DNA and subsequently baculovirus was expressed. (adapted from(*274*))

Generation of a recombinant bacmid

The baculovirus was generated by using the Bac-to-Bac® Baculovirus Expression System Kit (Invitrogen), which consists of the pFastBac1™ plasmid, MAX Efficiency® DH10Bac™ Competent *E. coli,* and Cellfectin™ II Reagent. All procedures were performed according to the manufacturer's instructions with slight modifications.

The gene of interest was cloned into the pFastBac1 plasmid as described above, and selected via ampicillin resistance followed by a screening PCR. Finally, the identity of the DNA was confirmed by Sanger sequencing.

The purified pFastBac™ construct was diluted to the desired concentration of 200 pg/μl in TE buffer pH 8. MAX Efficiency® DH10Bac™ Competent *E. coli* were thawed on ice, and an aliquot of 50 μl was used for transformation with 1 ng of plasmid. After a 30 min incubation on ice, the mixture was heat-pulsed for 45 sec at 42°C, immediately transferred to ice and chilled for 2 min. Thereafter 0.95 ml of SOC medium (Invitrogen) were added and incubated for 4 h at 37°C and 200rpm. After the incubation, 10-fold serial dilutions (10^{-1},10^{-2},10^{-3}) were prepared with SOC medium, and 100 μl were spread on LB agar plates containing 50 μg/ml of kanamycin (dissolved in water and filter-sterilized), 7μg/ml of gentamycin (dissolved in water and filter-sterilized), 10μg/ml of tetracycline (dissolved in 100% ethanol and filter-sterilized), 40 μg/ml of X-gal and 50 μg/ml of IPTG (X-gal and IPTG were dissolved in dimethylformamide). The bacmid itself contains a kanamycin resistance marker, the gentamycin resistance is on the donor plasmid, and the tetracycline resistance is on the helper plasmid. In addition to the selection by antibiotics, X-gal and IPTG were used for a blue/white screening. After 48 h of incubation at 37°C, colonies with successful transposition of the gene of interest into the bacmid DNA appeared white, while blue colonies contained the unaltered bacmid. Five white colonies were picked and restreaked on fresh LB agar plates containing 50 μg/ml of kanamycin, 7μg/ml of gentamycin, 10μg/ml of tetracycline, 40 μg/ml of X-gal and 50 μg/ml of IPTG and incubated overnight at 37°C. A single colony, with a confirmed white phenotype, was inoculated over-night at 37°C in 2ml of liquid LB medium containing 50 μg/ml of kanamycin, 7μg/ml of gentamycin, 10μg/ml of tetracycline.

Isolation of recombinant bacmid

The recombinant bacmid DNA was isolated from the bacterial culture using the PureLink™HiPure Plasmid Miniprep Kit (Invitrogen, Thermo Fischer Scientific AG, Reinach, Switzerland). An aliquot (1,5 ml) of the bacterial culture was treated according to the manufacturer's special protocol for the isolation of bacmid DNA, and extracted bacmid was dissolved in 20 μl of TE buffer for 60 min on ice.

Confirmation of gene transposition by PCR

PCR analysis was used to verify the presence of the gene of interest in the recombinant bacmid. pUC/M14 forward (5′-CCCAGTCACGACGTTGTAAAACG-3′) and reverse (5′-AGCGGATAACAATTTCACACAGG-3′) primers were used which hybridize to sites flanking the mini-*att*Tn7 site. (Figure 9, A)

PCR was performed under standard conditions with Taq polymerase and the supplied buffer. Amplification conditions needed to be modified, because the expected size of the PCR construct was over 4kb: For the reaction a final concentration of 3 mM $MgCl_2$, 0.25 μM of each primer was used, and 1μl of the bacmid solution served as a template. The annealing temperature was set to 55°C, and extension time was extended to 5 min.

A

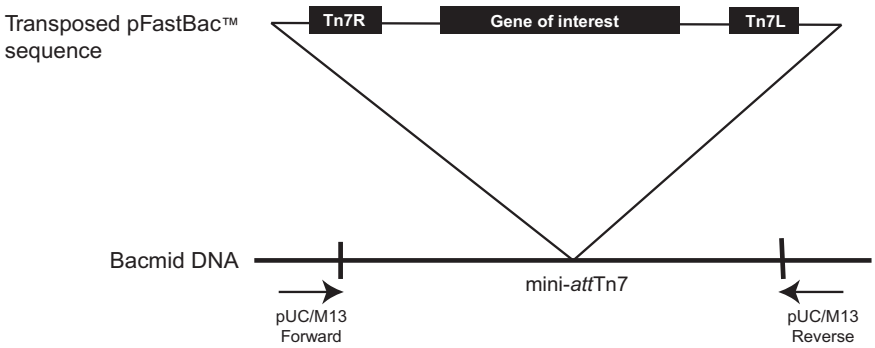

B

Sample	Size of PCR Product
Bacmid alone	~ 300 bp
Bacmid transposed with pFastBac	~ 2300 bp + size of insert

Figure 9: Scheme of the bacmid DNA

(A) Scheme illustrating the bacmid DNA and primer hybridization site flanking the mini-*att*Tn7 site and (B) the expected size of the PCR product.

5.3.1.3. Expression of recombinant proteins in Sf9 cells

Transfection of insect cells

Sf9 cells were transfected with the purified recombinant bacmid DNA. To this end, cells in the log phase (1.5-2.5 x 10^6) with greater viability than 95% were used and cultured without antibiotics in 6-well culture dishes. Two ml of unsupplemented (without serum and antibiotics) TC-100 medium were added. For each transfection, 8 μl of Cellfectin™ II, a cationic lipid formulation, were diluted in 100 μl of unsupplemented TC-100 insect medium. In a second tube, 1 ng of bacmid DNA was diluted in 100 μl of unsupplemented TC-100, mixed gently, and the diluted DNA was combined with the diluted

Cellfectin™ II. After a 30 min incubation at room temperature, the DNA-lipid mixture was added dropwise onto the cells. Cells were incubated for 4 h at 27°C, and subsequently the transfection mixture was removed and replaced with 2 ml of complete growth medium containing antibiotics. Cell viability was checked daily. After 72-96 h, clear signs of cell death, such as cell lysis and signs of clearing in the monolayer, were observed. Medium was collected from each well, and centrifuged at 500 x g for 5 min to remove cells and large debris. The clarified supernatant is the P1 viral stock, and was stored at 4 °C.

Amplification of the baculovirus stock

The viral P1 stock is a low-titer stock and was used to infect cells to generate a high-titer P2 stock. Therefore, a healthy (viability over 95%) Sf9 cell culture of low passage (5-20) was infected. The multiplicity of infection (MOI) is defined as the number of virus particles per cell. The following formula was used to calculate the amount P1 stock needed to obtain a specific MOI of 0.1. For the P1 stock, a titer of 5 x 10^6 pfu/ml was assumed.

$$\boldsymbol{Inoculum\ required\ (ml) = \frac{MOI(pfu/cell) \times\ number\ of\ cell}{titer\ of\ viral\ stock\ (pfu/ml)}}$$

About 48-72 h post infection, when 70-80% of cells were dead. The P2 viral stock was harvested as described before.

Expression of recombinant proteins in Sf9 cells

Numerous factors such as MOI and incubation time can influence the expression of proteins in Sf9 cells. To determine the optimal expression, an assay was adapted from reference (*275*). Cells were infected using MOIs from 0.5 to 10 (0.5, 1, 2, 5, 10), and harvested at different times post infection (24, 48, 72, 96 h post infection). For preparation of the time course, 6 x 10^5 cells were seeded per well in a 24-well plate, and baculoviral stock in the desired MOI was added. At the appropriate time, cells were dislodged with 1 ml of ice-cold PBS (Sigma-Aldrich), transferred to a 1.5 ml microcentrifuge tube, pelleted at 1000 x g for 5 min at 4°C, and lysed in 200 µl of urea-containing SDS sample buffer. Samples were stored at -20°C, and analysed by SDS-PAGE and immunoblotting.

Harvesting infected Sf9 cells

Infected cells were harvested on ice from a 175 cm^2 flask with a scraper. Suspended cells were pelleted at 4°C by centrifugation at 500 x g for 5 min, and washed twice with precooled PBS (Sigma-Aldrich) containing protease inhibitor cocktail. The Sf9 cell pellet was snap frozen in liquid nitrogen and stored at -80°C.

5.3.2. Protein detection by immunoblot

For all protein procedures ultrapure deionized water was used (PURELAB Ultra, Lab water purification system, ELGA, High Wycombe, United Kingdom)

Protein separation by SDS-PAGE

Protein samples were dissolved in an appropriate volume of SDS sample buffer, with or without urea, boiled for 3 min and separated by SDS-PAGE (**s**odium **d**odecyl **s**ulfate **p**oly**a**crylamide **g**el **e**lectrophoresis). Gel was casted as a separation gel (7.5%-10% acrylamide/0.2-0.27% bis-acrylamide (w/v) 375 mM Tris-HCl (pH 8.8) 0.1% SDS) and topped by a stacking gel (3.75% acrylamide/0.16% bis-acrylamide (w/v) 125 mM Tris-HCl (pH 6.8) 0.1% SDS). Polymerization of polyacrylamide was initiated by APS, and the reaction was accelerated by TEMED. In the separation gel 0.0325% (w/v) of APS and 0.5 µl/ml of TEMED and in the stacking gel 0.1% (w/v) APS and 1µl/ml of TEMED were used. Proteins were resolved at 80V in SDS running buffer (192 mM glycine, 25 mM Tris-HCl and 0.2% SDS) for 2-3 h. Prestained protein molecule weight marker (PageRuler Plus Prestained Protein Ladder) was loaded in parallel to monitor the protein separation during electrophoresis and assess blotting efficiency. The stacking gel was removed and the separation gel was either stained with Coomassie brilliant blue or used for western blotting.

staining solution	
acetic acid	10%
methanol	20%
Coomassie brilliant blue	0.05%
dH_2O	Ad 1000 ml

destaining solution	
acetic acid	10%
methanol	20%
dH_2O	Ad 1000 ml

Table 5: Composition of Coomassie brilliant blue staining- and destaining solution of SDS-PAGE gels

Protein Transfer onto PVDF membranes by semi-dry blotting

The separated proteins were transferred onto a polyvinylidene difluoride (PVDF) membrane. Therefore, a PVDF membrane (Immobilon-P, 0.45 μm) was activated in methanol for 7 min, and equilibrated in transfer buffer for 30 min. In addition, the acrylamide gel and two filter papers (Extra thick blot paper, Bio-Rad Laboratories AG, Cressier, Switzerland) were incubated in transfer buffer for 45 min. The transfer buffer with the gel was changed twice. Proteins were blotted onto the membrane by semi-dry blotting with 20 V and 0.04 A for 40 min (Trans Blot SD semi-dry Transfer Cell, Bio-Rad Laboratories AG, Cressier, Switzerland). Membrane was rinsed in Milli Q water five times to remove residual methanol and gel debris, and finally stored in PBS at 4°C.

The transfer buffer compromises out of 192 mM glycine, 25 mM Tris, 0.2% (w/v) SDS and 20% (v/v) methanol.

PBS (phosphate buffered saline) consists of 137 mM NaCl, 2.7 mM KCl, 6.5 mM Na_2HPO_4 and 1.5 mM KH_2PO_4.

Immunoblot detection of proteins

After protein transfer, blotting membrane was placed in blocking buffer and incubated for 1 h with gentle agitation, followed by 1 h of incubation with the primary antibody dilution. Next, the blot was washed four times for 5 min with PBST (phosphate buffered saline - tween), and incubated with POD-conjugated secondary antibody dilution for 30 min. The antibody solution was removed, and the membrane was washed 6x5 min each with PBST, followed by several washing step with PBS to remove residual detergents. Visualisation of bound antibody was performed with the chemiluminescence by ECL Wester Blotting detection reagent. Emitted light was visualized by X-ray films were exposed to the membrane. Subsequently, films were developed (Tetenal, Roentoroll HC) and fixed (Tetenal Superfix MRP).

5.3.2.1. Antibodies

The following **primary antibodies** were used for immunoblot and immunohistology detection or ELISA:

anti-GRK2 antibody is a goat polyclonal antibody raised against a peptide mapping near the C-terminus of human GRK2 (sc-18409, Santa Cruz Biotechnology, LabForce AG, Muttenz, Switzerland); anti-GRK5 antibodies, raised in rabbit against recombinant GRK5 protein (*220*); anti-Pparg antibody, raised in rabbit against an antigen encompassing amino acids 8 –106 of PPARG (Santa Cruz Biotechnology Inc.) or synthetic phosphopeptides derived from PPARG around the phosphorylation site of Ser-273 or Ser-112 (BIOSS antibodies; Abcam), polyclonal pS153 RKIP antibody raised in rabbit against a short amino acid sequence containing Ser 153 phosphorylated RKIP (sc-32623, Santa Cruz Biotechnology, LabForce AG, Muttenz, Switzerland); anti-SRSF1 antibody is a mouse monoclonal antibody, the epitope is mapping near the N-terminus of the SF2/ASF protein (sc-33652, Santa Cruz Biotechnology, LabForce AG, Muttenz, Switzerland), anti Gnb antibody is a monoclonal mouse antibody raised against an epitope mapping between amino acids 302-340 at the C-terminus of Gβ of mouse origin (sc-166123, Santa Cruz Biotechnology, LabForce AG, Muttenz, Switzerland), anti His-probe antibody is a monoclonal mouse antibody raised against a His-tagged recombinant protein (sc-8036, Santa Cruz Biotechnology, LabForce AG, Muttenz, Switzerland)

The following **secondary antibodies** were used for immunoblot and immunohistology detection or ELISA:

Peroxidase-conjugated AffiniPure F(ab')2 Fragment Goat-Anti-Rabbit (111-036-046) / goat anti-mouse (115-036-071) IgG, Fc Fragment Specific (Jackson ImmunoResearch Laboratories), peroxidase-conjugated Protein A (Merck, Millipore)

5.4. Protein purification of 6xHis-tagged proteins

A Ni-NTA purification system (QIAGEN) was used to purify 6xHis-tagged recombinant proteins expressed in bacteria and insect cells. The following general protocol was adapted and optimized for each protein.

Frozen bacterial or insect cell pellets were thawed on ice and resuspended in 10-20 ml of lysis buffer. Sonication was used to break cell walls and reduce viscosity by fragmentation of DNA (HD2200 set to 5-10 x 3 s with 30% cycle and 70% power; UW2200; MS73; BANDELIN electronic GmbH & Co.KG). Cellular debris was pelleted by centrifugation at 4500 x g for 45 min at 4°C. Meanwhile 500µl - 2000µl of 50% Ni-NTA slurry was equilibrated with 20 column volumes of lysis buffer. The cytosolic cell extract was added to the column and incubated for 1h at 4°C with gentle agitation to

keep the resin suspended. Unbound proteins were removed by washing with 40 column volumes of wash buffer, and subsequently proteins were eluted with 10 ml of elution buffer and collected in 1 ml fractions. Aliquots of every purification step were taken and analysed by SDS-PAGE.

Proteins were purified under native or denaturing conditions depending on protein location and solubility, downstream application and whether biological activity has to be retained.

	Lysis Buffer	**Wash Buffer**	**Elution Buffer**
NaCl	300 mM	300 mM	300 mM
Hepes	50 mM (pH 8)	50 mM (pH 8)	50 mM (pH 3)
Urea	8 M	8 M	8M
β-mercaptoethanol	10 mM	10 mM	10 mM
Imidazole	10 mM	50 mM	

Table 6: Buffer composition for purification of 6xHis-tagged proteins under denaturing conditions

	Lysis Buffer	**Wash Buffer**	**Elution Buffer**
NaCl	300 mM	300 mM	300 mM
Hepes	50 mM	50 mM	50 mM
IGEPAL	1 %		
PMSF	1 mM	1 mM	1 mM
Protease inhibitor cocktail	1:100	1:100	1:100
β-mercaptoethanol	10 mM	10 mM	
Imidazole		40 mM	300 mM

Table 7: Buffer composition for purification of 6xHis-tagged proteins under native conditions

5.4.1. Buffer exchange

Desalting columns (PD-10)

PD-10 desalting columns containing Sephadex G-25 resin were used for desalting and buffer exchange. Buffer exchange was performed according to the manufacturer's instruction (GE Healthcare). All procedures were performed at 4°C.

Desalting and concentrating of proteins

Amicon® Ultra-15 Centrifugal Filter Units with a cutoff of 10 kDa were used for further buffer exchange and concentration of the desired protein according to the manufacturer's protocol (Merck).

Solid phase renaturation

Sudden removal of denaturants can lead to precipitation of proteins. Solid-phase renaturation was used to avoid protein precipitation by sudden removal of denaturing agents. A series of washes removed step by step the denaturing agents before the target protein was eluted. To this end, the target protein was loaded onto the column and refolded by decreasing concentrations of urea (8, 6, 4, 2, 1; ten column volumes each). Thereafter, a final washing step with 20 column volumes without urea was performed. The target protein was eluted with 15 ml of elution buffer (pH 3). All procedures were performed at 4°C.

5.4.2. Protein quantifications

The protein concentration was measured by a Bradford assay (*276*) using Roti®-Qunat reagent. The method was performed in semi-micro cuvettes (Ratiolab GmbH, Dreieich, Germany) according to the manufacturer's instructions and the absorbance was measured at 595 nm in a Biophotometer.

5.5. ELISA technique

A 96-well plate (F8 Maxisorp Nunc-Immuno Module, Thermo Fisher Scientific AG) was coated with protein (in 100 mM $NaHCO_3$) overnight at 4°C. The plate was blocked for 1 h with blocking buffer (0.2% non fat dry milk in TBST (with 0.05% Tween 20) under gentle continuous agitation at room temperature. The blocking buffer was replaced with interaction partner in blocking buffer and incubated for 1 h. After washing with TBST 0.05%, the primary antibody was added in blocking buffer. Unbound antibody was removed by washing steps with TBST followed by the POD-conjugated secondary antibody. After the final washing steps, detection of bound antibody was performed with freshly prepared ABTS solution (36 µl of 30% H_2O_2 added to 21 ml of ABTS stock solution (22 mg ABTS in 100 ml of 50 mM sodium citrate solution, pH 4.0)). The reaction was allowed to proceed for 30 min and the absorbance was measured at 410 nm (VersaMax ELISA Microplate Reader, Molecular Devices). The data were evaluated with SoftMax Pro 5.4.5 software.

TBST: 150 mM NaCl, 50 mM Tris pH 7.5 supplemented with 0.05% (v/v) Tween 20.

5.6. In vitro phosphorylation assay

To identify new substrates of GRK2, an in vitro kinase assay was performed.

Phosphorylation reaction

The in vitro phosphorylation assay was performed using purified substrates, purified kinase from Sf9 cells and ^{32}P-labeled γ-ATP. The reaction was carried out in 50 µl of Tris reaction buffer (comprised of 20 mM Tris (pH7.5), 5 mM $MgCl_2$, and 2 mM EDTA) or Hepes reaction buffer (comprised of 20 mM Hepes (pH 7), 2 mM $MgCl_2$ and 0.025% DDM). GRK2 substrates were purified from bacterial culture. The in vitro phosphorylation was performed with 50 nM-120 nM of GRK and 300 nM - 1000 nM of substrate. The mixture was incubated for 30 min on ice, and the phosphorylation reaction was started by the addition of ATP (1-50µM) and [32] γ-ATP (10 µCi/ml, $1x10^6$ DPM) The reaction was allowed to proceed for 30 min at 30°C. The reaction was stopped by the addition of 20 µl of Bolt 4x LDS sample buffer and 8 µl of sample reducing agent. Next, samples were heated at 70°C for 10 min and separated on a 10% Bolt Bis-Tris Plus gel at 200V for 21 min in MOPS SDS running buffer.

Detection of protein phosphorylation by autoradiography

Protein phosphorylation was determined by autoradiography with a high sensitivity X-ray Hyperfilm (exposure time 4-16 h at -80°C). The film was developed as described before. The image was scanned and quantified using Image J software. Data were analysed via GraphPad Prism 6 and the inhibition curve was fitted with a three-variable dose-inhibitor response curve and a fixed Hill slope of 1.

5.7. Generation of transgenic mice

All animal experiments were performed in accordance with National Institute of Health guidelines and approved by the local committee on animal care and use (University of Zurich). All mice were kept on a 12h light/12 h dark regime and had free access to food and water.

Transgenic mice were generated according to an established protocol (*277*) with modifications. For the successful generation of transgenic mice, an exact time schedule is important and involves five basic steps: At first, the transgenic construct was designed, cloned and linearized. Male CD1 mice were vasectomized in order to engender pseudopregnacy in female foster mice in step 4. In the second step donor zygotes were harvested after hormone treatment and mating according to the schedule outlined in Table 8. The third step consists of the microinjectition of the transgenic construct and is followed by the implantation of microinjected zygotes into pseudo-pregnant recipient mice (step 4). About 21 days after implantation, pups were born. Finally, genotyping was performed and founder mice identified (step5).

	Day1	Day 2	Day 3		Day 4	Day 5
Donor F	10 U PMSG at 14:00		10 U hCG at 13:00	mating at 21:00	Collecting zygotes at 9:00	
Donor M						
Foster F CD1		Housing of 2x CD1 F with CD1 M vasect. Separated by a barrier			Mating at 21:00	Implantation of zygotes into pseudopregnant foster mice
Vasectomized CD1						

Table 8: Timeline of hormone application and matings required for the generation of donor zygotes

F: female mouse, M: male mouse

pcDNA3.1

pcDNA3.1 (Invitrogen) is designed for high-level stable and transient expression in mammalian cells. Expression of the gene of interest is under control of a human cytomegalovirus promoter (Figure 10) (*278, 279*).

CMV promoter: bases 209-863
T7 promoter: bases 864-882
Polylinker: bases 889-994
Sp6 promoter: bases 999-1016
BGH poly A: bases 1018-1249
SV40 promoter: bases 1790-2115
SV40 origin of replication: bases 1984-2069
Neomycin ORF: bases 2151-2945
SV40 poly A: bases 3000-3372
ColE1 origin: bases 3632-4305
Ampicillin ORF: bases 4450-5310

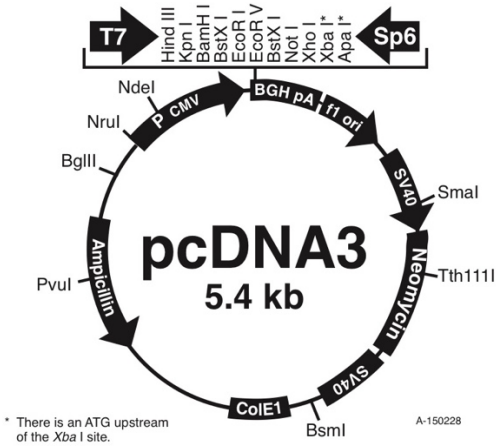

Figure 10: Vector map of pcDNA3

The vector map of pcDNA3 (Invitrogen) shows the CMV promoter followed by a multiple cloning site.

DNA preparation for pronuclear injection

For the successful generation of transgenic mice, DNA was linearized and the plasmid backbone was removed. For the endotoxin-free plasmid DNA preparation, the EndoFree Plasmid Maxi Kit was used according to the manufacturer's protocol. Plasmid sequence was removed by DraIII and MluI digestion, and DNA was purified by agarose gel electrophoresis. Linearized DNA was quantified by agarose gel electrophoresis with the commercial DNA ladder as reference and diluted to a concentration of 2 ng/µl in injection buffer (8 mM Tris-HCl pH7.4 (diluted from a 1M Trizma® hydrochloride solution, Sigma-Aldrich), 0.15 mM EDTA (diluted from a 0.5M EDTA solution, Sigma-Aldrich).

Mouse vasectomy

Male CD1 mice were anesthetized by intraperitoneal injection of ketamine/xylazine. Mice were laid in their back, abdomen side up, and the lower half of the abdomen was sterilized with ethanol (80%). A 1 cm incision was made and one side of the reproductive tract was pulled out. The vas deferens was identified and cauterized. The reproductive tract was returned back inside the body. The procedure was repeated with the other side of the reproductive tract. The body wall was sewed up and the remaining skin was clipped together.

Zygote collection

In order to produce zygotes for pronuclear injection, 10 female FVB mice underwent hormone treatment. At day one, female mice were injected i.p. with 10 IU pregnant mare serum gonatropin. On day 3 ovulation was induced by an i.p. injection by 10 IU human chorionic gonadotropin. After hCG injection, female and male mice were mated overnight (Table 8).

On day 4, fertilized oocytes were isolated. Briefly, plugged superovulated mice were killed by cervical dislocation, abdomen was opened, intestines were pushed aside and the uterine horn was identified. Fat was removed from the ovary and the uterus was cut near the oviduct. Ovary and oviduct were transferred to a 5 ml culture dish containing M2 medium supplemented with antibiotics (Penicillin–Streptomycin Solution Hybri-Max™, final concentration 50 IU penicillin and 50μg/ml streptomycin). The procedure was repeated with the other side of the uterine horn.

Under a stereo-microscope, the oviduct was separated from the ovary and transferred to dish containing hyaluronidase solution (final concentration: 0.3 mg/ml in M2 containing antibiotics). The most swollen part of the oviduct was cut open and zygotes were gently squeezed out, if they did not flow out by themselves. Zygotes were separated from the surrounding cluster of follicular transfer cells, using a mouth-controlled pipet assembly. Zygotes were transferred into a microdrop of 50 μl of M2 medium overlaid with mineral oil. Zygotes were cleaned from cell debris and all cumulus cells by transferring them from drop to drop and finally stored in drops of M16 medium overlaid with mineral oil at 37°C in a 5% CO_2 incubator.

Pronuclear Injection of DNA

The microinjection platform was prepared by putting two 50μl microdrops of M2 medium in the lid of a sterile 6 well plate (Costar, Corning Life Sciences, Tewksbury, USA). 20-25 zygotes were transferred to the M2 medium and the microinjection platform was carefully placed on the microscope stage.

The holding capillary (VacuTip; 5175108.000; Eppendorf) was filled up to 2 thirds with M2 medium using a microloader (5242956.003; Eppendorf) and placed into the connector piece of an oil-filled

manual microinjector. The injection capillary was filled with DNA solution and mounted to the micromanipulator and connected to the microinjector (FemtoJet; 5247000.013; Eppendorf).

The holding capillary was used to stabilize and hold the zygote. The pronucleus was penetrated with the injection capillary (BioMedical Instruments, Zöllnitz, Germany) and DNA was injected. Microinjected zygotes were maintained in M16 medium at 37°C and 5% CO_2 overnight until implantation.

Embryo-implantation in pseudopregnant foster mice

To obtain pseudopregnant female foster mice, two CD1 females were mated with one vasectomized male the day before implantation. In the morning of day 5, CD1 mice with a vaginal plug were identified and used for embryo implantation.

Pseudopregnant mice were anesthetized and were shaved on the side of the implantation. A 1 cm cut was made on the back, the fat pad attached to the ovary was pulled out and the fat pad was fixed with a vessel clip. The bursa was teared and the infundibulum was exposed. A reimplantation capillary (BioMedical Instruments) was loaded with 20 zygotes at the two-cell stage and the capillary was inserted into the infundibulum under a stereo-microscope. Zygotes were slowly blown into the oviduct. Ovary and fat pad were pushed back in the abdomen, musculature was sewed up and the skin was closed by wound clips.

5.8. Genotyping

Preparation of genomic DNA from mouse biopsies

Genomic DNA was extracted from ear-punch biopsies of 3-week-old mice by hot digestion. Briefly, biopsies were incubated overnight at 57°C on a shaking platform (1000 rpm) in 210 µl of lysis buffer supplemented with 10 µl of a 20 mg/ml proteinase K solution. The reaction was stopped and proteinase K was inactivated by boiling the sample for 30 min at 99°C. The supernatant was used as a template for the genotyping PCR.

tail lysis buffer	
10% sodium lauroyl sarcosinate	2.5 ml
5 M NaCl	1 ml
Chelex – 100	2.5 g
dH_2O	ad 50 ml

Table 9: Composition of the tail lysis buffer for DNA extraction from mouse biopsies

Genotyping PCR

Genotyping PCR was performed using *Taq* Polymerase in the supplied buffer supplemented with 250 μM $MgCl_2$ and 100 μM dNTPs. A primer specific for the CMV promoter of pcDNA3 (CMV2) and one primer specific for the GRK5 transgene (GRK532) were used at 0.625 μM. Amplification was performed in a reaction volume of 50 μl with 1 μl of genomic mouse DNA lysate with a standard program as detailed in Table 10:

Step	Temperature	Time	Cycles
1	95°C	2 min	1X
2	95°C	45 s	40X
3	60°C	60 s	
4	72°C	60 s	
5	72°C	10 min	1X

Table 10: Genotyping PCR program

Initial melting of the dsDNA (step 1) was followed by 25-30 cycles consisting each of melting of dsDNA (step 2) followed by annealing (step 3) and extension (step 4) of primers. PCR was finished with a final extension step (step 5).

5.9. Phenotyping of transgenic mice

5.9.1. Detection of the transgenic protein by immunoblotting

Increased protein levels indicative of increased expression of the transgene were determined by the western bolt technique as described in 5.3.2.

Protein extraction

Frozen tissue was grinded in liquid nitrogen using a mortar and pestle and the homogenized powder was lysed in 500 µl - 750 µl of extraction buffer on ice under continuous gentle agitation for 30 min. Cell debris was removed by centrifugation at 16 000 x g at 4°C for 10 min. Supernatant was transferred to a new 2 ml microcentrifuge tube and proteins were precipitated by adding 1 ml of acetone. After the 30 - 60min incubation at 4°C, precipitated proteins were pelleted, the supernatant was discarded and the pellet was dissolved in 300 µl sample buffer containing urea.

Extraction buffer	
Tris pH7.4	10 mM
Sodium desoxycholate	1%
SDS	0.1 %
EDTA	5 mM
β-glycerophosphate disodium	1 mM
NaF	20 mM
Sodium orthovanadate	1 mM
Sodium molybdate	1 mM
PMSF	1 mM
Protease inhibitor cocktail	1:100

Table 11: Composition of the extraction buffer

5.9.2. Preparation of tissue sections

Formalin-fixed paraffin embedded (FFPE) tissue

The deeply anesthetized mouse was perfused with ice-cold PBS (Sigma-Aldrich) in order to remove the blood from of the vasculature. Tissue was removed quickly and fixed by immersing in 10% neutral buffered formalin (100 x tissue volume) for at least 48 h at room temperature. After fixation, tissue was washed in water and afterwards, tissue samples underwent dehydration and paraffin infiltration using a tissue processing system (Leica ASP200). Samples were embedded in paraffin using the tissue embedding station Leica EG1160. The paraffin tissue block was cut into 10 μm thick sections with a microtome (Leica RM2265). Sections were transferred to a 37°C water bath. Floating tissue sections were transferred to a clean histological slide and dried overnight in an incubator at 37°C.

Dewaxing

For dewaxing and rehydration, tissue sections were heated to 60°C, followed by washing twice with xylene for dewaxing and rehydration through a graded series of ethanol and water composed of 100%, 95%, 90%, 80%, 70% of ethanol and water. Each step consisted of two 5 min incubation steps.

5.9.3. Hematoxylin and eosin staining

For the hematoxylin and eosin staining of nuclei and cytosol, dewaxed and rehydrated tissue sections were incubated in filtered Mayer's hemalum solution for 4 min and subsequently washed five times in hydrochloric acid 0,1%. Blueing was allowed to proceed for 5 min under running tap water. In the second step, cytoplasm was stained with aqueous Eosin Y solution (0,5%) and followed by a final washing step.

5.9.4. Immunohistology

For immunohistology, dewaxed and rehydrated tissue sections were incubated in antigen retrieval buffer (0,1 M citrate buffer pH 6 0,1%, (v/v) Triton X-100) for 30 min under continuous heat supply in a microwave oven. Sections were washed with PBS twice and then incubated in a 3% (v/v) hydrogen peroxide solution for 5 min in order to block endogenous peroxidase activity. Hydrogen peroxide was

washed away with water. Tissue sections were blocked with blocking solution (3% (w/v) BSA in PBST (0.05 % (v/v) tween-20 in PBS)) for 1 h at 37°C, and then incubated with the primary antibody for 1 h at 37°C. Unbound antibody was removed by washing three times with PBST. Sections were incubated with the secondary POD-conjugated antibody for 1 h at 37°C. Antibody was removed, washed in PBST and followed by a final washing step with PBS. For visualisation DAB (3,3'-diaminobenzidine tetrahydrochloride) enhanced liquid substrate system was used according to manufacturer's instructions. The reaction was stopped with water and sections were coverslipped using Poly-Mount Xylene.

5.9.5. Heart-weight to body-weight ratio determination

Mice were weighted, anaesthetised and chest cavity was opened quickly. Whole body perfusion was performed with ice cold PBS. Heart was removed, cleaned from connective tissue, blotted dry, weighted, and the body weight/heart weight ratio was calculated.

5.9.6. Plasma glucose measurement

Blood samples were withdrawn from the tail vein, and plasma glucose levels were measured by a Healthpro–X1 Glucometer (Axapharm AG, Baar, Switzerland)

5.9.7. Ejection fraction measurement by echocardiography

For transthoracic echocardiography, a Vivid 7 echocardiograph (GE Healthcare) with a 12 MHz linear array transducer was used. The left ventricular ejection fraction was calculated in the M-mode of the parasternal long axis view using the formula of Teichholz. Recordings were analysed off line using EchoPac Pc 3.0 software (GE Healthcare)

5.9.1. Determination of cellular cAMP level

Cellular cAMP levels were determined in neonatal cardiomyocytes isolated from Tg-RKIP, Tg-GRK2-K220R and B6 mice. Isolation of neonatal cardiomyocytes was performed at described before (*241*).

Isolated myocytes were washed with Hepes buffer (138 mM NaCl, 1 mM $CaCl_2$, 1 mM $MgCl_2$, 5 mM KCl, 20 mM Na-HEPES, pH 7.3) and incubated in the same buffer for 5 min at 37°C with 0.2 mM isobutyl methyl xanthine. Cardiomyocytes were stimulated with 100 nM of isoproterenol for 20 min at 37°C. The reaction was stopped by the addition of boiling water, the cellular cAMP was determined by a radioimmunoassay (Immunotech).

5.9.2. Cardiac lipid extraction

Total cardiac lipids were extraction by the method of Folch et al. (*280*). Frozen tissue of three hearts was grinded in liquid nitrogen using a mortar and pestle, and lipids were extracted from the homogenized powder with 10 ml of a chloroform/methanol (2:1) mixture for 10 min. The supernatant was collected after centrifugation at 620 g and the extraction step was repeated once with 10 ml chloroform/methanol (2:1) mixture followed by extraction with an acidified 10 ml of chloroform/methanol (2:1) mixture. Solvents of the combined supernatants were evaporated and the lipid extract was resolved in 4 ml of chloroform/methanol (2:1) mixture. Hydrophilic contaminants were extracted with 800 µl of 50 mM $CaCl_2$ and the lipid phase was stored for further analysis. Myocardial triacylglyceride (TAG) content was quantified using an enzymatic spectrophotometric kit according to the manufacturer`s instructions (Sigma). Cardiac contents of diacylglycerol (DAG) and ceramides were determined with the DAG kinase assay method as described (*281*).

5.9.3. Analysis of fatty acid methyl esters (FAME) by gas chromatography

Lipids were extracted from heart tissue as described in 5.9.2 and further analysed using gas chromatography. Gas chromatography was performed by Dr. Joshua Abd Alla. Briefly, the cardiac lipid extract of three mice was used for the formation of fatty acid methyl esters by transesterification and subsequently were separated on a Carbowax column. Helium was used as the carrier gas and detected by a flame ionization detector. A standard lipid mixture was used for calibration.

5.9.4. Microarray gene expression profiling

In order to stabilize the RNA, the whole animal was perfused with RNA*later* RNA stabilization Reagent, tissue was removed quickly and stored in RNA*later* RNA stabilization Reagent at -80°C. Total RNA was extracted using the RNeasy Midi kit. cDNA synthesis, labelling, and hybridization onto the Affymetrix Array Chip (Affymetrix GeneChip® Mouse genome MG430 2.0 Array) were carried out according to manufacturer's instructions.

5.9.5. Abdominal aortic constriction

Abdominal aortic constriction was performed in the Molecular Pharmacology Unit, ETH Zurich. Switzerland by Dr. Said Abd Alla as described (*282, 283*).

5.10. Statistical analysis

Experimental data were analysed using GraphPad Prism 6. If not stated otherwise, groups were analysed using a two-tailed student's t-test and p-values < 0.05 were considered as significant. Analysis of variances was performed between more than two groups followed by a post test. Data are shown as means $\pm$ S.D..

6. RESULTS

6.1. In vitro inhibition of GRK2 by RKIP compared to the ATP-site-directed inhibitor paroxetine

Inhibition of GRK2 is an emerging approach for the treatment of heart failure. There are different GRK2 inhibitors in preclinical and clinical development. The ATP-site directed GRK2 inhibitor, paroxetine, and the Raf kinase inhibitor protein (RKIP), which targets the receptor-GRK2 interaction, were selected for in vitro studies. My study focused on the analysis of non-receptor substrates of GRK2 because the function of non-receptor substrates of GRK2 are still under investigation, while the GPCR-phosphorylating activity of GRK2 is well established.

In order to compare substrate specificities of the GRK2 inhibitors, RKIP and paroxetine, an in vitro kinase assay was established. The test system used recombinant GRK2 purified from Sf9 (Spodoptera frugiperda) cells, which were infected with a recombinant GRK2-encoding baculovirus. As GRK2 substrates, I used the two non-receptor GRK2 substrates phosducin and SRSF1 (serine/arginine-rich splicing factor 1). The two non-receptor GRK2 substrates and the GRK2 inhibitor RKIP were expressed in and purified from E. coli BL21-DE3 bacteria with T7 RNA polymerase-directed expression of recombinant proteins applying the pET expression system.

6.1.1. Expression and purification of GRK2-substrates, SRSF1 and phosducin, and GRK2 inhibitor, RKIP

The N-terminally His-tagged phosducin, SRSF1 and the GRK2 inhibitor RKIP were cloned into the pET3d plasmid, which was used for the expression in *E.coli* BL21(DE3) pLysS. All purification steps were performed under denaturating conditions.

6.1.1.1. Phosducin

Expression of phosducin

The plasmid coding for N-terminally His-tagged PDC (pET3d6xHisPDC; U.Quitterer) was transformed into BL21(DE3) pLysS competent cells. Phosducin protein expression was induced with 1 mM IPTG and a time course analysis of protein induction was performed. Bacteria transformed with the pET3d plasmid without insert served as a negative control. Samples before and 1, 2 and 3 hours

after IPTG-induction were separated by SDS-PAGE. A clear additional band of 33 kDa was visible in the PDC samples, but was absent in the control samples. The molecular mass of approximately 33 kDa corresponds to the published size of PDC. Maximal expression of PDC was achieved 3 h after induction with IPTG.

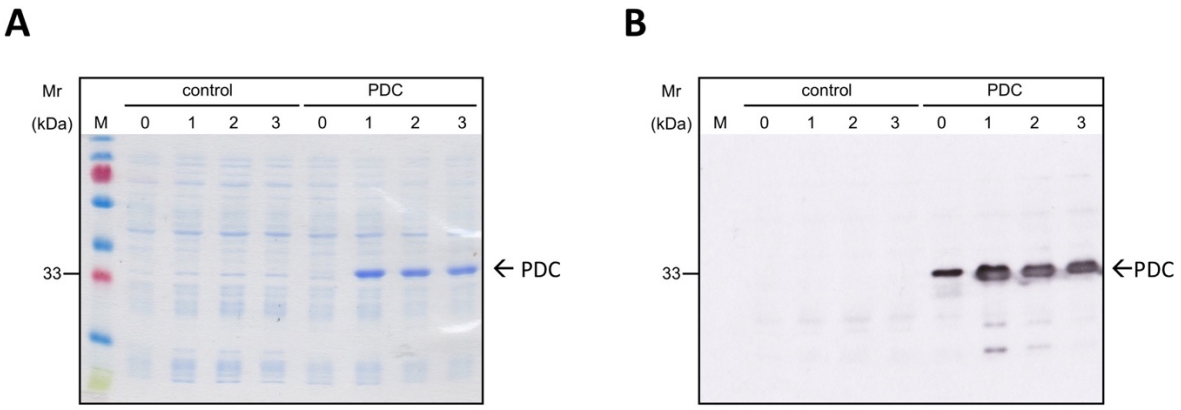

Figure 11: Protein expression of PDC

Samples taken before (0) and 1, 2, and 3 h after IPTG-induced protein expression were separated by SDS-PAGE followed by Coomassie brilliant blue staining (A). PDC expression was detected by immunoblotting with a monoclonal His-specific antibody (B).

Purification and buffer exchange of phosducin

Phosducin was purified under denaturing conditions by Ni-NTA chromatography and buffer exchange was performed by gel filtration over PD-10 column followed by centrifugation over Amicon® Ultra centrifugal filter device in order to remove urea. Briefly, bacteria of a 200 ml culture were harvested by centrifugation 3 h after IPTG induction. The resulting pellet was resuspended in lysis buffer containing 8 M urea and the suspension was incubated for 30 min at room temperature. Viscosity was reduced by sonication and the suspension was centrifuged. The clarified supernatant was incubated with 1 ml Ni-NTA agarose equilibrated resin for 1 h at 4°C. Unbound proteins were removed by washing with 40 ml of wash buffer containing 40 mM imidazole. His-tagged phosducin was eluted with 10 ml elution buffer pH 3 and collected in 1 ml aliquots.

The protein concentration of each elution sample was measured, and samples with the highest concentration were pooled to a final volume of 2.5 ml. All subsequent procedures were performed at 4°C in the cold-room. The PD-10 column was equilibrated with precooled storage buffer (300 mM NaCl, 50 mM Hepes (pH 8) and 10% glycerol) without urea. Pooled samples were added to column and eluted in 1 ml aliquots.

Five samples with the highest protein concentration were pooled and adjusted up to a volume of 15 ml with precooled storage buffer. The sample was loaded on the Amicon® Ultra centrifugal filter device with a cut off of 10 kDa. The Amicon® Ultra centrifugal filter device was spun at 4000 x g at 4°C for 45 min. To the remaining 200 µl, 14.8 ml of buffer consisting of 300 mM NaCl, 50 mM Hepes (pH 8) and 10% glycerol) were added and centrifugation was repeated for 30 min. The purified phosducin was stored in 20 µl aliquots at -80°C.

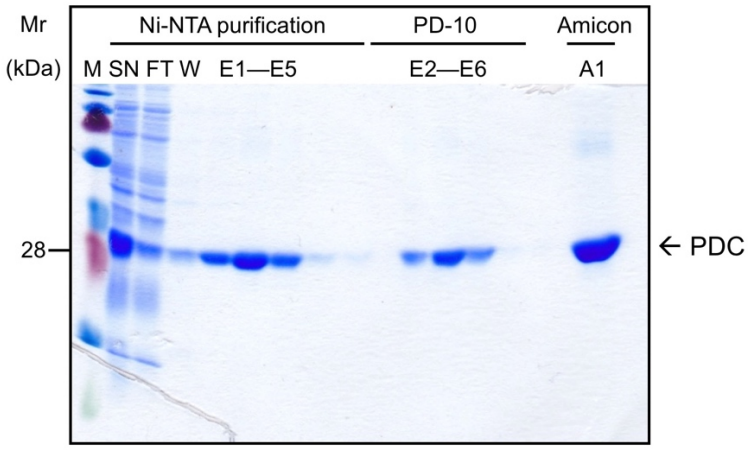

Figure 12: Phosducin purification by Ni-NTA affinity chromatography and subsequent buffer exchange

The image shows a Coomassie stained SDS-Gel. Aliquots from the supernatant (S), flow-through (FT), wash (W) and elution fractions (E1-E5) from the Ni-NTA purification, elution fractions (E2-E6) from the PD-10 and the concentrated eluate from the Amicon® Ultra centrifugal filter device (A1).

6.1.1.2. SRSF1

Expression of SRSF1

The expression of the non-receptor GRK2 substrate was also performed in E.coli BL21 with the pET3d expression plasmid. The plasmid coding for N-terminally His-tagged SRSF1 (pET3d6xHisSRSF1; U.Quitterer) was transformed into BL21(DE3) pLysS competent cells. SRSF1 expression was induced with 1 mM IPTG and a time course analysis of protein induction was performed. Bacteria transformed with pET3d without insert served as a negative control. Samples before and 1, 2, 3 and 4 hours after IPTG-induction were separated by SDS-PAGE. A clear additional

band of 28 kDa was visible in the SRSF1 samples, but was absent in the control samples. Maximal expression of SRSF1 was achieved 4 h after induction.

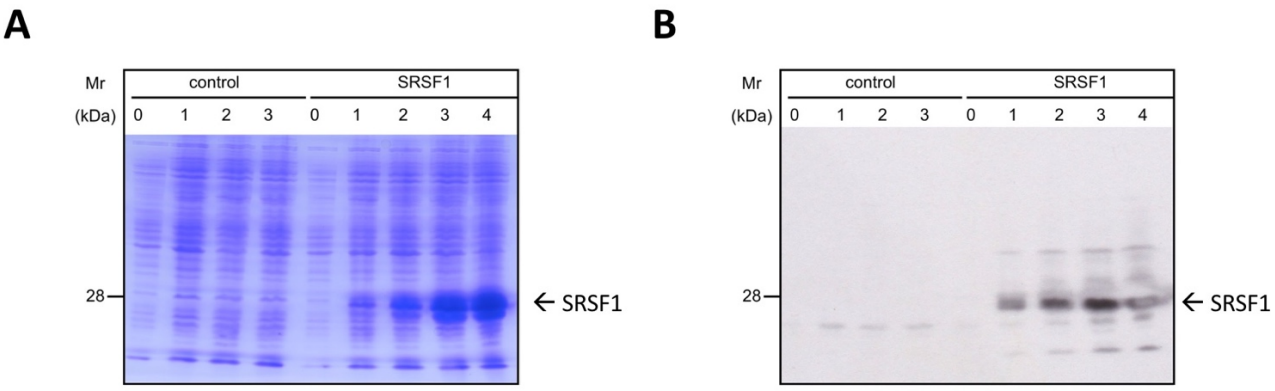

Figure 13: Protein expression of SRSF1

Samples taken before (0) and 1, 2, 3 and 4 h after IPTG-induction were separated by SDS-PAGE followed by Coomassie brilliant blue staining (A). SRSF1 expression was detected by immunoblotting with a polyclonal SRSF1-specific antibody (B).

Purification and solid phase renaturation of SRSF1

SRSF1 was purified under denaturing conditions by Ni-NTA affinity chromatography, followed by solid phase renaturation. A typical protein purification used 200 ml of bacterial culture which were pelleted 4h after IPTG induction and resuspended in lysis buffer containing 8 M urea and 10 % glycerol. The suspension was incubated for 30 min at room temperature, viscosity was reduced by sonication and the suspension was centrifuged. The clarified supernatant was incubated with 1 ml of equilibrated resin for 1 h. All the following steps were performed at 4°C. The SRSF1 protein was refolded by washing with 10 ml of each urea dilution (300 mM NaCl, 50 mM Hepes (pH8), 40 mM imidazole, 10% glycerol and 8, 6, 4, 2 or 1 M urea) and a final wash with 20 ml washing buffer without urea (300 mM NaCl, 50 mM Hepes (pH 8), 40 mM imidazole, 10% glycerol). His-tagged SRSF1 was eluted with 15 ml elution buffer (300 mM NaCl, 50 mM Hepes (pH 3) and 10% glycerol). The pH was adjusted to pH 8 by NaOH.

15 ml of the elution were loaded on the Amicon® Ultra centrifugal filter device with a cut off of 10 kDa. The Amicon® Ultra centrifugal filter device was spun at 4000 x g at 4°C for 45 min. To the remaining

200 µl, 14.8 ml buffer were added and centrifugation was repeated for 30 min. The purified SRSF1 protein was stored in 20 µl aliquots at -80°C.

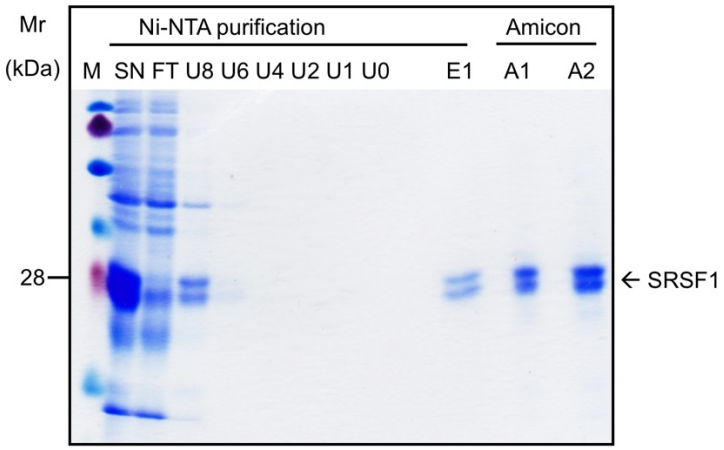

Figure 14: SRSF1 purification by Ni-NTA affinity chromatography and subsequent buffer exchange

Aliquots from the supernatant (S), flow-through (FT), renaturation buffers (8 M urea = U8 - 0 M urea = U0) and elution (E1) from Ni-NTA purification. Elute E1 from the Ni-NTA was concentrated by an Amicon® Ultra centrifugal filter device in 2 steps (A1 and A2).

6.1.1.3. RKIP

Expression of RKIP

RKIP was also expressed in bacteria with the pET expression system. BL21(DE3) pLysS competent cells were transformed with the plasmid coding for N-terminally His-tagged RKIP (pET3d6xHisRKIP; U.Quitterer). RKIP expression was induced with 1 mM IPTG and a time course analysis of protein induction was performed. Samples before and 1, 2, and 3 h after IPTG-induction were separated by SDS-PAGE. Coomassie brilliant blue staining showed that an additional band of 22 kDa was visible in the RKIP samples. Maximal expression of RKIP was achieved 3 h after IPTG induction.

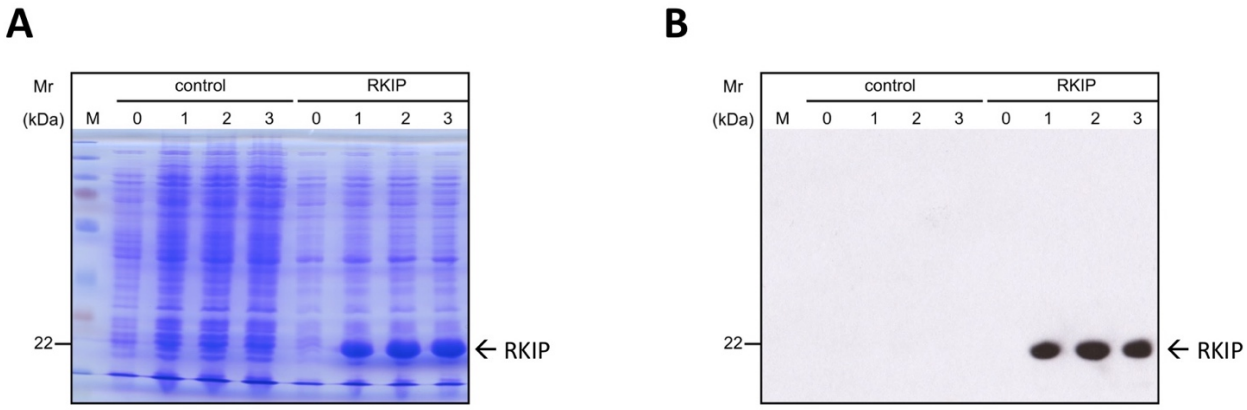

Figure 15: Protein expression of RKIP

Samples taken before (0) and 1, 2, and 3 h after IPTG-induction were separated by SDS-PAGE followed by Coomassie brilliant blue staining (A). RKIP expression was detected by immunoblotting with a polyclonal RKIP-specific antibody (B).

Purification and buffer exchange of RKIP

Ni-NTA chromatography was used for the purification of RKIP and a PD-10 column was used for subsequent buffer exchange. The final protein concentration of RKIP was done by an Amicon® Ultra centrifugal filter device. *E. coli* BL21(DE3) pLysS bacteria of a 200 ml culture were pelleted by centrifugation 4 h after induction. The resulting pellet was lysed in lysis buffer containing 8 M urea and the suspension was incubated for 30 min at room temperature. Viscosity was reduced by sonication and the suspension was centrifuged. The clarified supernatant was incubated with 1 ml of equilibrated resin for 1 h. Unbound proteins were removed by washing with 40 ml of wash buffer containing 40 mM imidazole. His-tagged RKIP was eluted with 10 ml of elution buffer, pH 3, and collected in 1 ml aliquots.

Samples with the highest protein concentration were pooled to a final volume of 2.5 ml. All subsequent procedures were performed at 4°C. Pooled samples were loaded onto the PD-10 column, equilibrated with precooled phosphorylation assay buffer (20 mM Tris, 5 mM $MgCl_2$, 2 mM EDTA, pH 7.5), and eluted in 1 ml aliquots.

Five samples with the highest protein concentration were pooled and adjusted to a volume of 15 ml with precooled phosphorylation assay buffer and loaded on the Amicon® Ultra centrifugal filter device

with a cut off of 10 kDa. The Amicon® Ultra centrifugal filter device was spun at 4000 x g at 4°C for 45 min, assay buffer was added and centrifuged again. RKIP solutions with a protein concentration of at least 1 mg/ml in assay buffer were stored at 4 °C.

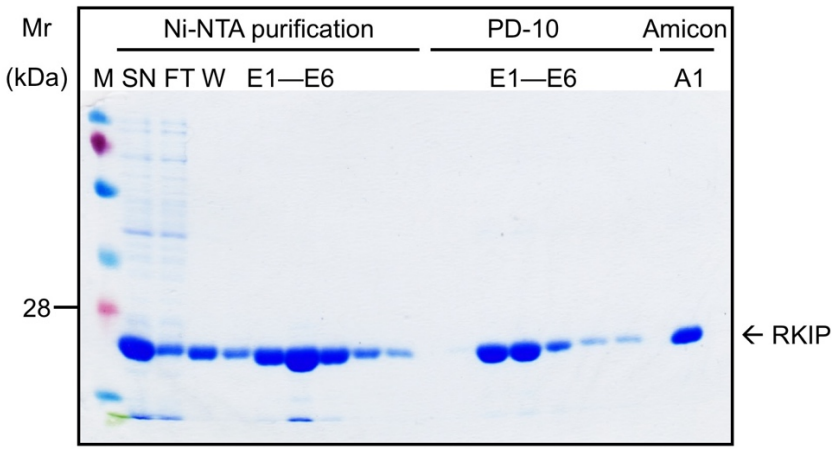

Figure 16: RKIP purification by Ni-NTA chromatography and subsequent buffer exchange

Aliquots from the supernatant (S), flow-through (FT), wash (W) and elution fractions (E1-E6) from the Ni-NTA purification, elution fractions (E1-E6) from PD-10 columns, and the concentrated elution from the Amicon® Ultra centrifugal filter device (A1) were separated by SDS-PAGE followed by Coomassie staining.

6.1.2. Expression of GRK2 in SF9 cells

Generation of pFastBac6xHisTEVGRK2

For cloning of GRK2, the cDNA of human GRK2 was amplified by PCR using suitable primers (GRK254 and GRK255) for introduction of an N-terminal His-tag followed by a TEV cleavage site. A recognition site for SalI/HindIII was also introduced by PCR. After restriction digest, the fragment was inserted into a SalI/HindIII cut pFastBac1 plasmid.

GRK254: Forward primer for GRK2 amplification and introduction of a N-terminal hexahistidine-tag and a cleavage site for TEV protease
SalI Start 6x His tag 5' - TAC TAT TAC GTC GAC ACC **ATG** TCG TAC TAC CAT CAC CAT CAC CAT CAC GAT TAC GAT ATC CCA TEV recognition site GRK2 ACG ACC GAA AAC CTG TAT TTT CAG GGC GCG GAC CTG GAG GCG GTG CTG GCC GAC GTG AGC – 3'

GRK255: Reverse primer for GRK2 amplification, which introduces a HindIII cleavage site for insertion into pFastBac1
HindIII 5' - TAT TAC AGG CTT TCA GAG GCCGTT GGC ACT GCC GCG CTG GAC – 3'

Table 12: Primers for cloning of His-tagged GRK2 into pFastBac1

Single colony screening was performed using the forward primer, GRK2seq32 (5'-TAT AAT TAT AAT TC ATG ACC CGC TCC CTG GAC TGG CAG ATG GTC-3') and GRK255. The single colony screening showed that 7 out of 9 clones were positive and DNA sequencing of clone 1 confirmed the identity of the DNA and its correct insertion into pFastBac1 (13.1).

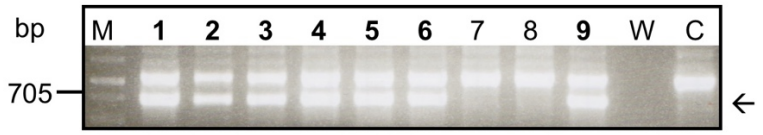

Figure 17: Single colony screening for pFastBac6HisTEVGRK2

Single colony screening PCR of bacterial clones: PCR product separation by agarose gel electrophoresis showed amplification of an approximately 705 bp fragment for clone 1-6 and 9. The control clone (C) and the water control (W) showed no PCR product of the right size.

6.1.2.1. Generation of the GRK2 encoding baculovirus

Generation of the recombinant bacmid

Bacmid DNA was generated according to the manufacturer's protocol as described before. Briefly, pFastBac6xHisTEVGRK2 DNA isolated from clone 1 was diluted to 200 pg/μl in supplied TE buffer and transformed into DH10Bac competent cells. For blue/white selection, transformed DH10Bac bacteria were incubated on LB agar plates containing 50 μg/ml kanamycin, 7 μg/ml gentamycin, 10 μg/ml tetracyclin, 40 μg/ml X-gal and 50 μg/ml IPTG. If transposition of GRK2 into the bacmid was successful, colonies were white and tended to be larger. The bacmid DNA was isolated and analysed by PCR using pUC/M13 forward and pUC/M13 reverse primers. All 4 clones showed amplification of an approximately 4440 bp fragment.

Production of the recombinant baculovirus

For baculovirus production, 8 x 10^5 Sf9 cells were transfected with 1 μg of recombinant bacmid DNA using 8 μl Cellfectin™ II. After 96 h, 80% of the cells appeared to be lysed and baculovirus stock (P1) was harvested.

Amplification of the GRK2 baculovirus stock (P2)

In order to generate a high-titer P2 virusstock, 2.4 x 10^7 cells were infected with 400 µl of the P1 stock and harvested after 72 h. The P2 stock was stored at 4°C, protected from light. For long term storage, aliquots were stored at -80°C.

6.1.2.2. Expression and purification of GRK2

Expression of GRK2

Expression in Sf9 cells was analysed as described before. Cells were infected with the baculoviral stock at different MOIs, samples were harvested after 24, 48 and 72 h and separated by urea-containing SDS-PAGE. A clear band was visible at 80 kDa after 48 and 72 h, which corresponds well to the expected mass of GRK2. Identity was confirmed by immunoblot detection with a polyclonal GRK2-specific antibody (1:1500). Maximum expression was achieved after 48 h at a MOI of 1.

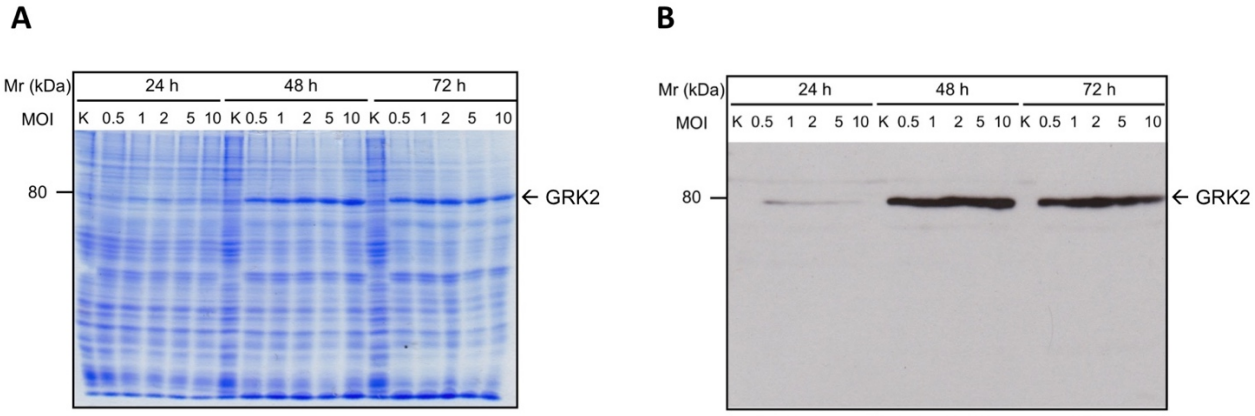

Figure 18: Expression of recombinant GRK2

Uninfected aliquots (K) and infected aliquots at a MOI of 0.5, 1, 2, 5, and 10 were taken 24 h, 48, and 72h after infection. Samples were separated by SDS-PAGE, and proteins were stained with Coomassie brilliant blue (A). GRK2 expression was detected by immunoblotting with a polyclonal GRK2-specific antibody (B).

Purification of GRK2

Sf9 cells were infected at a MOI of 1 for 48 h. All procedures were performed on ice at 4°C. 10^7 cells were harvested and washed twice with PBS containing protease inhibitor cocktail. The pellet was resuspended and cells were lysed in 10 ml of native lysis buffer (300 mM NaCl, 50 mM Hepes (pH 7), 1% NP40, 1 mM PMSF and 1:100 protease inhibitor cocktail) using a 27 G needle and a syringe. Next, cells were sonicated (3 x 3 sec with 30% cycle and 70% power) to reduce viscosity and centrifuged at 4600 x g at 4°C for 45 min. Cleared supernatant was loaded on 500 µl equilibrated Ni-NTA resin and incubated for 1 h with gentle agitation. After washing with 40 ml of wash buffer (300 mM NaCl, 50 mM Hepes (pH 7) and 40 mM imidazole), the purified protein was eluted with 300 mM imidazole. Buffer was exchanged using Amicon® Ultra centrifugal filter unit.

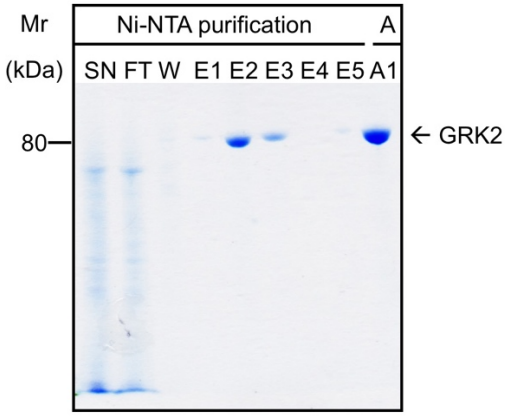

Figure 19: GRK2 was purified by Ni-NTA affinity chromatography followed by buffer exchange

Aliquots from the supernatant (S), flow-through (FT), wash (W) and elution fractions (E1-E5) from the Ni-NTA purification and the concentrated elution from the Amicon® Ultra centrifugal filter device (A1). Samples were separated by SDS-PAGE and proteins were stained with Coomassie brilliant blue.

6.1.3. Determination of the SRSF1-GRK2 interaction by ELISA

ELISA was utilized to analyse the interaction of GRK2 with SRSF1, which was identified by our group as a novel non-receptor substrate of GRK2 (*284*). Therefore, ELISA plates were coated with increasing concentrations (0.1, 0.32, 0.63, 1.25, 2.5, 5, 10 and 20 µg/ml) of recombinant GRK2 purified from Sf9 cells. Subsequently purified SRSF1 was added at a constant concentration of 5 µg/ml, and BSA served as a control. Binding was detected using a primary mouse monoclonal

SRSF1 antibody (1/300), and a secondary HRP-conjugated goat anti-mouse antibody (1/4000). The substrate reaction was allowed to proceed for 30 min and absorbance was measured at 410 nm. The ELISA showed that SRSF1 did interact with GRK2 in a concentration-dependent manner, whereas SRSF1 did not bind to the BSA protein control.

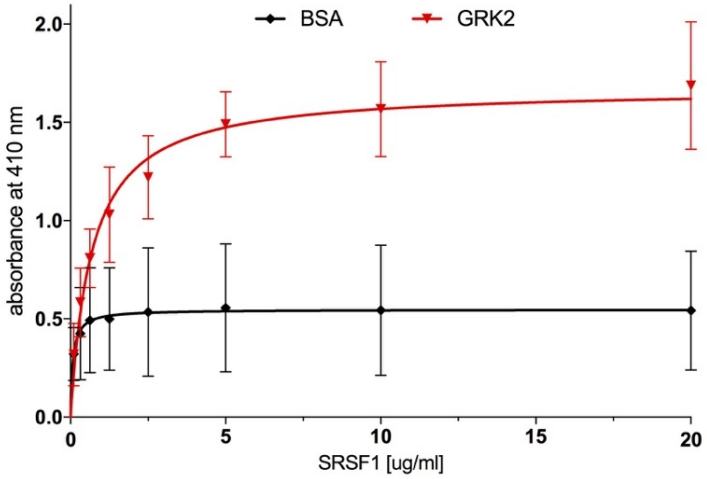

Figure 20: ELISA shows the interaction of GRK2 with SRSF1

Binding of SRSF1 (5μg/ml) to GRK2 or BSA (n=3, mean ± sd)

6.1.4. In vitro GRK2 phosphorylation assay

6.1.4.1. SRSF1 is a novel non-receptor substrate of GRK2 in vitro

The serine/arginine-rich splicing factor 1 (SRSF1) contains several phosphorylation sites and has been identified as a new substrate of GRK2 (*284*).

6.1.4.2. RKIP inhibited GRK2-mediated PDC phosphorylation, whereas SRSF1 phosphorylation was not altered

RKIP is a GRK2 inhibitor, which interferes with the interaction of GRK2 with the G protein-coupled receptor (GPCR) substrates. There are data which indicate that RKIP does not inhibit the phosphorylation of non-receptor GRK2-substrates (*245*). To further analyse the impact of RKIP on phosphorylation of non-receptor GRK2 substrates, I analysed whether RKIP inhibits the GRK2-

mediated phosphorylation of two different non-receptor substrates of GRK2, i.e phosducin and SRSF1.

The phosphorylation reaction was performed using 130 nM of recombinant GRK2 and 300 nM SRSF1 in a reaction buffer containing 20 mM Tris (pH7.5) 5 mM $MgCl_2$ and 2 mM EDTA. Purified RKIP was added in increasing concentrations from 10 nM to 30 μM. The reaction was started by the addition of [γ-32P]-labelled ATP (10 μCi/ml, total ATP concentration of 10 μM) and stopped after 30 min of incubation at 30°C by the addition of SDS sample buffer. After separation of proteins by SDS-PAGE and gels were exposed to X-ray films. The images were then scanned and quantified using Image J software. Data were analysed and inhibition curves were fit via GraphPad Prism. The data showed, that RKIP is able to inhibit the GRK2-mediated phosphorylation of PDC with an IC50 value of 950 nM (Figure 21). In contrast, GRK2 -mediated SRSF1 phosphorylation was not significantly decreased by RKIP up to 30 μM.

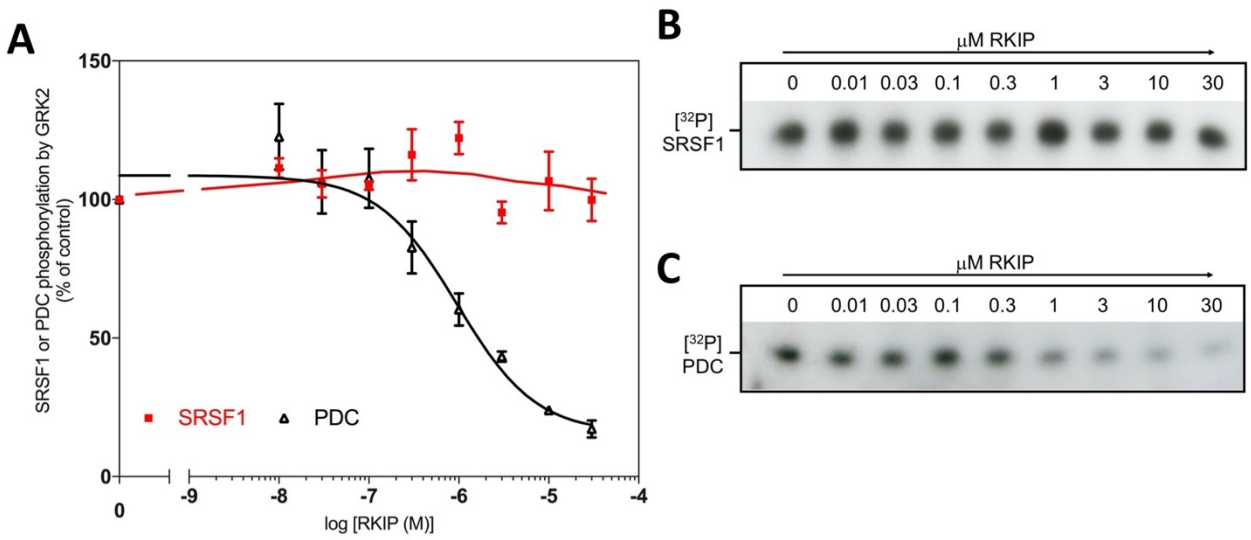

Figure 21: RKIP inhibited GRK2-mediated phosphorylation of phosducin, whereas SRSF1 phosphorylation remains unaltered.

(A) Dose response curves for RKIP-mediated effects on GRK2 induced phosphorylation of SRSF1 and PDC (n=6-8/each substrate) (B) Purified RKIP does not inhibit the phosphorylation of SRSF1 by purified GRK2 (representative autoradiogram) (C) Purified RKIP inhibits phosphorylation of PDC in vitro by purified GRK2 (representative autoradiogram).

6.1.4.3. The ATP-site-directed GRK2 inhibitor, paroxetine, interferes with the GRK2-mediated phosphorylation of SRSF1 and phosducin

The GRK2-inhibitory activity of RKIP was compared with paroxetine, which was identified as an ATP-sit directed inhibitor of GRK2 (*257*). To analyse the effect of paroxetine on GRK2-mediated phosphorylation of the non-receptor substrates, SRSF1 and phosducin, phosphorylation was performed using 50 nM of recombinant GRK2 S670A purified from Sf9 cells and 1 μM of PDC or SRSF1 purified from *E. coli* in reaction buffer (20 mM Hepes (pH 7), 2 mM $MgCl_2$ and 0.025% DDM). Paroxetine was added in increasing concentrations dissolved in DMSO yielding a final concentration of 2% total DMSO. The assay was performed and analysed as described before. Under these conditions an IC_{50} value of 1.7 μM for PDC and 6.13 μM for SRSF1 was determined, which correlates with the published IC_{50} value of 1.4 μM for tubulin for the paroxetine-mediated inhibition of tubulin phosphorylation, which is another non-receptor substrate of GRK2 (*263*).

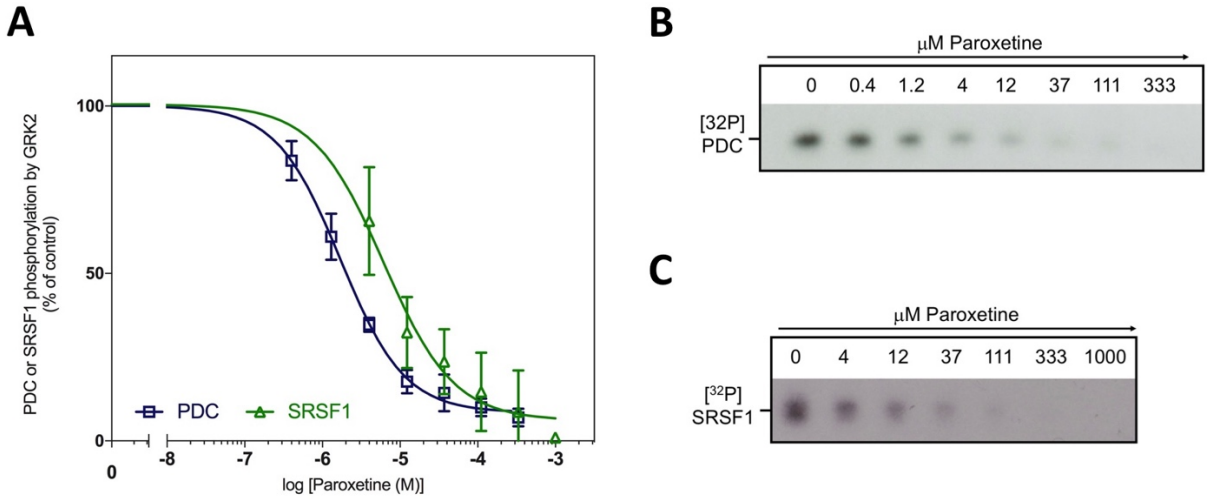

Figure 22: Paroxetine inhibits GRK2-mediated SRSF1 and PDC phosphorylation

(A) Dose response curve of paroxetine for inhibition of SRSF1 and PDC phosphorylation by GRK2 (n=3). Paroxetine inhibits phosphorylation of (B) PDC and (C) SRSF1 by purified GRK2 (representative autoradiogram).

6.2. Differential effects of RKIP and GRK2-K220R in vivo

In view of the observed in vitro differences between the GRK2 inhibitor RKIP compared to the ATP-site-directed inhibitor, paroxetine, the in vivo effects of RKIP were examined and compared with GRK2-K220R, which is the dominant-negative mutant of GRK2.

Transgenic mice were generated by our group with myocardium-specific overexpression of RKIP and GRK2-K220R. The dominant negative mutant GRK2-K220R lacks kinase activity and is able to inhibit wild type GRK2 phosphorylation of the β-AR (*285*). RKIP directly interacts with the N-terminal domain of GRK2, thereby interfering with GPCR substrate binding (*241*).

6.2.1. Generation of the transgenic mice with myocardium-specific RKIP and GRK2-K220R overexpression in a B6 background

Human RKIP cDNA sequence and point mutated GRK2-K220R sequence was cloned into a vector containing the α-myosin heavy chain promotor, thereby restricting protein expression to cardiac tissue (*286*). Transgenic mice were generated in the Molecular Pharmacology Unit ETH Zurich, Switzerland by Dr. Joshua Abd Alla and Dr. Said Abd Alla as described (*220*). Proteins were extracted from the heart as described before and protein expression was analysed by immunoblot detection with a polyclonal RKIP and GRK2 antibody. Two RKIP lines in a B6 (C57BL/6) background were established, Tg-RKIP2 showed a 3.5 ± 0.3-fold and Tg-RKIP3 showed a 2.9 ± 0.2-fold expression of myocardial RKIP compared with the levels of RKIP in non-transgenic B6-mice (Figure 23, A). Comparable cardiac RKIP up-regulation was also observed in cardiac biopsies from human heart failure patients (*245*). Tg-GRK-K220R lines in a B6 background showed a 3.4 ± 1-fold overexpression of GRK2/GRK2-K220R compared to non-transgenic B6 mice (Figure 23, B).

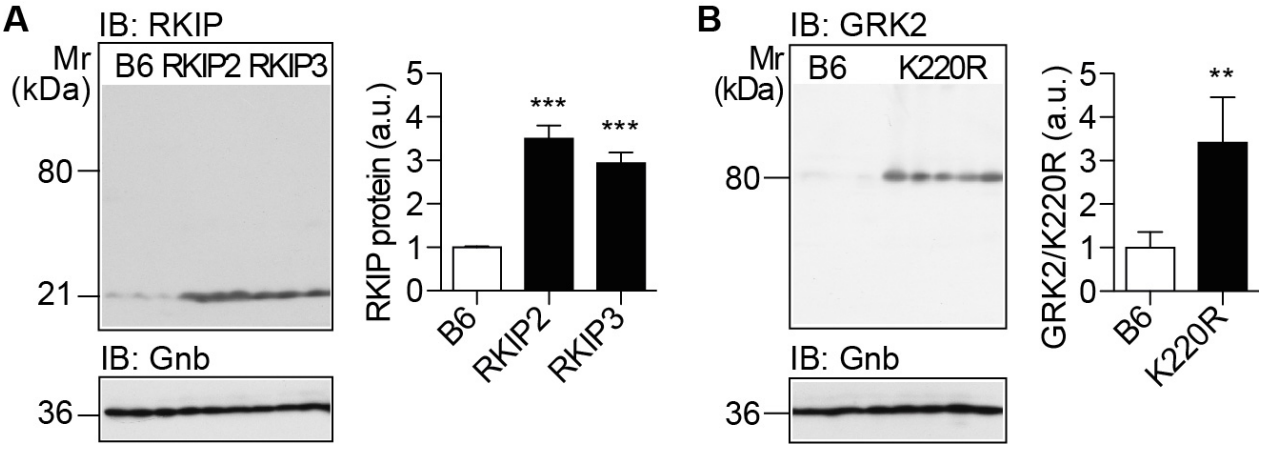

Figure 23: Immunoblot detection of cardiac RKIP and GRK2/GRK2-K220R protein levels

(A) Immunoblot detection revealed increased RKIP protein levels in two different Tg-RKIP mouse lines in B6 background (B) and of increased GRK2/GRK2-K220R protein level in B6 background compared to the non-transgenic control. (Bars represent mean ± S.D., RKIP: n=3/group, GRK2-K220R: n=5, **, $p \leq 0.01$; ***, $p \leq 0.001$)

6.2.2. Transgenic RKIP mice developed signs of heart failure, whereas transgenic GRK2-K220R mice did not

The cardiac phenotype of Tg-RKIP mice was investigated. Tg-RKIP mice developed cardiac hypertrophy with a significantly increased heart weight to body weight ratio and a decreased left ventricular ejection fraction relative to non-transgenic B6 controls. Cardiac performance of eight-month-old Tg-RKIP, Tg-GRK2-K220R and B6 control mice were measured by transthoracic echocardiography. The left ventricular ejection fraction of both RKIP mouse lines was significantly decreased to 28.2 ± 4.2 % (Tg-RKIP2) and 37.0 ± 3.6 % (Tg-RKIP3) compared to the B6 control (50.0 ± 5.1 %) and Tg-GRK2-K220R (56.8 ± 4.1 %). The dominant negative mutant showed a trend towards improved cardiac function over the B6 control (Figure 24, A). Cardiac dysfunction of RKIP transgenic B6 mice was accompanied by cardiac heart dilatation at advanced age, which is clearly visible in hematoxylin-eosin-stained heart sections (Figure 24, C). B6 mice and GRK2-K220R did not develop cardiac dilatation (Figure 24, C). Heart-weight to body-weight ratio of Tg-RKIP mice (RKIP2: 5.8 ± 0.3 mg/g) was significantly increased compared to B6 control mice (5.0 ± 0.1 mg/g) and Tg-GRK2-K220R mice (5.1 ± 0.2 mg/g).

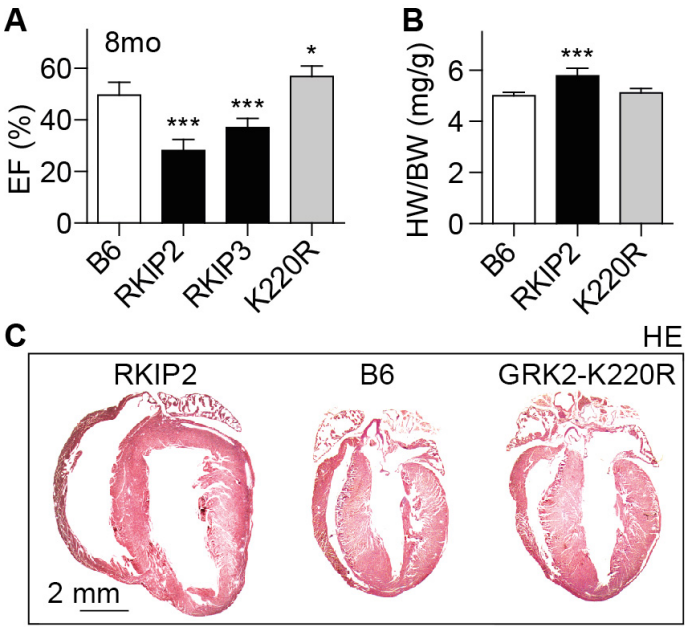

Figure 24: Transgenic RKIP overexpression triggered signs of heart failure in B6 mice

(A) Measurement of left ventricular ejection fraction (%) by transthoracic echocardiography, and (B) determination of heart weight to body weight ratio (HW/BW, mg/g) of B6 control, Tg-RKIP, and Tg-GRK2-K220R (age: 8 month). Data represent mean ± S.D., A: n=5/group, B: n=6/group (***, $p \leq 0.001$ (C) Representative hematoxylin-eosin (H&E)-stained heart sections of an 8-month-old Tg-RKIP, a B6 control, and Tg-GRK2-K220R mouse (bar, 2 mm).

6.2.3. Heart failure-related Pparg targets were upregulated in Tg-RKIP hearts, but not in Tg-GRK2-K220R hearts

Whole genome microarray gene expression profiling further confirmed the heart failure phenotype of Tg-RKIP hearts by demonstrating the significant up-regulation of the heart failure-related cardiac Pparg targets. RNA was extracted from heart tissue of 6-month-old B6 control, Tg-RKIP, and Tg-GRK2-K220R mice and whole genome microarrays gene expression profiling was performed as described.

Microarray data were normalized to a target value of 200 and analysed. Probe sets with significant difference (P value ≤ 0,01) and ≥6-fold upregulated signal intensities between heart tissue of RKIP transgenic and B6 control mice were identified. Analysis revealed upregulation of heart failure-related Pparg targets. Highly up-regulated heart failure genes, such as uncoupling protein-1 (*Ucp1*) (21.0-fold), adipsin (*Adn*) (14.7-fold), adiponectin (*Adipoq*) (11.0-fold), and resistin (*Retn*) (9.9-fold), are reportedly induced by ERK inhibition and serine 273 dephosphorylated Pparg (*287*). None of these genes were altered in GRK2-K220R transgenic mice.

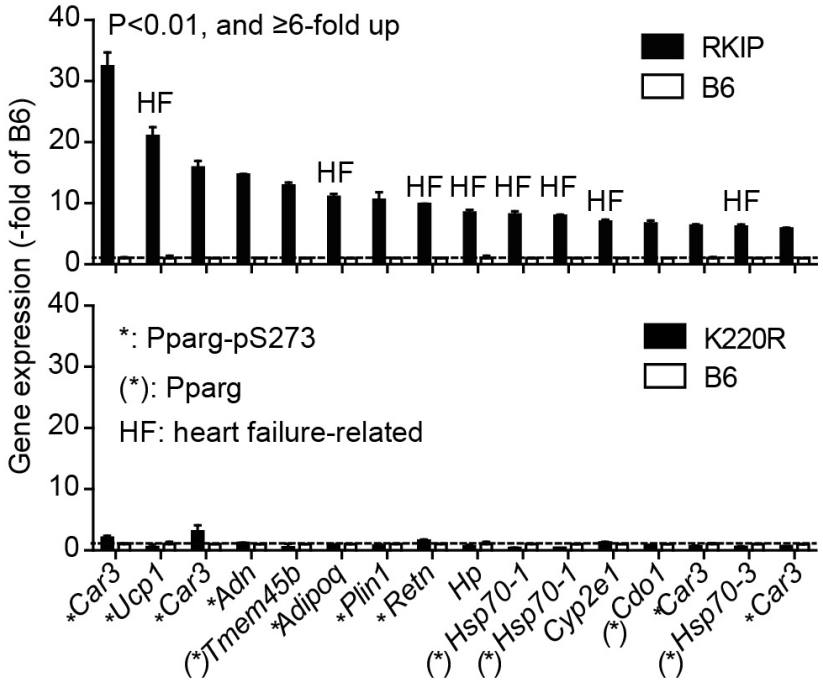

Figure 25: Upregulation of Pparg target genes in heart tissue of transgenic RKIP mice, but not in heart tissue of GRK2-K220R mice

Data of whole genome microarray gene expression profiling of 6-month-old Tg-RKIP mice showed up-regulation of cardiac Pparg-dependent heart failure-related targets compared to B6 mice. Expression of Pparg-dependent heart failure-related targets of Tg-GRK2-K220R heart tissue remained unaltered. (fold-change relative to B6)

6.2.4. Tg-RKIP hearts display cardiac lipid over load, whereas Tg-GRK2-K220R hearts did not

PPARG signalling could be influenced from the Raf/ERK axis in two ways: direct binding of MAPK to PPARG leads to sequestration of PPARG in the cytosol (*288*), and ERK is capable to phosphorylate PPARG on serine 273 and serine 112. Phosphorylation decreases canonical PPARG activation PPARG target gene induction (*287, 289, 290*). Vice versa, Raf/ERK axis inhibition decreases inactivating PPARG phosphorylation and thereby triggers heart failure-related PPARG targets, resulting in development of cardiac lipid overload and dysfunction (*220*).

Total cardiac Pparg and pS273 Pparg protein levels were detected by immunoblotting. Cardiac tissue extracts of Tg-RKIP, B6 control, and GRK2-K220R mice were separated by SDS-PAGE and detected with a specific antibody raised against a synthetic phosphopeptide derived from Pparg around the phosphorylation site serine 273 and a specific antibody raised against Pparg. Transgenic hearts which express RKIP were characterised by a significantly decreased phosphorylation of Pparg on serine-273 compared to B6 control and Tg-GRK2K220R hearts (Figure 26, A). Thus, RKIP leads to a decreased cardiac content of serine 273 phosphorylated Pparg, which is the active form of Pparg.

Total cardiac lipids were extracted by the method of Folch et al. (*280*) and analysed as described before (5.9.2). Concomitantly to the increased RKIP protein level and Pparg activation, cardiac palmitate (Figure 26, B), triacylglycerol (TAG) (Figure 26, C), ceramide (Figure 26, D) and diacylglycerol (DAG) (Figure 26, E) content of RKIP hearts were significantly elevated compared to B6 and Tg-GRK2-K220R mice. Palmitate is synthesized by the Pparg-target fatty acid synthase (FASN). Together, thus cardiac lipid accumulations could be involved in the heart failure phenotype of Tg-RKIP mice.

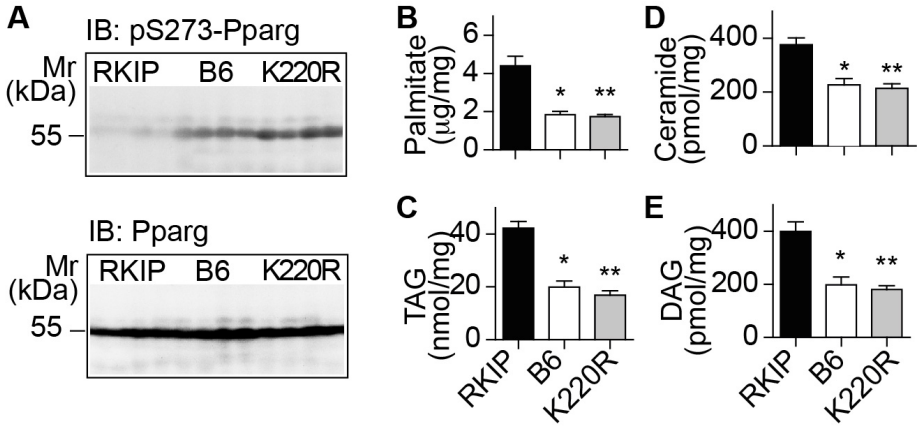

Figure 26: Immunoblot detection of Pparg activation and lipid overload in Tg-RKIP hearts

(A) Immunoblot detection of pS273-Pparg (upper panel) and total Pparg (lower panel) in cardiac tissue extract of RKIP transgenic mice relative to GRK2-K220R and B6 controls (n=4 mice/group). Measurement of plamitate (B), triacylglyerol (TAG) (C), diacylglycerol (DAG) (E) and total ceramide (D) contents of Tg-RKIP mice relative to Tg-GRK2-K220R and B6 controls. (mean±S.D., n=7; *, $p < 0.05$; **, $p \leq 0.01$; ***, $p \leq 0.001$)

6.2.5. Moderately increased RKIP protein levels in FVB background

To determine whether the genetic background of B6 mice is linked to the different phenotype of the two GRK2 inhibitors, transgenic FVB mice with myocardium-specific RKIP overexpression were generated. Analogous to Tg-RKIP B6 mice, moderate overexpression of RKIP occurs in cardiac tissue of Tg-RKIP FVB mice. Two different mouse lines were generated and a 2.7-fold and 3.4-fold expression of RKIP compared to the non-transgenic FVB mice were detected by immunoblotting (Figure 27, A). For immunohistological detection, paraffin sections of mouse heart specimens were incubated with blocking solution, followed by anti-RKIP antibody and detection as described (5.9.4). Final HE staining was performed as described (5.9.3). Immunohistology showed the increased RKIP protein on the cardiac section from the Tg-RKIP1 mouse, whereas the RKIP protein was low on the non-transgenic FVB control. In addition to the increased RKIP-protein, the transgenic RKIP heart showed cardiac hypertrophy (Figure 27, B).

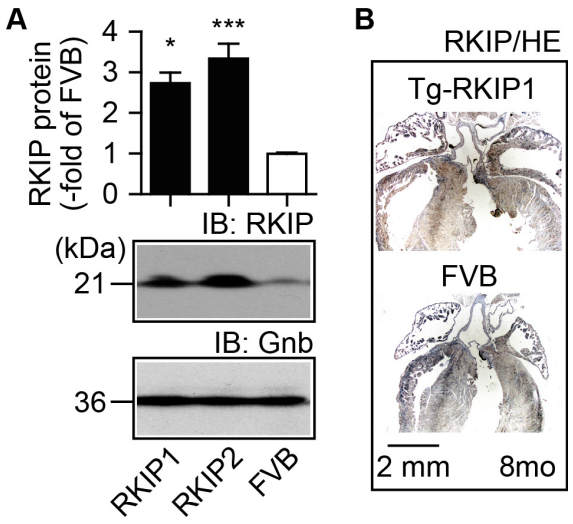

Figure 27: Transgenic RKIP overexpression triggered signs of heart failure in FVB mice

(A) Immunoblot detection and quantification of RKIP protein in cardiac extracts and (B) representative immunohistological detection of RKIP on cardiac sections of a Tg-RKIP1 FVB mouse relative to a non-transgenic FVB control (bar, 2mm).

6.2.6. Tg-RKIP FVB mice show signs of heart failure

Analogous to Tg-RKIP B6 mice, 8-month-old Tg-RKIP FVB mice developed signs of cardiac hypertrophy with dilatation and cardiac dysfunction (see Figure 27). Histological analysis confirmed that hearts from 8-month-old Tg-RKIP FVB mice showed ventricular and atrial enlargement and dilation relative to an age-matched non-transgenic FVB mouse (Figure 27, A). Heart-weight to body-weight ratio was significantly increased in both Tg-RKIP FVB mouse lines (RKIP1: 5.9 ± 0.3 mg/g; RKIP2: 6.3 ± 0.4 mg/g; and FVB: $4.9 \pm 0{,}3$ mg/g) (Figure 27,B) and left ventricular ejection fraction was also significantly and strongly decreased (RKIP1: 30.9 ± 2.5 %; RKIP2: 25.9 ± 4.4 %; and FVB: 49.3 ± 3.4 %) (Figure 27,C).

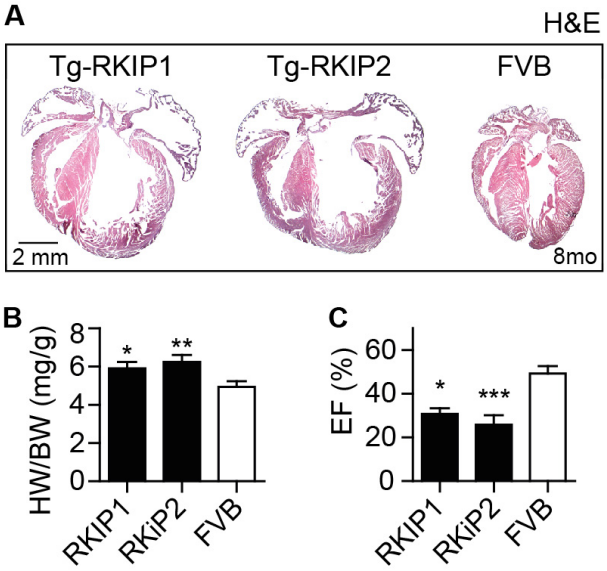

Figure 28: Aged Tg-RKIP FVB mice develop signs cardiac hypertrophy with dilatation and heart failure

(A) Representative H&E-stained heart sections of both 8-month-old Tg-RKIP FVB mouse lines and age-matching FVB control (bar, 2 mm) (B) determination of heart weight to body weight ratio (HW/BW, mg/g) n=6 mice/group, (C) measurement of left ventricular ejection fraction (%) by transthoracic echocardiography. (Data represent mean±S.D., n=8/group, *, $p < 0.05$; **, $p \leq 0.01$; ***, $p \leq 0.001$)

6.2.7. Tg-RKIP FVB mice show cardiac lipid overload

The lipid content of the cardiac tissue was elevated in Tg-RKIP mice in FVB background. In this study, we analysed the composition of the lipid content by gas chromatography. Therefore, total cardiac lipids were extracted from pulverized cardiac tissue and further analysed using gas chromatography. The cardiac lipid extract of three Tg-RKIP FVB mice were separated on a Carbowax column. Helium was used as the carrier gas and detected by a flame ionization detector. A standard lipid mixture was used for calibration. Age-matched FVB mice served as a control. A variety of different saturated and unsaturated lipids were strongly increased in the Tg-RKIP lipid extract (Figure 29, A), such as palmitic acid (16:0), which is the major synthesis product of FASN, palmitoleic acid (16:1 n7), which is synthesized from palmitic acid by SCD1, and stearic acid (18:0), which is the synthesized form of palmitate undergoing elongation by ELOVL1 and ELOVL6.

In agreement with the cardiac lipid load, cardiac palmitate (2.3-fold) (Figure 29, B) and triacylglycerol (TAG) (2.4-fold) (Figure 29, C), ceramide (1.7-fold) (Figure 29, D) and diacylglycerol (2.6-fold) (DAG) (Figure 29, E) content of RKIP hearts were significantly elevated.

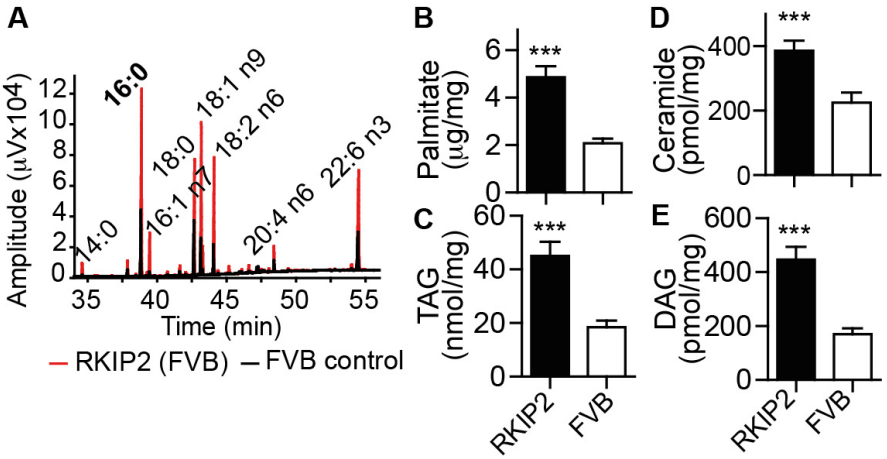

Figure 29: Analysis of lipid content and fatty acid composition in Tg-RKIP FVB mice

(A) FAME chromatogram of cardiac lipid extracts from Tg-RKIP FVB mice relative to non-transgenic FVB mice. Measurements of palmitate (B), triacylglyerol (TAG) (C), diacylglycerol DAG (E) and total ceramide (D) contents of Tg-RKIP FVB mice relative to FVB controls (mean±S.D., n=6, ***p<0.0001, unpaired t-test)

6.2.8. RKIP acts as a GRK2 inhibitor in vivo

My data show, that for cardioprotective GRK2 inhibition an intact Raf/Erk axis is required. RKIP is a dual inhibitor, which switches upon PKC-mediated phosphorylation on serine 153 from Raf to GRK2 inhibition (*241*). To determine if RKIP acts as a GRK2 inhibitor in vivo, immunoblot detection was performed using a phosphor-specific polyclonal p-S153 RKIP antibody. In cardiac extract from Tg-RKIP B6 mice, the total RKIP content was elevated as shown before and the majority of RKIP was phosphorylated on serine 153 (Figure 30, A). In order to assess the extent of GRK2 inhibition by RKIP and GRK2-K220R, a cAMP assay with isolated neonatal cardiomyocytes was performed. GRK2 inhibition reduces agonist-induced phosphorylation and internalization of the β-adrenergic receptors by mediated GRK2. As a consequence, β-AR mediated cAMP concentrations are enhanced after GRK2 inhibition. In cardiomyocytes isolated form Tg-RKIP (124 ± 5 %, p<0.01) and

Tg-GRK2-K220R (118 ± 4 %, p<0.05, Dunn's test) hearts cAMP concentrations were elevated in a similar extent compared to the B6 control. In conclusion, RKIP shows a comparable inhibitory potency against GRK2 like GRK2-K220R. In agreement with increased cAMP levels, gene expression analysis showed significant up-regulation of the cAMP-inducible gene, Ttc14, in Tg-RKIP and Tg-GRK2-K220R hearts.

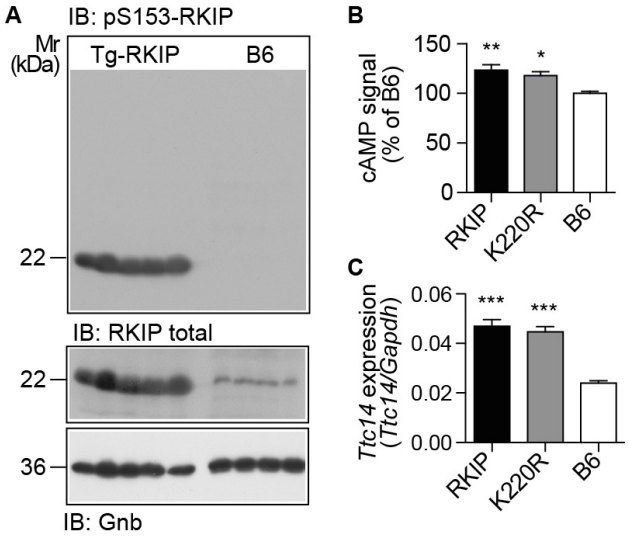

Figure 30: RKIP acts as a GRK2 inhibitor in vivo

(A) immunoblot detection of pS153-RKIP (upper panel), total RKIP (mid panel) and loading control (lower panel) in cardiac tissue extracts of Tg-RKIP mice relative to B6 controls (n=5/group) (B) isoproterenol-stimulated (100nM) cAMP levels in neonatal cardiomyocytes isolated from RKIP-transgenic, GRK2-K220R-transgenic and B6 mice. (mean±S.D.,n=6) (C) Gene expression data show up-regulation of cardiac cAMP-depended Ttc14 expression. (mean±S.D., n=3)

The effective GRK2 inhibition of both models is also evident in the microarray gene expression profiling. RNA was isolated and analysed as described before. In Tg-RKIP mice, 200 probes were identified, which were significantly changed and 98 probes in Tg-GRK2-K220R mice. More than 45% of regulated probe sets of Tg-GRK2-K220R hearts show concordant regulation with Tg-RKIP hearts.

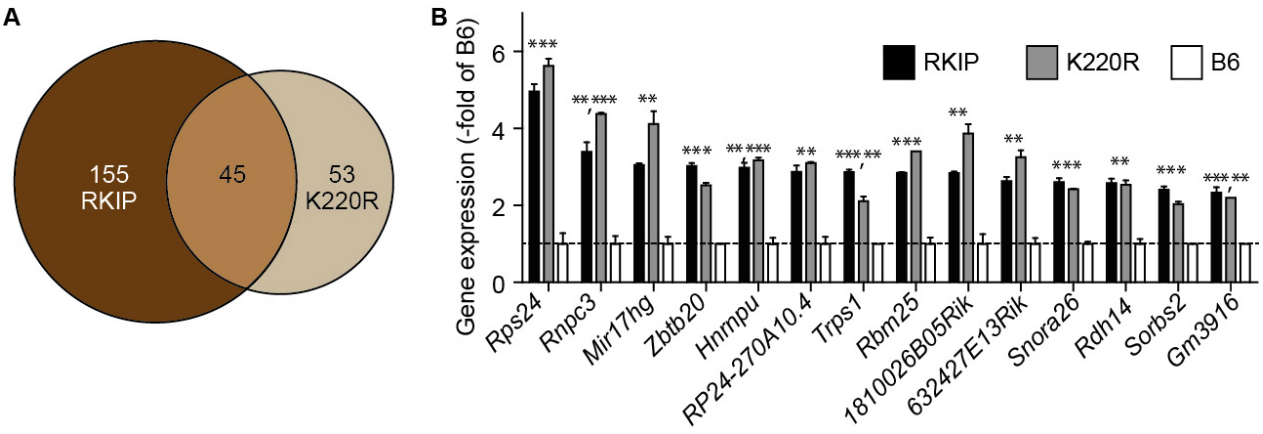

Figure 31: Concordant gene regulation by RKIP and GRK2-K220R

(A) The Venn diagram illustrates the number of significantly regulated probe sets for each model. 45 probe sets (i.e. 45 %) of Tg-GRK2-K220R hearts showed concordant regulation with Tg-RKIP mice. (B) Whole genome microarray gene expression profiling of heart tissue identified concordant regulation of Tg-RKIP and Tg-GRK2-K220R hearts. Data filtering identified probe sets with significant up-regulation in Tg-GRK2-K220R and Tg-RKIP hearts relative to B6. (fold-change relative to B6) (*, $p < 0.05$; **, $p \leq 0.01$; ***, $p \leq 0.001$ versus the respective control)

6.2.9. GRK2-K220R retards chronic pressure overload-induced heart failure

Abdominal aortic constriction (AAC) was performed in 8-week-old GRK2-K220R transgenic mice to trigger pressure-overload induced cardiac hypertrophy and heart failure. The age matched control group underwent identical surgical procedure. After 8 weeks of AAC, at an age of 4 month development of cardiac dysfunction was assessed by left ventricular ejection fraction (EF). Cardiac function of GRK2-K220R-transgenic mice were significantly improved (EF of 29.8 ± 5.2 %; $p<0.01$, Dunn's test) compared to the non-transgenic control (EF of 24.0 ± 4.9 %).

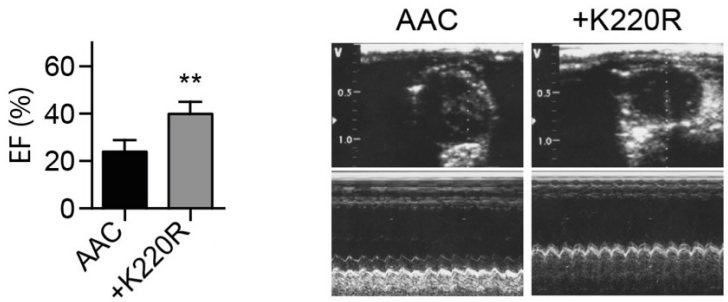

Figure 32: GRK2 K220K retarded chronic pressure overload-induced heart failure

Determination of left ventricular ejection fraction (%) by transthoracic echocardiography of Tg-GRK2-K220R mice and non-transgenic FVB mice. (mean±S.D., n=6, $p<0.01$)

6.3. Establishment of a transgenic mouse model with ubiquitous GRK5 overexpression

6.3.1. Generation of transgenic GRK5 mice

For the generation of a transgenic mouse model with a ubiquitous overexpression of GRK5, the corresponding cDNA was cloned into a vector containing the human cytomegalovirus promoter (*291*). For cloning of GRK5, the cDNA of human GRK5 was amplified by PCR using suitable primers for introduction of recognition sites for SalI/HindIII. After restriction digest of the fragment, it was inserted into a SalI/HindIII cut pcDNA3 plasmid (pcDNA3GRK5, U. Quitterer). The DNA was sequenced and endotoxin-free plasmid DNA was prepared and linearized by restriction digest with MluI/DraIII.

Approximately 100 fertilized zygotes were collected from superovulate female FVB mice. Linearized DNA was injected into the pronucleus of each cell and subsequently injected zygotes were reimplanted into pseudopregnant CD1 foster mice. After 3 weeks, 14 pubs were born.

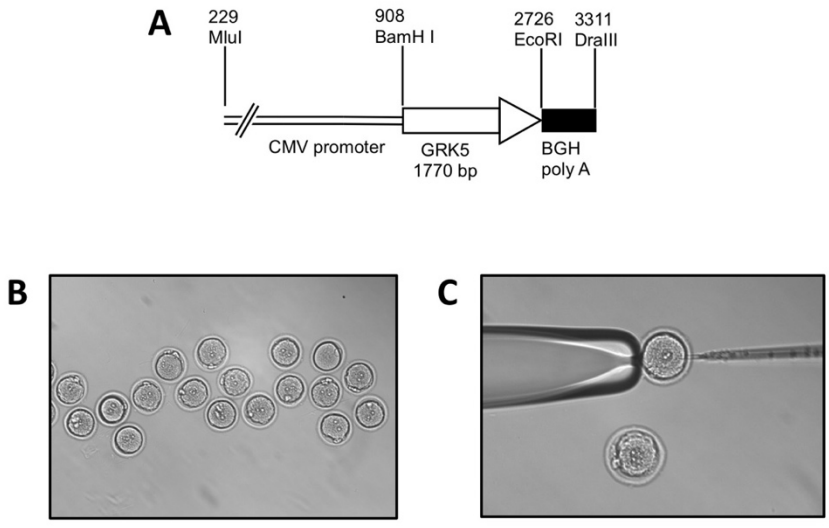

Figure 33: Generation of transgenic GRK5 mice

(A) Diagram of transgene: expression of GRK5 under control of the CMV immediate-early promoter/enhancer. (B) Collected fertilized zygotes and (C) pronuclear DNA injection.

6.3.2. Identification of Tg-GRK5 founder mice by PCR genotyping

To identify founder mice with stable genome integration of the transgene, genomic DNA was isolated from ear punch biopsies and analysed by PCR. The vector-specific forward primer CMV2-for (5' CGC AAA TGG GCG GTA GGC GTG TAC GGT GGG 3') and the insert-specific primer reverse GRK532 (5' CCA GCC CAG GCC TGG TTT CAC 3') were used. Three founder mice could be identified under standard genotyping PCR at 60°C annealing temperature (Figure 24, A). In order to reduce unspecific amplifications, the annealing- and extension-step was combined at 72°C for 60 s. Modified genotyping PCR was performed with mice from the F2 generation and results are shown in Figure 24 B.

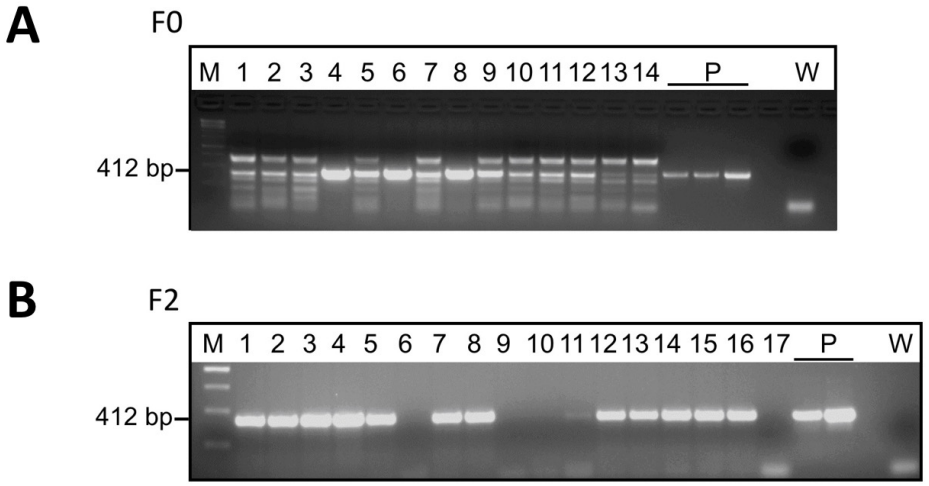

C

Step	Temperature	Time	Cycles
1	95°C	2 min	1X
2	95°C	40 s	40X
3	72°C	60 s	
4	72°C	10 min	1X

Figure 34: Identification of the CMVGRK5 transgene in the genomic DNA of mice by PCR

Isolated genomic DNA was used for genotyping PCR with CMV2/GRK532 primers, which identified three founder mice. M=Marker; P=positive control; W=negative control (A) Genotyping PCR of mice from generation F0 under standard conditions. (B) Modified genotyping PCR of mice from generation F2. (C) Modified genotyping PCR program with combined annealing- and extension-step.

6.3.3. Phenotype characterization of Tg-GRK5 mice

6.3.3.1. Moderately increased GRK5 protein levels in heart tissue

The phenotype of Tg-GRK5 mice was determined. Groups of 6-month-old male mice were weighted and sacrificed. Hearts were removed quickly and hearts were weighted and snap frozen immediately. Proteins were extracted as described (5.9.1) and GRK5 protein level in cardiac tissue of Tg-GRK5 mice was analysed by immunoblot detection using an anti-GRK5 antibody, raised in rabbit against recombinant GRK5 protein (U. Quitterer (*220*)). Age-matched non-transgenic FVB mice served as control. Tg-GRK5 showed a 2.09 ± 0.45-fold expression of myocardial GRK5 compared with the levels of GRK5 in non-transgenic FVB mice (1 ± 0.21-fold; n=5-7; p=0,0006) (Figure 35). Comparable cardiac GRK5 up-regulation was observed in heart failure patients and it reproduces the GRK5 up-regulation induced by GRK2 inhibition (*292*). Thus, the generated Tg-GRK5 mice reproduce the up-regulated GRK5 level observed in human heart failure patients.

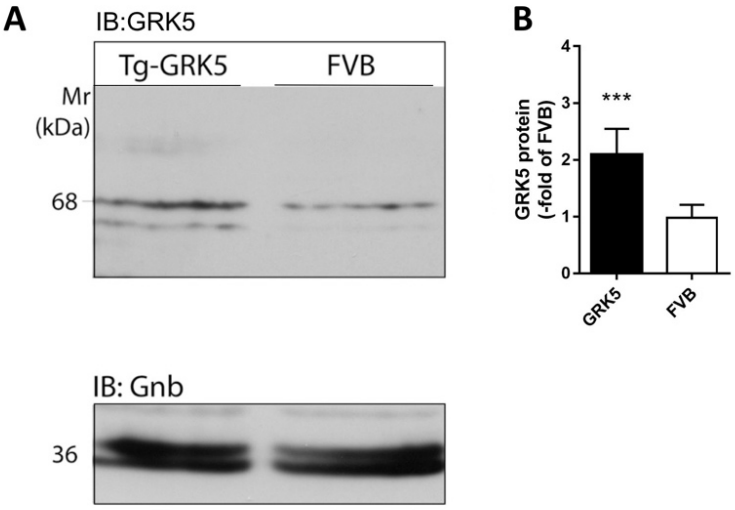

Figure 35: GRK5 protein levels in Tg-GRK5 heart tissue

(A) Immunoblot detection of cardiac extracts revealed (B) 2-fold increased GRK5 levels in Tg-GRK5 mice compared to the non-transgenic FVB control. The graph represents mean ± SD, n=5-7 mice/group, p=0,0006.

6.3.3.2. Hearts of Tg-GRK5 mice did not show signs of cardiac hypertrophy and had normal blood glucose level

The phenotype of 6-month-old Tg-GRK5 mice was determined. Therefore, mice were weighted and blood samples were withdrawn from the tail vein. Blood glucose level was measured as described before (5.9.6). Hearts were perfused with ice-cold PBS, weighted, fixed by immersing in 10% neutral buffered formalin, and tissue sections were prepared as described (5.9.2). Tg-GRK5 mice did not show any signs of cardiac hypertrophy. The heart weight (GRK5: 153 ± 17 mg and FVB: 156 ± 25 mg; p=0.81), body weight (GRK5: 35.83 ± 2.23 g and FVB 35.38 ± 1.60 g; p=0.66) and the heart weight to body weight ratio (GRK5: 4.28 ± 0.48 and FVB 4.43 ± 0.80; p=0.69) was not significantly different from non-transgenic controls. Also, the blood glucose level remained unaltered (GRK5: 10.56 ± 1.58 mmol/l and FVB: 10.64 ± 0.80 mmol/l; p=0.92).

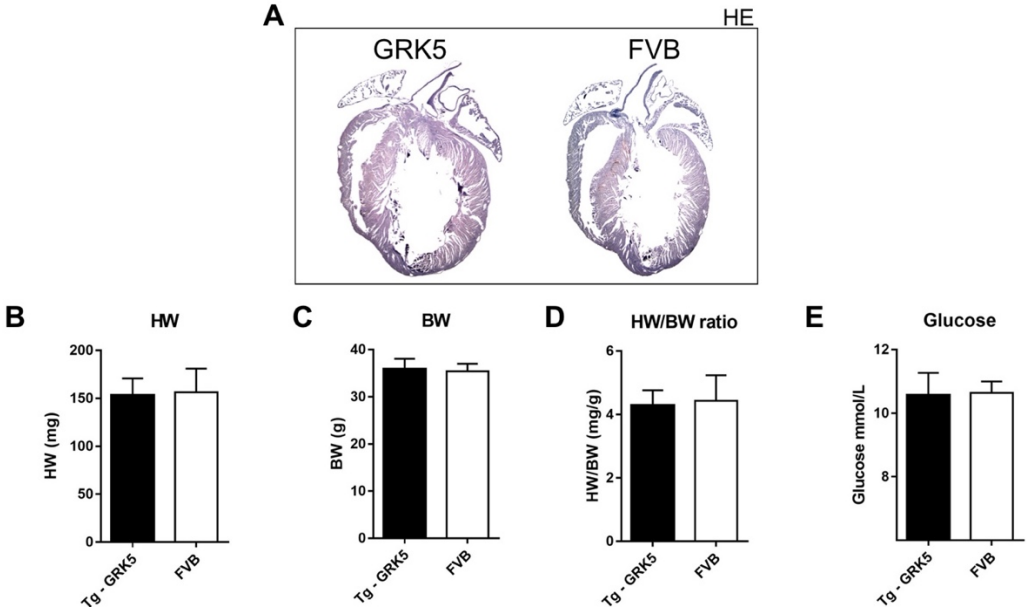

Figure 36: Hearts of Tg-GRK5 mice did not show any signs of cardiac hypertrophy and had normal blood glucose level

(A) Representative H&E-stained heart sections of a 6-month-old Tg-GRK5 FVB mouse lines and age-matching FVB control. (B) Determination of heart-weight (HW, mg), (C) body-weight (BW, g), (D) heart-weight to body-weight ratio (HW/BW, mg/g) and (E) blood glucose level (mmol/l) Data represent mean±S.D, n=5-7/group.

Histology analysis of hematoxylin-eosin-stained heart sections further documented that moderate GRK5 overexpression did not cause any cardiac abnormalities. Thus, my data show that moderate GRK5 expression had no adverse cardiac effects (Figure 36 A).

6.3.3.3. Increased GRK5 protein level in frontal cortex and hippocampus

The CMV promoter directs ubiquitous expression of a transgene. To determine the transgenic GRK5 protein in a non-cardiac tissue, I chose the brain, because GRK5 is reported to exert a neuroprotective function in the brain (*228-231*). Brain was carefully dissected out from the skull and placed on ice. Cortex was removed from the hippocampus and subsequently hippocampus was isolated and freed from residual cortex by rolling free from cortex and frozen in liquid nitrogen. A section of the frontal cortex was cut off and also snap frozen in liquid nitrogen. Proteins were extracted as described (5.9.1). Western bolt analysis was performed using an anti-GRK5 antibody, raised in rabbit against recombinant GRK5 protein (U. Quitterer (*220*)). Immunoblot analysis showed a clearly increased protein level of GRK5 in extracts from the frontal cortex and the hippocampus of Tg-GRK5 mice, while endogenous GRK5 could not be detected in extracts from FVB controls. Extracts from HEK293 cells transfected with pcDNA3GRK5 served as a control.

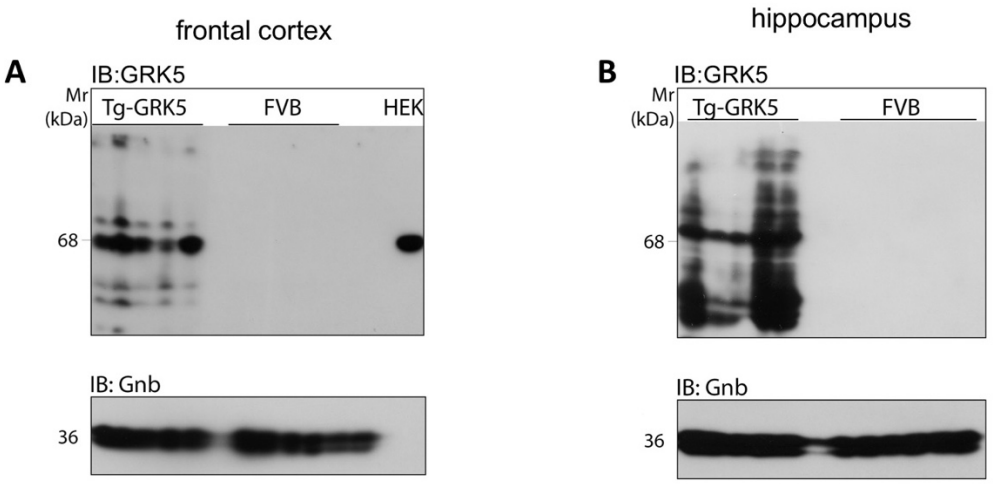

Figure 37: GRK5 protein levels in brain tissue from Tg-GRK5 mice

Immunoblot detection of GRK5 in (A) frontal cortex and (B) hippocampus extract revealed increased GRK5 levels compared to the non-transgenic FVB control in Tg-GRK5 mice. Extracts from HEK293 cells transfected with pcDNA3GRK5 served as a control (HEK) n=5.

7. DISCUSSION

7.1. Different strategies of GRK2 inhibition

Cardioprotective GRK2 inhibition seems to be a promising approach in the treatment of heart failure. All three domains contribute to the activity of GRK2 and allow a range of approaches to inhibit GRK2 effector functions.

Targeting the N-terminal domain of GRK2 may inhibit the recognition and binding of GPCR substrates and may block $G\alpha_q$-mediated effects. Compounds which interact with the enzymatically active kinase domain, may prevent phosphorylation activity, but do not alter the kinase-independent functions. Interference with the C-terminal domain could prevent the $G\beta\gamma$-mediated GRK2 activation and membrane translocation to receptor substrates.

In the present study I compared different approaches of GRK2 inhibition:

- **RKIP** is a dual-specific inhibitor of GRK2 and the Raf/Erk axis, and was used for in vitro and in vivo experiments. The Raf kinase inhibitor protein (RKIP) inhibits GRK2 in vivo (*188, 245*) and in vitro (*241*). RKIP does not inhibit the catalytic domain but interferes with the GRK2-receptor interaction via binding to the amino-terminal domain of GRK2 (*241*).

- The small molecule and ATP site inhibitor **paroxetine** was used for in vitro experiments. Paroxetine fits in the enzymatic pocket of GRK2 and stabilizes it in an inactive state. GPCR and non-GPCR substrate phosphorylation were inhibited by paroxetine in vitro and in living cells (*261*).

- The dominant-negative GRK2-inhibitory mutant, **GRK2-K220R**, was used for the in vivo experiments. GRK2-K220R lacks kinase activity and is able to inhibit GRK2-mediated phosphorylation of GPCR substrates such as the β-AR (*285*).

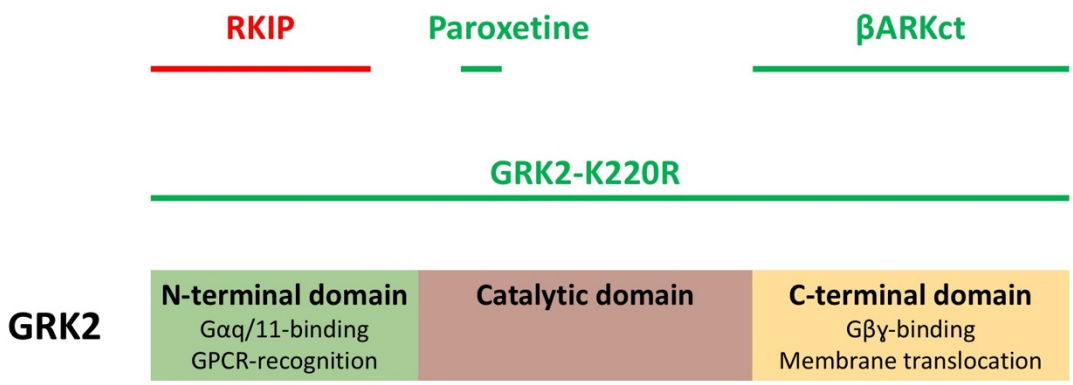

Figure 38: Different approaches of GRK2 inhibition

RKIP interferes with the GRK2-receptor interaction via binding to the N-terminal domain of GRK2 and inhibits GPCR-recognition. **Paroxetine** fits in the enzymatic pocket of GRK2 and stabilizes it in an inactive state. **βARKct** prevents the activation and translocation of endogenous GRK2 to the plasma membrane. The effect of **GRK2-K220R** could be attributed to kinase-mediated effects and kinase-independent effects because GRK2-K220R also inhibits Gβγ- and $G\alpha_q$-mediated signalling.

7.2. GRK2 inhibitors, RKIP and paroxetine, display different substrate specificities in an in vitro phosphorylation assay

GRK2 is well known for its ability to phosphorylate various substrates, most prominently GPCRs (*293*). In addition to canonical function of GRK2, over the last year an increasing number of non-GPCR targets were established (*123*). In frame of this theses I used two different non-GPCR substrates of GRK2, i.e. phosducin and SRSF1. Phosducin is a previously characterized GRK2 substrate (*131*) and SRSF1 is a novel non-receptor substrate of GRK2, which was recently identified by our group (*284*). In the present study, the GRK2-SRSF1 interaction was investigated in vitro by ELISA technique and kinase assay. The protein-protein binding of SRSF1 and GRK2 was confirmed with ELISA, in which SRSF1 interacted with GRK2 in a concentration-dependent manner, whereas SRSF1 did not bind to the BSA protein control. In addition, SRSF1 was confirmed as a novel non-GPCR substrate of GRK2 as shown in the in vitro phosphorylation assay. Purified SRSF1 was markedly phosphorylated in the presence of GRK2.

To characterize the effect of RKIP and paroxetine as GRK2 inhibitors, I used the non-GPCR substrates phosducin and SRSF1. The in vitro phosphorylation assay detected different modes of GRK2 inhibition by RKIP compared to paroxetine. RKIP only inhibited the GRK2-mediated phosphorylation of phosducin with an IC_{50} value of 980 nM whereas SRSF1-mediated GRK2 inhibition was not significantly decreased by RKIP up to 30 microM. Phosducin is known for its high affinity for Gβγ subunits, which is in a range of 20 nM (*294*). Overexpression of truncated phosducin enhances the contractility in both normal and failing cardiomyocytes by scavenging of Gβγ subunits (*295*). Phosphorylation of phosducin by GRK2 (*131*) or PKA (*294*) markedly reduces its binding ability to Gβγ subunits. Although the cellular concentration of phosducin in the heart is 1 μM (*296*), its regulatory relevance in the heart is unclear, in its phosphorylated as well as in its unphosphorylated form. However, the inhibitory effect of RKIP on a soluble substrate such as phosducin was not expected. GRK2 inhibition by RKIP was considered as GPCR specific, whereas GRK2-phosphorylation of cytosolic substrates such as tubulin, ezrin, radixin and moesin was not affected by RKIP (*245*). In agreement with the notion that RKIP does not inhibit the GRK2-mediated phosphorylation of most non-receptor substrates, I also found that RKIP did not inhibit the phosphorylation of SRSF1 by GRK2.

However, there is little data on the interaction of cytosolic substrates with GRK2. The substrate specificity of RKIP points to a possible interaction-site. Whereas an interaction between phosducin and the N-terminal domain of GRK2 seems possible, the binding of SRSF1 to the N-terminal domain of GRK2 can be excluded. Further investigations are needed to clarify this proposed mechanism of action. In contrast to RKIP, the ATP-site directed inhibitor paroxetine inhibited the phosphorylation of phosducin and SRSF1.

SRSF1 phosphorylation has a major impact in vivo and is essential for preventing exon skipping, ensuring the accuracy of splicing and regulating alternative splicing (*297*). SRSF1 consists out of functional modules: two arginine-serine rich regions (RS region, RS1 and RS2), where SRSF1 is regulated via phosphorylation, and two RNA recognition motifs, which interact with RNA and other splicing factors (*298, 299*). Its function and localization are regulated by phosphorylation. Serine/threonine-protein kinase (SRPK1) phosphorylates up to twelve serines in the RS region of SRSF1 (*298*). Phosphorylation of the RS1 region mediates nuclear import of SRSF1 when localized in the cytosol and phosphorylation in the RS2 region by the dual specificity protein kinase CLK1 in the nucleus activates transcription and consequently splicing (*300*). For the proper transitions between the different steps of the splicing process, sequential phosphorylation and dephosphorylation are necessary (*301*).

Chronic pressure overload induced cardiac hypertrophy is associated with an increased expression of SRSF1 (*302*). SRSF1 regulates alternative splicing and constitutive splicing of the Ca^{2+}/calmodulin-dependent kinase II (CaMKII). Cardiac specific knockout of SRSF1 leads to a hypercontraction phenotype due to a defect in splicing of CaMKIIδ transcripts. SRSF1 is an important player for the switch in splicing of the CaMKIIδ transcripts in the juvenile-to-adult transition of cardiac function (*303*). PKA phosphorylates SRSF1 in vivo (*26*), enhances SRSF1 activity and promotes a dysregulation in the alternative splicing of CaMKIIδ, which may contribute to cardiomyopathy and heart failure (*304*).

Altered cardiac Ca^{2+} homoeostasis plays an important role in cardiac hypertrophy and heart failure. CaMKII is a critical player in intracellular Ca^{2+} handling. Upregulation of CaMKII levels and activity have been reported in the pathogenesis of heart failure in humans and in animal models (*305-308*).

Future studies will have to investigate the role GRK2-mediated SRSF1 phosphorylation in vivo. But these different substrate specificities of the GRK2 inhibitors paroxetine and RKIP could be of relevance in vivo, because paroxetine showed cardioprotection against myocardial infarction-induced heart failure whereas the in vivo function of RKIP is according to our transgenic models is not cardioprotective 7.3.

7.3. GRK2 inhibition by RKIP and GRK2-K220R show contrasting cardiac phenotypes in vivo in transgenic mouse models

In the present study, I compared two different GRK2 inhibitors in vivo i.e. GRK2-K220R and RKIP. The dominant-negative GRK2-K220R is an inhibitor, which lacks kinase activity and is able to inhibit GRK2-mediated phosphorylation of GPCRs such as the β-AR (*285*). In addition to the competitive binding to GPCR and non-GPCR substrates, GRK2-K220R displays all kinase independent functions of GRK2. While the dominant-negative GRK2-K220R mutant displayed a healthy cardiac phenotype, GRK2 inhibition with RKIP showed the opposite effect. In eight-month-old transgenic RKIP mice, signs of cardiac dysfunction, cardiac hypertrophy with dilation and cardiac lipid overload were evident.

7.3.1. Cardioprotective GRK2 inhibition

It is widely accepted, that GRK2 inhibition is cardioprotective. There are several mechanisms which could account for cardioprotection, but the most prominent is the restoration of the β-AR system. β-ARs that are activated by catecholamines are well known for the regulatory function in the heathy heart. Cardiac injury and cardiac stress induced constant release of these hormones and persistent β-AR activation. Sustained β-AR stimulation is cardiotoxic and noradrenaline plasma levels correlate with the degree of cardiac dysfunction and mortality of heart failure patients (*309, 310*). Continuous hyperstimulation of β-ARs is regulated by GRKs and followed by profound desensitization and chronical receptor downregulation (*311*). The hallmark characteristic of heart failure is the loss of the β-AR-mediated inotropic reserve by loss of about 50% of β-AR density attributed to increased GRK2 activity (*163, 312*). Several mouse models of GRK2 inhibition showed restoration of the β-AR system and reversal of cardiac dysfunction.

RKIP and GRK2-K220R both induce comparable signs of GRK2 inhibition

GRK2-RKIP binding prevents GPCR internalisation resulting in enhanced GPCR signalling. Recently, RKIP was suggested to stimulate cardiac contractility and reconstitute β-AR signalling in heart failure (*245*). In addition, RKIP is a dual-specific inhibitor which also blocks the pro-survival Raf/Erk axis. Upon PKC-mediated phosphorylation on serine 153, RKIP dissociates from Raf-1 to dimerize and associate with GRK2 (*241, 244*). However, as described above, RKIP is considered to be cardioprotective only upon phosphorylation. In the present study, the phosphorylation status of RKIP was determined in vivo by immunoblot analysis. In cardiac extract from Tg-RKIP B6 mice the majority of RKIP was phosphorylated on serine 153 (Figure 30).

In addition, both transgenic mouse lines Tg-GRK2-K220R and Tg-RKIP display restoration of the β-AR system. Isolated neonatal cardiomyocytes from Tg-RKIP and Tg-GRK2-K220R mice show comparable enhancement of isoprenaline stimulated cAMP levels. This result confirms that both mouse lines show equivalent GRK2 inhibition with regard to the β-adrenergic receptor response (Figure 30). In conclusion, RKIP is active as a GRK2 inhibitor and is able to modulate the β-AR system. In addition, in microarray gene expression profiling more than 45% of regulated probe sets of GRK2-K220R-transgenic hearts showed concordant regulation with hearts expressing RKIP. This is a further proof, that GRK2 inhibition was effective in both models.

The cardioprotective effect of the dominant-negative GRK2-K220R mutant was analysed in a chronic pressure overload-induced heart failure model imposed by abdominal aortic constriction (AAC). In agreement with data of other GRK2 inhibitors, AAC promoted cardiac dysfunction, as assessed by left ventricular ejection fraction, in non-transgenic mice, whereas in Tg-GRK2-K220R mice, cardiac dysfunction was retarded (Figure 32).

GRK2-K220R is cardioprotective whereas RKIP promotes signs of heart failure

The cardioprotective effect of Tg-GRK2-K220R could be attributed to kinase-mediated effects (see above) and kinase-independent effects because GRK2-K220R also inhibits Gβγ- and $G\alpha_q$-mediated signalling. The regulator of G protein signalling (RGS) domain within the amino terminal domain of GRK2 interacts with and inhibits $G\alpha_q$ (*138, 139, 313*). $G\alpha_q$ is a trigger of maladaptive cardiac hypertrophy after pressure overload (*314*). Transgenic mice with cardiac-specific overexpression of $G\alpha_q$ show a phenotype of decompensated cardiac hypertrophy (*315-317*). A cardiac-specific expression of the RGS domain of GRK2 had an antihypertrophic effect in a mouse model of pressure overload (*318*). In addition to the $G\alpha_q$-inhibitory RGS domain of GRK2, a peptide derived from the carboxyl terminal domain of GRK2, βARKct, sequesters Gβγ proteins to prevent the Gβγ/L-type calcium channel interaction and thereby improves cardiac contractility by increasing the intracellular calcium levels (*248*). GRK2-K220R is able to bind both, $G\alpha_q$ and Gβγ, which could be an explanation for the improved cardiac function in aged Tg-GRK2-K220R mice compared to the B6 control.

In contrast to GRK2-K220R, transgenic hearts which expressed the dual-specific GRK2/Raf inhibitor, RKIP, showed cardiac hypertrophy with a significantly increased heart weight to body weight ratio and a decreased left ventricular ejection fraction.

GRK2 restrains the MAPK pathway by GRK2-mediated desensitization of MAPK-activating GPCRs (*136, 319*). Nuclear MAPK signalling inhibition could be mediated by GRK2-dependent recruitment of β-arrestin (*320-322*). Consequently, GRK2 suppresses MAPK activation and nuclear translocation. Vice versa, GRK2 inhibition activates the nuclear MAPK pathway, and induces nuclear ERK1/2 targets (*220*). Inhibition of GRK2 leads to an activation of the pro-survival Raf/ERK cascade, which overlaps with the cardioprotective properties of the MAPK pathway. Promotion of cell growth protects the failing hearts against cell-death-promoting signals (*323, 324*). Activation of ERK1/2 protects the myocardium against pressure overload-induced hypertrophic cardiomyopathy (*324*) and genetic inhibition of ERK1/2 promotes cardiomyocytes apoptosis (*325*). As discussed in the next chapter,

findings in the here presented thesis strongly suggest, that for cardioprotective GRK2 inhibition an intact Raf/ERK axis is needed.

7.3.2. Inhibition of the Raf/Erk axis by RKIP promotes signs of heart failure

RKIP, which is a dual inhibitor of GRK2 and the Raf/ERK axis, induces signs of heart failure, when overexpressed in the heart. There are several lines of evidence, which provide strong evidence that inhibition of the Raf/ERK axis by RKIP contributes to this heart failure phenotype. Cardiac muscle-specific Raf-1-knockout mice show increased number of apoptotic cardiomyocytes (*326*). Zebrafish treated with sorafenib, a small inhibitor of several tyrosine protein kinases and Raf kinase, show cardiotoxicity, by inhibition of Raf/MEK/ERK (*327*). In agreement with this to the cardiotoxic function of RAF inhibition, RKIP-mediated damage of the heart could be due to a lack of cardioprotective MAPK activation (*323, 324, 328*).

Another target downstream of the Raf/MEK/ERK axis is the PPARG. PPARG is regulated by ERK-mediated phosphorylation on serine 273. Enhanced ERK activity induced by GRK2 inhibition and increased Pparg phosphorylation is part of the cardioprotective gene expression program (*188, 220, 329*), whereas inhibition of the ERK axis with subsequent decrease of Pparg phosphorylation leads to the induction of heart-failure promoting Pparg targets. In the present study, hearts of Tg-RKIP mice showed a significantly decreased phosphorylation of Pparg on serine-273 compared to B6 control and Tg-GRK2-K220R hearts (Figure 26, A). Gene expression analysis revealed the up-regulation of heart failure-related Pparg targets, which are triggered by RKIP, resulting in development of cardiac lipid load and cardiac dysfunction. In B6- and Tg-GRK2-K220R mice none of these genes were upregulated.

Pparg is a transcription factor, which is a main regulator of cardiac energy metabolism. So, cardiomyocyte-specific knockout of Pparg causes cardiac hypertrophy and heart failure (*330*). On the other hand, agonist stimulation and overexpression of PPARG in vivo leads to cardiac hypertrophy, dysfunction and lipid overload (*330, 331*). The Raf/ERK axis could influence PPARG signalling in two ways: MAPK binds directly to PPARG, leading to sequestration PPARG in the cytosol (*288*) and ERK is capable to phosphorylate PPARG on serine 273 and serine 112. Phosphorylation decreases PPARG activation and shifts PPARG target gene expression (*287, 289, 290*). Notable, an inhibition of the Raf/ERK axis by RKIP triggers heart failure-related PPARG targets, resulting in development of cardiac lipid overload and dysfunction (*220*). Excessive lipid accumulation in the heart leads to

decreased cardiac function and is associated with increased PPARG expression. PPARG regulates genes mediating lipid uptake, synthesis, oxidation, lipolysis, and storage, such as fatty acid translocase (*Cd36*), fatty acid synthase (*Fasn*), acyl-CoA oxidase (*AOX*), adipose TAG lipase (*Atgl*), adipose differentiation related protein (*Adrp*), and diacylglycerol acyltransferase1 (*Dgat1*) (*332*). FASN is upregulated in patients with heart failure (*283, 333*) and FASN-transgenic mice develop a heart-failure like phenotype (*188*).

Whole genome microarray gene expression profiling showed up-regulation of heart failure-related Pparg targets in Tg-RKIP mice

Whole genome microarray gene expression profiling showed up-regulation of heart failure-related Pparg target genes in RKIP-transgenic hearts with signs of heart failure. All genes with ≥6-fold upregulated signal intensities between heart tissue of RKIP transgenic, GRK2-K220R transgenic and B6 control mice are discussed below. In transgenic RKIP mice unphosphorylated Pparg is a key player in the gene expression of uncoupling proteins and adipokines, such as adipsin, adiponectin (*334*), and resistin (*335*).

Uncoupling protein 1 (**Ucp1**) is regulated by an Erk1/2-controlled phosphorylation of Pparg (*289, 336*) and is known to exert mitochondrial uncoupling, which is a major feature of failing heart metabolism (*337*). Excessive mitochondrial uncoupling contributes to inefficient cardiac ATP generation and lipid-induced death (*338, 339*). Aged transgenic mice with cardiac-specific UCP1 expression developed cardiac dysfunction, signs of heart failure, and increased mitochondrial uncoupling (*188*).

Adipsin (**Adn**) is a key metabolic regulator and was the first fat-cell selective gene whose expression is altered in obesity (*340*). In heart failure patients increased levels of adipsin were found. Levels of adipsin in heart failure patients were correlated with measures of systemic inflammation, cardiac function and deteriorated diastolic function (*341*).

Adiponectin (**Adipoq**) is a circulating insulin sensitivity factor secreted from adipocytes and essential for maintaining insulin responsiveness (*342*). Adiponectin increases glucose and free fatty acid utilization and stimulates mitochondrial biogenesis (*342*). The role of adiponectin in heart failure is discussed controversially. On one hand reduced adiponectin levels are correlated with increased acute myocardial infarction risk (*343*) and worse cardiac functional recovery after myocardial

infarction with reperfusion (*344*). On the other hand, several clinical studies showed that hyperadiponictemia is associated with poor cardiac function and increased mortality (*345-347*). Transgenic mice with cardiac mutated Pparg-S273A expression show clear signs of hypertrophy and increased adiponectin levels compared to transgenic wildtype-Pparg and B6 control mice (*188*).

Resistin (**Retn**) plays an important regulatory role in obesity, insulin resistance and diabetes (*348*), inflammation and arteriosclerosis (*349*) and cardiovascular diseases. Resistin, originally described as an adipocyte-specific hormone, is also expressed in cardiomyocytes and was shown upregulated by mechanical stress (*350*). Recent studies showed that resistin contributes to cardiac dysfunction, because adenoviral overexpression of resistin can induce hypertrophy in rats (*351*) and resistin blood levels are elevated in patients with heart failure (*352*).

Carbonic anhydrase 3 (**Car3**) in mice is highly abundant in tissues that can store lipids: liver, brown and white fat tissue (*353*). A high-fat-diet-induced phosphorylated Pparg reduced Car 3 expression in fat tissue (*287*).

Perilipin 1 (**Plin1**) is the most abundant protein on the surface of lipid droplets and is responsible for the basal and hormonal regulation of lipolysis (*354*).

Haptoglobin (**Hp**) is expressed in adipose tissue and directly regulated by Pparg during adipocyte differentiation (*355*). Hp is an acute reactant inflammation plasma protein and a significant risk factor for acute myocardial infarction and heart failure (*356*).

Heat shock 70 kDa protein 1 (**Hsp70-1**) is a chaperone protein and contributes to biological processes such as signal transduction, apoptosis, cell growth and differentiation (*357*). High levels of Hsp70-1 are associated with increased mortality in patients with systolic heart failure (*358*).

Cystein dioxygenase type 1 (**Cdo1**) expression is upregulated during adipogenic differentiation and is required for Pparg binding to the target gene promoters (*359*).

In conclusion, most of the 6-fold and higher up-regulated genes in RKIP hearts are Pparg targets and related to heart failure.

7.3.3. Cardiotoxic lipid overload

The heart is by far the most energy-requiring tissue in the body, and under healthy conditions fatty acids are the major substrate of ATP generation (*360*). Lipids trigger a wide spectrum of cardiotoxic mechanisms, such as excessive formation of reactive oxygen species, increased endoplasmic reticulum stress, enhanced apoptosis, and mitochondrial dysfunction (*281, 361*). Lipid accumulation in the myocardium is associated with decreased cardiac function (*362*).

Concomitantly to the increased RKIP protein level and Pparg activation, cardiac palmitate, triacylglycerol (TAG), ceramide and diacylglycerol (DAG) contents of RKIP hearts were elevated compared to Tg-GRK2-K220R and non-transgenic control mice.

Ceramide is involved in many pathogenic components of chronic heart failure, such as apoptosis, inflammation and stress response (*363*). Increased ceramide levels mediate apoptosis through a mitochondrial-dependent pathway of cytochrome c release (*364*). In patients with heart failure, increased plasma ceramide levels correlated with the severity of heart failure (*365*).

An increased cardiac **DAG** and ceramide content could mediate the activation of protein kinase C, which decreases heart function (*281, 366, 367*). In addition, increased PKC activity, could phosphorylate RKIP and switches RKIP from Raf inhibition to more GRK2 inhibition.

Although the heart is able to store some surplus **TAG**, excessive TAG accumulation in the heart correlates with mitochondrial dysfunction or apoptosis (*368*).

In this thesis, the composition of the cardiac lipid content was analysed in detail by gas chromatography. Results showed increased cardiac levels of palmitate and stearate in Tg-RKIP hearts with signs of heart failure. The increased palmitate and stearate contents could contribute to cardiomyocyte death because in primary cardiac myocytes treated with palmitoleate (**C16:1**) or oleate (**cis-C18:1**) did not alter cell viability, while 24 h of treatment with palmitate (**C16:0**) or stearate (**C18:0**) precipitated apoptosis (*369*).

Palmitate is synthesised by FASN in cardiomyocytes and is responsible for the energy supply to the heart muscle. Uncontrolled accumulation of palmitate can induce apoptotic signalling through dissipation of the mitochondrial membrane potential and overproduction of ROS (*370, 371*). In addition, the palmitate-accumulation promotes pro-apoptotic signalling and inhibits the ERK axis (*372*). As a result, the Erk1/2 inhibition triggers an enhanced expression of heart failure-associated Pparg targets. Taken together, my data present strong evidence that inhibition of the Raf/Erk axis by RKIP contributes to signs of heart failure in Tg-RKIP mice.

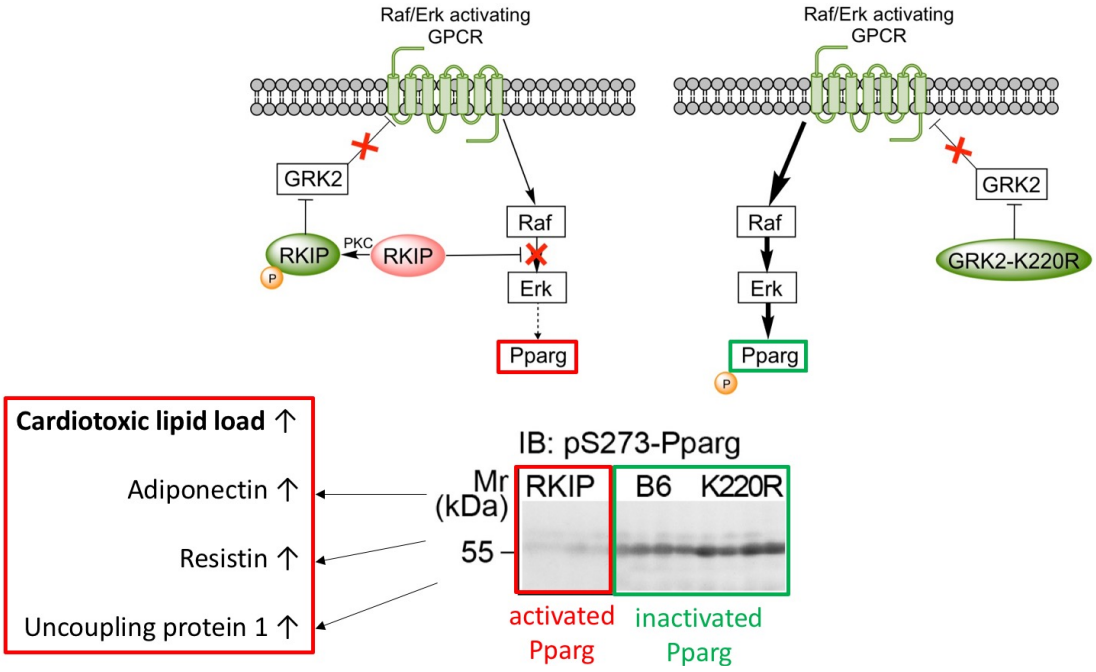

Figure 39: The scheme illustrates inhibition of Raf/Erk axis by RKIP, which results in cardiotoxic Pparg activation

Inhibition of GRK2 leads via reduced desensitisation of Raf/Erk activating GPCR to an activation of the Raf/Erk axis. Activated Erk1/2 is capable to phosphorylate Pparg on serine 273, which decreases Pparg activation. Vice versa, the inhibition of the Raf/Erk axis by RKIP decreases inactivating Pparg phosphorylation and thereby triggers heart failure-related Pparg targets, resulting in development of cardiac lipid overload and dysfunction. Immunoblot detection of pS273-Pparg in cardiac tissue extract of RKIP transgenic mice relative to GRK2-K220R-transgenic mice and non-transgenic B6 controls (6.2.4).

7.3.4. Safety of GRK2-inhibition

GRK2 is an important regulator of signalling and trafficking of GPCRs in many physiological processes in the body. Side effects of GRK2 inhibition need to be addressed, considering that knockout of GRK2 in mice is embryonic lethal (*186*). This lethality stems not from a specific role in heart development, rather from a general role of GRK2 during embryogenesis, because mice with cardiac specific GRK2 ablation develop normally (*373*).

Paroxetine was previously established as a cardioprotective ATP-site GRK2 inhibitor by drug repurposing (*261*). Paroxetine, which was released to the market in 1992, shows a similar safety profile like other antidepressants, which do not inhibit GRK2 (*374*). Compatible with the role of GRK2 in heart development, paroxetine treatment during the first trimester is associated with an increased prevalence of cardiac defects (*375*).

As discussed in the present study, the induction of the Raf/ERK axis by GRK2 inhibition is essential for the cardioprotective effect. Adenovirus-mediated RKIP gene delivery for the treatment of heart failure was currently patented (*376*). This treatment approach bears the risk of cardiotoxic Raf inhibition with subsequent worsening of cardiac function. Notable, cardiomyocyte-specific expression of RKIP triggered heart failure with cardiac hypertrophy and dilatation in different genetic backgrounds. The cardioprotective activity of the Raf/ERK cascade overlaps with the tumor growth-promoting properties of the Raf/ERK axis triggered by GRK2 inhibition (*220*). Thus, GRK2 inhibition and subsequent Raf/ERK induction could be counterproductive in cancer patients.

7.4. GRK2-GRK5 interplay in the heart

GRK2 and GRK5 are both highly abundant in humans. They are both able to modulate the signalling of β-AR and angiotensin II receptor and through those, the performance of the heart.

As discussed before, heart failure is associated with downregulating βAR signalling by increased GRK2 expression or activity. Several strategies of GRK2 inhibition in vivo can improve cardiac function in models of heart failure (*168, 377*), and cardiac-specific knock-out of GRK2 in mice ameliorates symptoms of catecholamine-induced heart failure (*373*). The role of GRK2 seems to depend both on its expression and on the pathophysiological context. The role of the second GRK in the heart, GRK5, is not as well defined. Knock-out of GRK5 is not associated with a cardiac phenotype in mice (*378*), but a massive 30-fold cardiac expression of bovine GRK5 depresses cardiac βAR responsiveness (*174, 193*). GRK2 and GRK5 have a different subcellular localization, receptor specificity and mechanism of activation. This suggests that they have a nonredundant modulatory role in heart failure. GRK2 is rapidly up- and downregulated and its activity is correlated with its ventricular function (*166, 167*). GRK2 is predominantly responsible for the acute regulation of βAR signalling. GRK5 is more important for chronic regulation and seems to be less dynamic (*172, 379*). GRK5-mediated βAR desensitization has adaptive, beneficial effects during early ventricular decompensation. However, inhibition of GRK2 causes upregulation of GRK5. In a study, GRK2 was inhibited by βARKct and 4 weeks after myocardial infarction GRK5 was 2-fold upregulated (*292*).

7.5. Controversial role of GRK5 in heart failure

GRK5 is related to the development of heart failure and cardiac hypertrophy, but its role in these processes is not clear. In the failing heart, GRK5 levels are increased 1.68-fold in the left ventricle (*172*). But the role of GRK5 is still unclear. In 1995 the group of Robert Lefkowitz generated two mouse lines with cardiac specific expression of bovine GRK5 (*174*). One of the mouse lines expressed GRK5 at a low level, whereas the other had a 30-fold increased level of GRK5. Only the high-expressing line was used for further experiments and developed spontaneous heart failure (*193*). By comparison, mouse lines with a four- to six-fold increased expression level of human GRK5-Gln41 and GRK5-Leu41 showed no abnormalities of cardiac size, histological appearance or basal contractile function up to an age of 6 months (*202*). My results are in accordance with these findings. We generated GRK5-transgenic mice with a 2-fold upregulation of GRK5 in heart tissue, which reproduces the GRK5 up-regulation induced by GRK2 inhibition, and the up-regulation seen in human heart failure patients. Tg-GRK5 mice did not show any signs of cardiac hypertrophy, i.e. the heart weight to body weight ratio was not significantly different from non-transgenic controls. Histology analysis of hematoxylin-eosin-stained heart sections further documented that moderate GRK5 overexpression did not cause any cardiac abnormalities. Thus, my data showed that moderate GRK5 expression had no adverse cardiac effect. With the newly established GRK5-transgenic model, future studies will have to investigate the role of GRK5 under pathophysiological conditions. For example, we could use a model of abdominal aortic constriction to determine whether increased cardiac GRK5 levels influence myocardial response to ventricular pressure overload.

In our Tg-GRK5 mice, GRK5 is expressed under control of the human cytomegalovirus immediate-early promoter/enhancer, which directs ubiquitous expression of the transgene. These transgenic mice can be also used to study the role of GRK5 upregulation in virtually every tissue. GRK5 levels in the frontal cortex and hippocampus were highly increased. GRK5 could counteract the pathogenesis of Alzheimer's and Parkinson's disease. In this respect, the herein generated Tg-GRK5 model could be used to identify potential neuroprotective mechanisms initiated by GRK5. Finally, GRK5 expression levels in other tissues also need to be analysed, in order to investigate the potential role of GRK5 in hypertension or diabetes, which was suggested by previous studies.

7.6. Conclusion

GRK2 is widely accepted as a drug target in the treatment of heart failure. To date, all efforts towards a clinically approved drug were not successful, yet. This is also owed to the fact, that the underlying mechanism of GRK2 inhibition is not fully understood.

In the present study, I identified mechanisms that are required for cardioprotective GRK2-inhibition. I established SRSF1 as a new substrate of GRK2 and compared substrate specificity of the GRK2 inhibitors, RKIP and paroxetine. Paroxetine is able to inhibit GRK2 mediated SRSF1 phosphorylation, whereas RKIP does not. This could be of major relevance in vivo, because paroxetine showed cardioprotection against myocardial infarction-induced heart failure whereas RKIP promotes heart failure. This heart failure-enhancing activity of RKIP was further established by the present study. RKIP led to activation of the adipogenic and heart failure-promoting transcription factor Pparg by inhibition of the Raf-Erk axis-mediated serine-273 phosphorylation of Pparg. In contrast, GRK2 inhibition by transgenic expression of the dominant-negative GRK2-K220R mutant did not activate Pparg and retarded the development of chronic pressure overload-induced cardiac dysfunction imposed by abdominal aortic constriction. From these data it is concluded that an intact Raf-Erk axis is required for cardioprotective GRK2 inhibition. In addition, a new transgenic model was established, which allows to study the impact of compensatory GRK5 up-regulation under conditions of GRK2 inhibition. The newly established GRK5-transgenic model showed that moderate GRK5 expression had no adverse cardiac effect. However, further research is needed to characterize the role of GRK5 under pathophysiological conditions.

8. Acknowledgments

I would like to thank Prof. Dr. Ursula Quitterer for giving me the opportunity to work on this exciting project as part of my PhD thesis and for her support throughout the years. I would also like to thank Prof. Dr. Jonathan Hall for being my co-supervisor.

Special thanks to Dr. Andreas Langer for his assistance with various laboratory techniques.

Thanks go to Dr. Joshua Abd Alla for introduction into transgenic mouse techniques and to my fellow PhD students Dr. Muriel Grämer and Alexander Perhal, for scientific and non-scientific exchange and to our animal caretaker, Marianne Antony.

Finally, I would like to thank my master students Philipp Hanke, Clara Schölly, Kira Heusler, Olivia Bolli, Melanie Saxer, Andrea Tanner and Ladina Cabalzar.

Big thanks go to my family and especially to Susanne Stranimaier for the great patience and support over the past years.

9. Curriculum vitae

Stefan Wolf

Ph.D. Student
Molecular Pharmacology
ETH Zurich
Winterthurerstrasse 190
8057 Zürich
Switzerland
E-Mail: stefan.wolf@pharma.ethz.ch

Personal information

Date of birth:	July 17th, 1987
Place of birth:	Graz
Nationality:	Austrian

Education

July 2014 – present	Ph.D. Student in the group of Prof. Dr. Ursula Quitterer, Institute of Pharmaceutical Sciences, ETH Zurich, Molecular Pharmacology
2013	Austrian Pharmacist's Diploma
June 2012 – June 2013	12-month internship in two public pharmacies
March 2011 – June 2012	Master Thesis in the group of Prof. Dr. Klaus Groschner, Institute of Pharmaceutical Sciences, Karl-Franzens-University of Graz, Department of Pharmacology
2006 – 2012	Master's Degree in Pharmaceutical Sciences, Karl-Franzens-University of Graz, Austria

10. Publications

Patent application

Abd Alla J, **Wolf S**, and Quitterer U. (2018), Cell-protective compounds and their use, WO2018130537

Abd Alla J, Graemer M, **Wolf S**, and Quitterer U. (2016), Invention of a prototype, which is cardioprotective by inhibition of GRK2-mediated phosphorylation of a novel non-receptor GRK2 substrate, the Serine/arginine-rich splicing factor 1 (SRSF1), patent application approved by ETH Transfer (ETH 2016-138)

Peer-reviewed publications

Doleschal B, Primessnig U, Wölkart G, **Wolf S**, Schernthaner M, Lichtenegger M, Glasnov TN, Kappe OC, Mayer B, Antoons G, Heinzel F, Poteser M, and Groschner K. (2015) TRPC3 contributes to regulation of cardiac contractility and arrhythmogenesis by dynamic interaction with NCX1. Cardiovascular Research, **106**, 163-73

Other publications (not peer-reviewed)

Wolf S, Graemer M, Langer A and Quitterer U. (2016) Myocardium-specific expression of the human raf kinase inhibitor protein (RKIP) induces cardiac hypertrophy, ECG abnormalities and signs of heart failure. Naunyn-Schmiedeber`s Arch Pharmacol, 389 (Supplement 1): 39-39,

Abd Alla J, Graemer M, **Wolf S**, Quitterer U. (2016). Inhibition of GRK2 counteracts the dysfunctional cardiac substrate metabolism of late-stage heart failure. Naunyn- Schmiedebergs`s Arch. Pharmacol 389 (Supplement 1), S39

Conference contributions

Short talk:

Wolf S, Abd Alla J, and Quitterer U (2018) RKIP Induces Heart Failure by Promoting Angiotensin II AT1 Receptor Hypersensitivity. Talk. KININ2018CLE, Cleveland, Ohio, USA, June 17-20 **(selected short talk at KININ2018Cle, awarded with a "Travel Award")**

Poster presentations:

Wolf S, Abd Alla J, and Quitterer U (2018) RKIP Induces Heart Failure by Promoting Angiotensin II AT1 Receptor Hypersensitivity. Poster. KININ2018CLE, Cleveland, Ohio, USA, June 17-20

Langer A, Abd Alla J, **Wolf S** and Quitterer U. (2017) The serine/arginine-rich splicing factor (SRSF1) is a non-receptor substrate of GRK2. Poster. GRKs and Arrestins: From Structure to Disease, Saxtone River, Vermont, USA, June 11-16

Wolf S, Abd Alla J, Quitterer U. (2017) Cardioprotective GRK2 inhibition down-regulates the heart failure-promoting cardiotoxic lipid metabolic process. Poster. Keystone Symposia on Molecular and Cellular Biology: Mitochondria, Metabolism and Heart, Santa Fe, New Mexico, USA, May 8-12

Wolf S, Graemer M, Langer A, Quitterer U. (2016) Myocardium-specific expression of the human raf kinase inhibitor protein (RKIP) induces cardiac hypertrophy, ECG abnormalities and signs of heart failure. Poster. 82th Annual Meeting of the German Society of Experimental and Clinical Pharmacology and Toxicology, Berlin, Germany, February 28 – March 3.

Wolf S, Doleschal B, Huber M.-S, Wölkart G, Groschner K. (2012) Schlüsselrolle von TRPC3 in der Angiotensin II – vermittelten kardialen Dysfunktion. Annual Congress of the Austrian Society of Cardiology. Poster, Salzburg, Austria May 30 - June 2

Other conference contributions

Abd Alla J, **Wolf S**, Quitterer U. (2017) Development of a non-peptide GRK2 inhibitor. Poster. DDNZ Zurich, 3rd Symposium, February 10

Abd Alla J, Graemer M, **Wolf S**, Quitterer U. (2016) Inhibition of GRK2 counteracts the dysfunctional cardiac substrate metabolism of late-stage heart failure. Poster. 82th Annual Meeting of the German Society of Experimental and Clinical Pharmacology and Toxicology, Berlin, Germany, February 28 – March 3.

Doleschal B, **Wolf S**, Schernthaner M, Wölkart G, Antoons G, Heinzel F, Groschner K. (2013) Remodelling of the Cardiac NCX1-TRPC3 Signaling Complex promotes Angiotensin II – induced Arrhythmogenesis. Poster. 57th Annual Meeting of the Biophysical-Society, Philadelphia, USA, February 02-06

Doleschal B, **Wolf S**, Huber M.-S, Wölkart G, Groschner K. (2012) TRPC3 overexpression promotes Angiotensin II induced cardiac dysfunction. Poster. 78th Annual Congress of the German Society of Cardiology, Mannheim, Germany, April 11-14

11. List of figures

12. References

1. K. L. Pierce, R. T. Premont, R. J. Lefkowitz, Seven-transmembrane receptors. *Nat Rev Mol Cell Biol* **3**, 639-650 (2002).

2. D. R. Flower, Modelling G-protein-coupled receptors for drug design. *Biochim Biophys Acta* **1422**, 207-234 (1999).

3. E. S. Lander, L. M. Linton, B. Birren, C. Nusbaum, M. C. Zody, J. Baldwin, K. Devon, K. Dewar, M. Doyle, W. FitzHugh, R. Funke, D. Gage, K. Harris, A. Heaford, J. Howland *et al.*, Initial sequencing and analysis of the human genome. *Nature* **409**, 860-921 (2001).

4. R. Fredriksson, M. C. Lagerstrom, L. G. Lundin, H. B. Schioth, The G-protein-coupled receptors in the human genome form five main families. Phylogenetic analysis, paralogon groups, and fingerprints. *Mol Pharmacol* **63**, 1256-1272 (2003).

5. X. Lv, J. Liu, Q. Shi, Q. Tan, D. Wu, J. J. Skinner, A. L. Walker, L. Zhao, X. Gu, N. Chen, L. Xue, P. Si, L. Zhang, Z. Wang, V. Katritch *et al.*, In vitro expression and analysis of the 826 human G protein-coupled receptors. *Protein Cell* **7**, 325-337 (2016).

6. T. K. Bjarnadottir, D. E. Gloriam, S. H. Hellstrand, H. Kristiansson, R. Fredriksson, H. B. Schioth, Comprehensive repertoire and phylogenetic analysis of the G protein-coupled receptors in human and mouse. *Genomics* **88**, 263-273 (2006).

7. M. C. Lagerstrom, H. B. Schioth, Structural diversity of G protein-coupled receptors and significance for drug discovery. *Nat Rev Drug Discov* **7**, 339-357 (2008).

8. E. J. Neer, G proteins: critical control points for transmembrane signals. *Protein science : a publication of the Protein Society* **3**, 3-14 (1994).

9. J. Wess, G-protein-coupled receptors: molecular mechanisms involved in receptor activation and selectivity of G-protein recognition. *FASEB journal : official publication of the Federation of American Societies for Experimental Biology* **11**, 346-354 (1997).

10. D. L. Farrens, C. Altenbach, K. Yang, W. L. Hubbell, H. G. Khorana, Requirement of rigid-body motion of transmembrane helices for light activation of rhodopsin. *Science* **274**, 768-770 (1996).

11. J. A. Ballesteros, A. D. Jensen, G. Liapakis, S. G. Rasmussen, L. Shi, U. Gether, J. A. Javitch, Activation of the beta 2-adrenergic receptor involves disruption of an ionic lock between the cytoplasmic ends of transmembrane segments 3 and 6. *The Journal of biological chemistry* **276**, 29171-29177 (2001).

12. D. A. Shapiro, K. Kristiansen, D. M. Weiner, W. K. Kroeze, B. L. Roth, Evidence for a model of agonist-induced activation of 5-hydroxytryptamine 2A serotonin receptors that involves the disruption of a strong ionic interaction between helices 3 and 6. *The Journal of biological chemistry* **277**, 11441-11449 (2002).

13. S. J. Han, F. F. Hamdan, S. K. Kim, K. A. Jacobson, L. M. Bloodworth, B. Li, J. Wess, Identification of an agonist-induced conformational change occurring adjacent to the ligand-binding pocket of the M(3) muscarinic acetylcholine receptor. *The Journal of biological chemistry* **280**, 34849-34858 (2005).

14. M. Han, M. Groesbeek, T. P. Sakmar, S. O. Smith, The C9 methyl group of retinal interacts with glycine-121 in rhodopsin. *Proceedings of the National Academy of Sciences of the United States of America* **94**, 13442-13447 (1997).

15. T. W. Hunt, T. A. Fields, P. J. Casey, E. G. Peralta, RGS10 is a selective activator of G alpha i GTPase activity. *Nature* **383**, 175-177 (1996).

16. E. J. Neer, Heterotrimeric G proteins: organizers of transmembrane signals. *Cell* **80**, 249-257 (1995).

17. G. B. Downes, N. Gautam, The G protein subunit gene families. *Genomics* **62**, 544-552 (1999).

18. M. I. Simon, M. P. Strathmann, N. Gautam, Diversity of G proteins in signal transduction. *Science* **252**, 802-808 (1991).

19. W. M. Oldham, H. E. Hamm, Heterotrimeric G protein activation by G-protein-coupled receptors. *Nat Rev Mol Cell Biol* **9**, 60-71 (2008).

20. F. Li, M. De Godoy, S. Rattan, Role of adenylate and guanylate cyclases in beta1-, beta2-, and beta3-adrenoceptor-mediated relaxation of internal anal sphincter smooth muscle. *J Pharmacol Exp Ther* **308**, 1111-1120 (2004).

21. T. Flock, A. S. Hauser, N. Lund, D. E. Gloriam, S. Balaji, M. M. Babu, Selectivity determinants of GPCR-G-protein binding. *Nature* **545**, 317-322 (2017).

22. P. Y. Sato, J. K. Chuprun, M. Schwartz, W. J. Koch, The evolving impact of g protein-coupled receptor kinases in cardiac health and disease. *Physiol Rev* **95**, 377-404 (2015).

23. J. K. Northup, P. C. Sternweis, M. D. Smigel, L. S. Schleifer, E. M. Ross, A. G. Gilman, Purification of the regulatory component of adenylate cyclase. *Proceedings of the National Academy of Sciences of the United States of America* **77**, 6516-6520 (1980).

24. A. E. Leroux, J. O. Schulze, R. M. Biondi, AGC kinases, mechanisms of regulation and innovative drug development. *Semin Cancer Biol* **48**, 1-17 (2018).

25. T. J. Kamp, J. W. Hell, Regulation of cardiac L-type calcium channels by protein kinase A and protein kinase C. *Circulation research* **87**, 1095-1102 (2000).

26. J. Shi, W. Qian, X. Yin, K. Iqbal, I. Grundke-Iqbal, X. Gu, F. Ding, C. X. Gong, F. Liu, Cyclic AMP-dependent protein kinase regulates the alternative splicing of tau exon 10: a mechanism involved in tau pathology of Alzheimer disease. *The Journal of biological chemistry* **286**, 14639-14648 (2011).

27. R. Taussig, J. A. Iniguez-Lluhi, A. G. Gilman, Inhibition of adenylyl cyclase by Gi alpha. *Science* **261**, 218-221 (1993).

28. S. J. Taylor, J. A. Smith, J. H. Exton, Purification from bovine liver membranes of a guanine nucleotide-dependent activator of phosphoinositide-specific phospholipase C. Immunologic identification as a novel G-protein alpha subunit. *The Journal of biological chemistry* **265**, 17150-17156 (1990).

29. A. M. Lyon, J. J. G. Tesmer, Structural Insights into Phospholipase C-beta Function. *Molecular pharmacology* **84**, 488-500 (2013).

30. M. J. Berridge, Cardiac calcium signalling. *Biochem Soc T* **31**, 930-933 (2003).

31. E. A. Woodcock, D. R. Grubb, T. M. Filtz, S. Marasco, J. T. Luo, T. J. McLeod-Dryden, D. M. Kaye, J. Sadoshima, X. J. Du, C. Wong, J. R. McMullen, A. M. Dart, Selective activation of the "b" splice variant of phospholipase C beta 1 in chronically dilated human and mouse atria. *Journal of Molecular and Cellular Cardiology* **47**, 676-683 (2009).

32. H. Jiang, Y. Kuang, Y. Wu, W. Xie, M. I. Simon, D. Wu, Roles of phospholipase C beta2 in chemoattractant-elicited responses. *Proceedings of the National Academy of Sciences of the United States of America* **94**, 7971-7975 (1997).

33. Z. Li, H. Jiang, W. Xie, Z. Zhang, A. V. Smrcka, D. Wu, Roles of PLC-beta2 and -beta3 and PI3Kgamma in chemoattractant-mediated signal transduction. *Science* **287**, 1046-1049 (2000).

34. K. S. Murthy, G. M. Makhlouf, Opioid mu, delta, and kappa receptor-induced activation of phospholipase C-beta 3 and inhibition of adenylyl cyclase is mediated by Gi2 and G(o) in smooth muscle. *Molecular pharmacology* **50**, 870-877 (1996).

35. Y. L. Wu, G. Pei, G. H. Fan, Inhibition of phospholipase C blocks opioid receptor-mediated activation of Gi proteins. *Neuroreport* **9**, 99-103 (1998).

36. J. L. Mathews, A. V. Smrcka, J. M. Bidlack, A novel Gbetagamma-subunit inhibitor selectively modulates mu-opioid-dependent antinociception and attenuates acute morphine-induced antinociceptive tolerance and dependence. *J Neurosci* **28**, 12183-12189 (2008).

37. S. S. Palaniyandi, L. Sun, J. C. Ferreira, D. Mochly-Rosen, Protein kinase C in heart failure: a therapeutic target? *Cardiovasc Res* **82**, 229-239 (2009).

38. A. C. Newton, Protein kinase C: poised to signal. *Am J Physiol Endocrinol Metab* **298**, E395-402 (2010).

39. M. P. Strathmann, M. I. Simon, G alpha 12 and G alpha 13 subunits define a fourth class of G protein alpha subunits. *Proceedings of the National Academy of Sciences of the United States of America* **88**, 5582-5586 (1991).

40. S. Fukuhara, H. Chikumi, J. S. Gutkind, RGS-containing RhoGEFs: the missing link between transforming G proteins and Rho? *Oncogene* **20**, 1661-1668 (2001).

41. P. Dutt, N. Nguyen, D. Toksoz, Role of Lbc RhoGEF in G alpha 12/13-induced signals to Rho GTPase. *Cellular Signalling* **16**, 201-209 (2004).

42. V. P. Sah, T. M. Seasholtz, S. A. Sagi, J. H. Brown, The role of Rho in G protein-coupled receptor signal transduction. *Annu Rev Pharmacol* **40**, 459-489 (2000).

43. M. A. Wall, D. E. Coleman, E. Lee, J. A. Iniguez-Lluhi, B. A. Posner, A. G. Gilman, S. R. Sprang, The structure of the G protein heterotrimer Gi alpha 1 beta 1 gamma 2. *Cell* **83**, 1047-1058 (1995).

44. W. F. Simonds, J. E. Butrynski, N. Gautam, C. G. Unson, A. M. Spiegel, G-protein beta gamma dimers. Membrane targeting requires subunit coexpression and intact gamma C-A-A-X domain. *The Journal of biological chemistry* **266**, 5363-5366 (1991).

45. D. E. Clapham, E. J. Neer, G protein beta gamma subunits. *Annu Rev Pharmacol Toxicol* **37**, 167-203 (1997).

46. D. E. Logothetis, Y. Kurachi, J. Galper, E. J. Neer, D. E. Clapham, The beta gamma subunits of GTP-binding proteins activate the muscarinic K+ channel in heart. *Nature* **325**, 321-326 (1987).

47. K. D. Wickman, J. A. Iniguez-Lluhl, P. A. Davenport, R. Taussig, G. B. Krapivinsky, M. E. Linder, A. G. Gilman, D. E. Clapham, Recombinant G-protein beta gamma-subunits activate the muscarinic-gated atrial potassium channel. *Nature* **368**, 255-257 (1994).

48. J. A. Pitcher, J. Inglese, J. B. Higgins, J. L. Arriza, P. J. Casey, C. Kim, J. L. Benovic, M. M. Kwatra, M. G. Caron, R. J. Lefkowitz, Role of beta gamma subunits of G proteins in targeting the beta-adrenergic receptor kinase to membrane-bound receptors. *Science* **257**, 1264-1267 (1992).

49. M. Camps, A. Carozzi, P. Schnabel, A. Scheer, P. J. Parker, P. Gierschik, Isozyme-selective stimulation of phospholipase C-beta 2 by G protein beta gamma-subunits. *Nature* **360**, 684-686 (1992).

50. S. Diel, K. Klass, B. Wittig, C. Kleuss, G beta gamma activation site in adenylyl cyclase type II Adenylyl cyclase type III is inhibited by G beta gamma. *Journal of Biological Chemistry* **281**, 288-294 (2006).

51. W. J. Tang, A. G. Gilman, Type-specific regulation of adenylyl cyclase by G protein beta gamma subunits. *Science* **254**, 1500-1503 (1991).

52. R. K. Sunahara, R. Taussig, Isoforms of mammalian adenylyl cyclase: multiplicities of signaling. *Mol Interv* **2**, 168-184 (2002).

53. S. Herlitze, D. E. Garcia, K. Mackie, B. Hille, T. Scheuer, W. A. Catterall, Modulation of Ca2+ channels by G-protein beta gamma subunits. *Nature* **380**, 258-262 (1996).

54. S. R. Ikeda, Voltage-dependent modulation of N-type calcium channels by G-protein beta gamma subunits. *Nature* **380**, 255-258 (1996).

55. P. Crespo, N. Xu, W. F. Simonds, J. S. Gutkind, Ras-dependent activation of MAP kinase pathway mediated by G-protein beta gamma subunits. *Nature* **369**, 418-420 (1994).

56. W. J. Koch, B. E. Hawes, L. F. Allen, R. J. Lefkowitz, Direct evidence that Gi-coupled receptor stimulation of mitogen-activated protein kinase is mediated by G beta gamma activation of p21ras. *Proceedings of the National Academy of Sciences of the United States of America* **91**, 12706-12710 (1994).

57. O. A. Coso, H. Teramoto, W. F. Simonds, J. S. Gutkind, Signaling from G protein-coupled receptors to c-Jun kinase involves beta gamma subunits of heterotrimeric G proteins acting on a Ras and Rac1-dependent pathway. *The Journal of biological chemistry* **271**, 3963-3966 (1996).

58. J. J. Yamauchi, M. Nagao, Y. Kaziro, H. Itoh, Activation of p38 mitogen-activated protein kinase by signaling through G protein-coupled receptors - Involvement of G beta gamma and G alpha(q/11) subunits. *Journal of Biological Chemistry* **272**, 27771-27777 (1997).

59. U. Wilden, S. W. Hall, H. Kuhn, Phosphodiesterase activation by photoexcited rhodopsin is quenched when rhodopsin is phosphorylated and binds the intrinsic 48-kDa protein of rod outer segments. *Proceedings of the National Academy of Sciences of the United States of America* **83**, 1174-1178 (1986).

60. K. L. Pierce, R. J. Lefkowitz, Classical and new roles of beta-arrestins in the regulation of G-protein-coupled receptors. *Nat Rev Neurosci* **2**, 727-733 (2001).

61. W. E. Miller, R. J. Lefkowitz, Expanding roles for beta-arrestins as scaffolds and adapters in GPCR signaling and trafficking. *Curr Opin Cell Biol* **13**, 139-145 (2001).

62. M. J. Lohse, J. L. Benovic, J. Codina, M. G. Caron, R. J. Lefkowitz, Beta-Arrestin - a Protein That Regulates Beta-Adrenergic-Receptor Function. *Science* **248**, 1547-1550 (1990).

63. H. Attramadal, J. L. Arriza, C. Aoki, T. M. Dawson, J. Codina, M. M. Kwatra, S. H. Snyder, M. G. Caron, R. J. Lefkowitz, Beta-arrestin2, a novel member of the arrestin/beta-arrestin gene family. *The Journal of biological chemistry* **267**, 17882-17890 (1992).

64. Y. Kang, X. E. Zhou, X. Gao, Y. He, W. Liu, A. Ishchenko, A. Barty, T. A. White, O. Yefanov, G. W. Han, Q. Xu, P. W. de Waal, J. Ke, M. H. Tan, C. Zhang *et al.*, Crystal structure of rhodopsin bound to arrestin by femtosecond X-ray laser. *Nature* **523**, 561-567 (2015).

65. A. K. Shukla, G. H. Westfield, K. Xiao, R. I. Reis, L. Y. Huang, P. Tripathi-Shukla, J. Qian, S. Li, A. Blanc, A. N. Oleskie, A. M. Dosey, M. Su, C. R. Liang, L. L. Gu, J. M. Shan *et al.*, Visualization of arrestin recruitment by a G-protein-coupled receptor. *Nature* **512**, 218-222 (2014).

66. M. Szczepek, F. Beyriere, K. P. Hofmann, M. Elgeti, R. Kazmin, A. Rose, F. J. Bartl, D. von Stetten, M. Heck, M. E. Sommer, P. W. Hildebrand, P. Scheerer, Crystal structure of a common GPCR-binding interface for G protein and arrestin. *Nat Commun* **5**, 4801 (2014).

67. O. B. Goodman, J. G. Krupnick, F. Santini, V. V. Gurevich, R. B. Penn, A. W. Gagnon, J. H. Keen, J. L. Benovic, beta-arrestin acts as a clathrin adaptor in endocytosis of the beta(2)-adrenergic receptor. *Nature* **383**, 447-450 (1996).

68. R. H. Oakley, S. A. Laporte, J. A. Holt, L. S. Barak, M. G. Caron, Association of beta-arrestin with G protein-coupled receptors during clathrin-mediated endocytosis dictates the profile of receptor resensitization. *The Journal of biological chemistry* **274**, 32248-32257 (1999).

69. J. Trejo, S. R. Coughlin, The cytoplasmic tails of protease-activated receptor-1 and substance P receptor specify sorting to lysosomes versus recycling. *The Journal of biological chemistry* **274**, 2216-2224 (1999).

70. K. J. Morrison, R. H. Moore, N. D. Carsrud, J. Trial, E. E. Millman, M. Tuvim, R. B. Clark, R. Barber, B. F. Dickey, B. J. Knoll, Repetitive endocytosis and recycling of the beta 2-adrenergic receptor during agonist-induced steady state redistribution. *Molecular pharmacology* **50**, 692-699 (1996).

71. D. Calebiro, V. O. Nikolaev, M. C. Gagliani, T. de Filippis, C. Dees, C. Tacchetti, L. Persani, M. J. Lohse, Persistent cAMP-Signals Triggered by Internalized G-Protein-Coupled Receptors. *Plos Biol* **7**, (2009).

72. S. Ferrandon, T. N. Feinstein, M. Castro, B. Wang, R. Bouley, J. T. Potts, T. J. Gardella, J. P. Vilardaga, Sustained cyclic AMP production by parathyroid hormone receptor endocytosis. *Nat Chem Biol* **5**, 734-742 (2009).

73. F. Mullershausen, F. Zecri, C. Cetin, A. Billich, D. Guerini, K. Seuwen, Persistent signaling induced by FTY720-phosphate is mediated by internalized S1P1 receptors. *Nat Chem Biol* **5**, 428-434 (2009).

74. T. N. Feinstein, N. Yui, M. J. Webber, V. L. Wehbi, H. P. Stevenson, J. D. King, K. R. Hallows, D. Brown, R. Bouley, J. P. Vilardaga, Noncanonical Control of Vasopressin Receptor Type 2 Signaling by Retromer and Arrestin. *Journal of Biological Chemistry* **288**, 27849-27860 (2013).

75. J. P. Vilardaga, F. G. Jean-Alphonse, T. J. Gardella, Endosomal generation of cAMP in GPCR signaling. *Nat Chem Biol* **10**, 700-706 (2014).

76. A. R. Thomsen, B. Plouffe, T. J. Cahill, 3rd, A. K. Shukla, J. T. Tarrasch, A. M. Dosey, A. W. Kahsai, R. T. Strachan, B. Pani, J. P. Mahoney, L. Huang, B. Breton, F. M. Heydenreich, R. K. Sunahara, G. Skiniotis *et al.*, GPCR-G Protein-beta-Arrestin Super-Complex Mediates Sustained G Protein Signaling. *Cell* **166**, 907-919 (2016).

77. E. Reiter, R. J. Lefkowitz, GRKs and beta-arrestins: roles in receptor silencing, trafficking and signaling. *Trends Endocrin Met* **17**, 159-165 (2006).

78. L. M. Luttrell, S. S. Ferguson, Y. Daaka, W. E. Miller, S. Maudsley, G. J. Della Rocca, F. Lin, H. Kawakatsu, K. Owada, D. K. Luttrell, M. G. Caron, R. J. Lefkowitz, Beta-arrestin-dependent formation of beta2 adrenergic receptor-Src protein kinase complexes. *Science* **283**, 655-661 (1999).

79. L. M. Luttrell, F. L. Roudabush, E. W. Choy, W. E. Miller, M. E. Field, K. L. Pierce, R. J. Lefkowitz, Activation and targeting of extracellular signal-regulated kinases by beta-arrestin scaffolds. *Proceedings of the National Academy of Sciences of the United States of America* **98**, 2449-2454 (2001).

80. K. A. DeFea, J. Zalevsky, M. S. Thoma, O. Dery, R. D. Mullins, N. W. Bunnett, beta-Arrestin-dependent endocytosis of proteinase-activated receptor 2 is required for intracellular targeting of activated ERK1/2. *J Cell Biol* **148**, 1267-1281 (2000).

81. Y. Sun, Z. J. Cheng, L. Ma, G. Pei, beta-arrestin2 is critically involved in CXCR4-mediated chemotaxis, and this is mediated by its enhancement of p38 MAPK activation. *Journal of Biological Chemistry* **277**, 49212-49219 (2002).

82. P. H. McDonald, C. W. Chow, W. E. Miller, S. A. Laporte, M. E. Field, F. T. Lin, R. J. Davis, R. J. Lefkowitz, beta-Arrestin 2: A receptor-regulated MAPK scaffold for the activation of JNK3. *Science* **290**, 1574-1577 (2000).

83. H. Gao, Y. Sun, Y. L. Wu, B. Luan, Y. Y. Wang, B. Qu, G. Pei, Identification of beta-arrestin2 as a G protein-coupled receptor-stimulated regulator of NF-kappa B pathways. *Molecular Cell* **14**, 303-317 (2004).

84. J. S. Smith, R. J. Lefkowitz, S. Rajagopal, Biased signalling: from simple switches to allosteric microprocessors. *Nat Rev Drug Discov*, (2018).

85. S. Nuber, U. Zabel, K. Lorenz, A. Nuber, G. Milligan, A. B. Tobin, M. J. Lohse, C. Hoffmann, beta-Arrestin biosensors reveal a rapid, receptor-dependent activation/deactivation cycle. *Nature* **531**, 661-664 (2016).

86. M. H. Lee, K. M. Appleton, E. G. Strungs, J. Y. Kwon, T. A. Morinelli, Y. K. Peterson, S. A. Laporte, L. M. Luttrell, The conformational signature of beta-arrestin2 predicts its trafficking and signalling functions. *Nature* **531**, 665-668 (2016).

87. J. W. Wisler, S. M. DeWire, E. J. Whalen, J. D. Violin, M. T. Drake, S. Ahn, S. K. Shenoy, R. J. Lefkowitz, A unique mechanism of beta-blocker action: carvedilol stimulates beta-arrestin signaling. *Proceedings of the National Academy of Sciences of the United States of America* **104**, 16657-16662 (2007).

88. S. K. Shenoy, R. J. Lefkowitz, beta-Arrestin-mediated receptor trafficking and signal transduction. *Trends in pharmacological sciences* **32**, 521-533 (2011).

89. K. N. Nobles, K. Xiao, S. Ahn, A. K. Shukla, C. M. Lam, S. Rajagopal, R. T. Strachan, T. Y. Huang, E. A. Bressler, M. R. Hara, S. K. Shenoy, S. P. Gygi, R. J. Lefkowitz, Distinct

phosphorylation sites on the beta(2)-adrenergic receptor establish a barcode that encodes differential functions of beta-arrestin. *Sci Signal* **4**, ra51 (2011).

90. J. L. Benovic, A. DeBlasi, W. C. Stone, M. G. Caron, R. J. Lefkowitz, Beta-adrenergic receptor kinase: primary structure delineates a multigene family. *Science* **246**, 235-240 (1989).

91. R. T. Premont, A. D. Macrae, S. A. Aparicio, H. E. Kendall, J. E. Welch, R. J. Lefkowitz, The GRK4 subfamily of G protein-coupled receptor kinases. Alternative splicing, gene organization, and sequence conservation. *The Journal of biological chemistry* **274**, 29381-29389 (1999).

92. H. G. Dohlman, J. Thorner, M. G. Caron, R. J. Lefkowitz, Model systems for the study of seven-transmembrane-segment receptors. *Annu Rev Biochem* **60**, 653-688 (1991).

93. J. L. Benovic, J. J. Onorato, J. L. Arriza, W. C. Stone, M. Lohse, N. A. Jenkins, D. J. Gilbert, N. G. Copeland, M. G. Caron, R. J. Lefkowitz, Cloning, expression, and chromosomal localization of beta-adrenergic receptor kinase 2. A new member of the receptor kinase family. *The Journal of biological chemistry* **266**, 14939-14946 (1991).

94. P. Kunapuli, J. L. Benovic, Cloning and expression of GRK5: a member of the G protein-coupled receptor kinase family. *Proceedings of the National Academy of Sciences of the United States of America* **90**, 5588-5592 (1993).

95. C. Y. Chen, S. B. Dion, C. M. Kim, J. L. Benovic, Beta-adrenergic receptor kinase. Agonist-dependent receptor binding promotes kinase activation. *The Journal of Biological Chemistry* **268**, 7825-7831 (1993).

96. B. Haribabu, R. Snyderman, Identification of additional members of human G-protein-coupled receptor kinase multigene family. *Proceedings of the National Academy of Sciences of the United States of America* **90**, 9398-9402 (1993).

97. J. M. Willets, R. A. Challiss, S. R. Nahorski, Non-visual GRKs: are we seeing the whole picture? *Trends in pharmacological sciences* **24**, 626-633 (2003).

98. W. Lorenz, J. Inglese, K. Palczewski, J. J. Onorato, M. G. Caron, R. J. Lefkowitz, The receptor kinase family: primary structure of rhodopsin kinase reveals similarities to the beta-adrenergic receptor kinase. *Proceedings of the National Academy of Sciences of the United States of America* **88**, 8715-8719 (1991).

99. O. Hisatomi, S. Matsuda, T. Satoh, S. Kotaka, Y. Imanishi, F. Tokunaga, A novel subtype of G-protein-coupled receptor kinase, GRK7, in teleost cone photoreceptors. *FEBS Lett* **424**, 159-164 (1998).

100. R. T. Premont, A. D. Macrae, R. H. Stoffel, N. Chung, J. A. Pitcher, C. Ambrose, J. Inglese, M. E. MacDonald, R. J. Lefkowitz, Characterization of the G protein-coupled receptor kinase GRK4. Identification of four splice variants. *The Journal of biological chemistry* **271**, 6403-6410 (1996).

101. K. Palczewski, J. Buczylko, L. Lebioda, J. W. Crabb, A. S. Polans, Identification of the N-terminal region in rhodopsin kinase involved in its interaction with rhodopsin. *The Journal of biological chemistry* **268**, 6004-6013 (1993).

102. J. J. Tesmer, Structure and function of regulator of G protein signaling homology domains. *Prog Mol Biol Transl Sci* **86**, 75-113 (2009).

103. J. A. Pitcher, N. J. Freedman, R. J. Lefkowitz, G protein-coupled receptor kinases. *Annu Rev Biochem* **67**, 653-692 (1998).

104. C. Ribas, P. Penela, C. Murga, A. Salcedo, C. Garcia-Hoz, M. Jurado-Pueyo, I. Aymerich, F. Mayor, Jr., The G protein-coupled receptor kinase (GRK) interactome: role of GRKs in GPCR regulation and signaling. *Biochimica et Biophysica Acta* **1768**, 913-922 (2007).

105. J. Inglese, J. F. Glickman, W. Lorenz, M. G. Caron, R. J. Lefkowitz, Isoprenylation of a protein kinase. Requirement of farnesylation/alpha-carboxyl methylation for full enzymatic activity of rhodopsin kinase. *The Journal of biological chemistry* **267**, 1422-1425 (1992).

106. W. J. Koch, J. Inglese, W. C. Stone, R. J. Lefkowitz, The binding site for the beta gamma subunits of heterotrimeric G proteins on the beta-adrenergic receptor kinase. *The Journal of biological chemistry* **268**, 8256-8260 (1993).

107. S. K. DebBurman, J. Ptasienski, J. L. Benovic, M. M. Hosey, G protein-coupled receptor kinase GRK2 is a phospholipid-dependent enzyme that can be conditionally activated by G protein betagamma subunits. *The Journal of biological chemistry* **271**, 22552-22562 (1996).

108. T. Eichmann, K. Lorenz, M. Hoffmann, J. Brockmann, C. Krasel, M. J. Lohse, U. Quitterer, The amino-terminal domain of G-protein-coupled receptor kinase 2 is a regulatory Gbeta gamma binding site. *The Journal of biological chemistry* **278**, 8052-8057 (2003).

109. M. M. Thiyagarajan, R. P. Stracquatanio, A. N. Pronin, D. S. Evanko, J. L. Benovic, P. B. Wedegaertner, A predicted amphipathic helix mediates plasma membrane localization of GRK5. *The Journal of biological chemistry* **279**, 17989-17995 (2004).

110. X. Jiang, J. L. Benovic, P. B. Wedegaertner, Plasma membrane and nuclear localization of G protein coupled receptor kinase 6A. *Mol Biol Cell* **18**, 2960-2969 (2007).

111. J. A. Pitcher, Z. L. Fredericks, W. C. Stone, R. T. Premont, R. H. Stoffel, W. J. Koch, R. J. Lefkowitz, Phosphatidylinositol 4,5-bisphosphate (PIP2)-enhanced G protein-coupled receptor kinase (GRK) activity. Location, structure, and regulation of the PIP2 binding site distinguishes the GRK subfamilies. *The Journal of biological chemistry* **271**, 24907-24913 (1996).

112. C. A. Boguth, P. Singh, C. C. Huang, J. J. Tesmer, Molecular basis for activation of G protein-coupled receptor kinases. *The EMBO journal* **29**, 3249-3259 (2010).

113. R. H. Stoffel, R. R. Randall, R. T. Premont, R. J. Lefkowitz, J. Inglese, Palmitoylation of G protein-coupled receptor kinase, GRK6. Lipid modification diversity in the GRK family. *The Journal of biological chemistry* **269**, 27791-27794 (1994).

114. L. R. Johnson, M. G. Scott, J. A. Pitcher, G protein-coupled receptor kinase 5 contains a DNA-binding nuclear localization sequence. *Mol Cell Biol* **24**, 10169-10179 (2004).

115. L. R. Johnson, J. D. Robinson, K. N. Lester, J. A. Pitcher, Distinct structural features of G protein-coupled receptor kinase 5 (GRK5) regulate its nuclear localization and DNA-binding ability. *PloS one* **8**, e62508 (2013).

116. D. T. Lodowski, V. M. Tesmer, J. L. Benovic, J. J. Tesmer, The structure of G protein-coupled receptor kinase (GRK)-6 defines a second lineage of GRKs. *The Journal of biological chemistry* **281**, 16785-16793 (2006).

117. U. Wilden, S. W. Hall, H. Kuhn, Phosphodiesterase Activation by Photoexcited Rhodopsin Is Quenched When Rhodopsin Is Phosphorylated and Binds the Intrinsic 48-Kda Protein of Rod Outer Segments. *Proceedings of the National Academy of Sciences of the United States of America* **83**, 1174-1178 (1986).

118. C. V. Carman, T. Som, C. M. Kim, J. L. Benovic, Binding and phosphorylation of tubulin by G protein-coupled receptor kinases. *The Journal of biological chemistry* **273**, 20308-20316 (1998).

119. J. L. Benovic, L. J. Pike, R. A. Cerione, C. Staniszewski, T. Yoshimasa, J. Codina, M. G. Caron, R. J. Lefkowitz, Phosphorylation of the mammalian beta-adrenergic receptor by cyclic AMP-dependent protein kinase. Regulation of the rate of receptor phosphorylation and dephosphorylation by agonist occupancy and effects on coupling of the receptor to the stimulatory guanine nucleotide regulatory protein. *The Journal of biological chemistry* **260**, 7094-7101 (1985).

120. M. Bouvier, L. M. Leeb-Lundberg, J. L. Benovic, M. G. Caron, R. J. Lefkowitz, Regulation of adrenergic receptor function by phosphorylation. II. Effects of agonist occupancy on phosphorylation of alpha 1- and beta 2-adrenergic receptors by protein kinase C and the cyclic AMP-dependent protein kinase. *The Journal of biological chemistry* **262**, 3106-3113 (1987).

121. S. Inagaki, R. Ghirlando, S. A. Vishnivetskiy, K. T. Homan, J. F. White, J. J. Tesmer, V. V. Gurevich, R. Grisshammer, G Protein-Coupled Receptor Kinase 2 (GRK2) and 5 (GRK5) Exhibit Selective Phosphorylation of the Neurotensin Receptor in Vitro. *Biochemistry* **54**, 4320-4329 (2015).

122. J. Kim, S. Ahn, X. R. Ren, E. J. Whalen, E. Reiter, H. Wei, R. J. Lefkowitz, Functional antagonism of different G protein-coupled receptor kinases for beta-arrestin-mediated angiotensin II receptor signaling. *Proceedings of the National Academy of Sciences of the United States of America* **102**, 1442-1447 (2005).

123. E. V. Gurevich, J. J. G. Tesmer, A. Mushegian, V. V. Gurevich, G protein-coupled receptor kinases: More than just kinases and not only for GPCRs. *Pharmacol Therapeut* **133**, 40-69 (2012).

124. J. A. Pitcher, R. A. Hall, Y. Daaka, J. Zhang, S. S. G. Ferguson, S. Hester, S. Miller, M. G. Caron, R. J. Lefkowitz, L. S. Barak, The G protein-coupled receptor kinase 2 is a microtubule-associated protein kinase that phosphorylates tubulin. *Journal of Biological Chemistry* **273**, 12316-12324 (1998).

125. K. Haga, H. Ogawa, T. Haga, H. Murofushi, GTP-binding-protein-coupled receptor kinase 2 (GRK2) binds and phosphorylates tubulin. *Eur J Biochem* **255**, 363-368 (1998).

126. S. H. Cant, J. A. Pitcher, G protein-coupled receptor kinase 2-mediated phosphorylation of ezrin is required for G protein-coupled receptor-dependent reorganization of the actin cytoskeleton. *Mol Biol Cell* **16**, 3088-3099 (2005).

127. A. W. Kahsai, S. Zhu, G. Fenteany, G protein-coupled receptor kinase 2 activates radixin, regulating membrane protrusion and motility in epithelial cells. *Biochim Biophys Acta* **1803**, 300-310 (2010).

128. P. K. Chakraborty, Y. Zhang, A. S. Coomes, W. J. Kim, R. Stupay, L. D. Lynch, T. Atkinson, J. I. Kim, Z. Nie, Y. Daaka, G protein-coupled receptor kinase GRK5 phosphorylates moesin and regulates metastasis in prostate cancer. *Cancer Res* **74**, 3489-3500 (2014).

129. A. N. Pronin, A. J. Morris, A. Surguchov, J. L. Benovic, Synucleins are a novel class of substrates for G protein-coupled receptor kinases. *The Journal of biological chemistry* **275**, 26515-26522 (2000).

130. S. Muller, A. Straub, S. Schroder, P. H. Bauer, M. J. Lohse, Interactions of phosducin with defined G protein beta gamma-subunits. *The Journal of biological chemistry* **271**, 11781-11786 (1996).

131. A. Ruiz-Gomez, J. Humrich, C. Murga, U. Quitterer, M. J. Lohse, F. Mayor, Jr., Phosphorylation of phosducin and phosducin-like protein by G protein-coupled receptor kinase 2. *The Journal of biological chemistry* **275**, 29724-29730 (2000).

132. G. Barthet, G. Carrat, E. Cassier, B. Barker, F. Gaven, M. Pillot, B. Framery, L. P. Pellissier, J. Augier, D. S. Kang, S. Claeysen, E. Reiter, J. L. Baneres, J. L. Benovic, P. Marin *et al.*, Beta-arrestin1 phosphorylation by GRK5 regulates G protein-independent 5-HT4 receptor signalling. *The EMBO journal* **28**, 2706-2718 (2009).

133. J. S. Martini, P. Raake, L. E. Vinge, B. R. DeGeorge, Jr., J. K. Chuprun, D. M. Harris, E. Gao, A. D. Eckhart, J. A. Pitcher, W. J. Koch, Uncovering G protein-coupled receptor kinase-5 as a histone deacetylase kinase in the nucleus of cardiomyocytes. *Proceedings of the National Academy of Sciences of the United States of America* **105**, 12457-12462 (2008).

134. J. Ho, E. Cocolakis, V. M. Dumas, B. I. Posner, S. A. Laporte, J. J. Lebrun, The G protein-coupled receptor kinase-2 is a TGFbeta-inducible antagonist of TGFbeta signal transduction. *The EMBO journal* **24**, 3247-3258 (2005).

135. S. Patial, J. Luo, K. J. Porter, J. L. Benovic, N. Parameswaran, G-protein-coupled-receptor kinases mediate TNFalpha-induced NFkappaB signalling via direct interaction with and phosphorylation of IkappaBalpha. *Biochem J* **425**, 169-178 (2009).

136. N. J. Freedman, L. K. Kim, J. P. Murray, S. T. Exum, L. Brian, J. H. Wu, K. Peppel, Phosphorylation of the platelet-derived growth factor receptor-beta and epidermal growth factor receptor by G protein-coupled receptor kinase-2. Mechanisms for selectivity of desensitization. *The Journal of biological chemistry* **277**, 48261-48269 (2002).

137. J. H. Wu, R. Goswami, X. Cai, S. T. Exum, X. Huang, L. Zhang, L. Brian, R. T. Premont, K. Peppel, N. J. Freedman, Regulation of the platelet-derived growth factor receptor-beta by G protein-coupled receptor kinase-5 in vascular smooth muscle cells involves the phosphatase Shp2. *The Journal of biological chemistry* **281**, 37758-37772 (2006).

138. C. V. Carman, J. L. Parent, P. W. Day, A. N. Pronin, P. M. Sternweis, P. B. Wedegaertner, A. G. Gilman, J. L. Benovic, T. Kozasa, Selective regulation of Galpha(q/11) by an RGS domain in the G protein-coupled receptor kinase, GRK2. *The Journal of biological chemistry* **274**, 34483-34492 (1999).

139. R. Sterne-Marr, J. J. Tesmer, P. W. Day, R. P. Stracquatanio, J. A. Cilente, K. E. O'Connor, A. N. Pronin, J. L. Benovic, P. B. Wedegaertner, G protein-coupled receptor Kinase 2/G alpha q/11 interaction. A novel surface on a regulator of G protein signaling homology domain for binding G alpha subunits. *The Journal of biological chemistry* **278**, 6050-6058 (2003).

140. P. W. Day, C. V. Carman, R. Sterne-Marr, J. L. Benovic, P. B. Wedegaertner, Differential interaction of GRK2 with members of the G alpha q family. *Biochemistry* **42**, 9176-9184 (2003).

141. K. Touhara, J. Inglese, J. A. Pitcher, G. Shaw, R. J. Lefkowitz, Binding of G protein beta gamma-subunits to pleckstrin homology domains. *The Journal of biological chemistry* **269**, 10217-10220 (1994).

142. A. Raveh, A. Cooper, L. Guy-David, E. Reuveny, Nonenzymatic rapid control of GIRK channel function by a G protein-coupled receptor kinase. *Cell* **143**, 750-760 (2010).

143. R. T. Premont, A. Claing, N. Vitale, J. L. Freeman, J. A. Pitcher, W. A. Patton, J. Moss, M. Vaughan, R. J. Lefkowitz, beta2-Adrenergic receptor regulation by GIT1, a G protein-coupled

receptor kinase-associated ADP ribosylation factor GTPase-activating protein. *Proceedings of the National Academy of Sciences of the United States of America* **95**, 14082-14087 (1998).

144. R. J. Hoefen, B. C. Berk, The multifunctional GIT family of proteins. *J Cell Sci* **119**, 1469-1475 (2006).

145. T. Shiina, K. Arai, S. Tanabe, N. Yoshida, T. Haga, T. Nagao, H. Kurose, Clathrin box in G protein-coupled receptor kinase 2. *The Journal of biological chemistry* **276**, 33019-33026 (2001).

146. K. Haga, T. Haga, Activation by G protein beta gamma subunits of agonist- or light-dependent phosphorylation of muscarinic acetylcholine receptors and rhodopsin. *The Journal of biological chemistry* **267**, 2222-2227 (1992).

147. C. M. Kim, S. B. Dion, J. L. Benovic, Mechanism of beta-adrenergic receptor kinase activation by G proteins. *The Journal of biological chemistry* **268**, 15412-15418 (1993).

148. J. A. Pitcher, K. Touhara, E. S. Payne, R. J. Lefkowitz, Pleckstrin homology domain-mediated membrane association and activation of the beta-adrenergic receptor kinase requires coordinate interaction with G beta gamma subunits and lipid. *The Journal of biological chemistry* **270**, 11707-11710 (1995).

149. D. T. Lodowski, J. F. Barnhill, R. M. Pyskadlo, R. Ghirlando, R. Sterne-Marr, J. J. Tesmer, The role of G beta gamma and domain interfaces in the activation of G protein-coupled receptor kinase 2. *Biochemistry* **44**, 6958-6970 (2005).

150. S. K. DebBurman, J. Ptasienski, E. Boetticher, J. W. Lomasney, J. L. Benovic, M. M. Hosey, Lipid-mediated regulation of G protein-coupled receptor kinases 2 and 3. *The Journal of biological chemistry* **270**, 5742-5747 (1995).

151. J. J. Onorato, M. E. Gillis, Y. Liu, J. L. Benovic, A. E. Ruoho, The beta-adrenergic receptor kinase (GRK2) is regulated by phospholipids. *The Journal of biological chemistry* **270**, 21346-21353 (1995).

152. S. Sarnago, A. Elorza, F. Mayor, Jr., Agonist-dependent phosphorylation of the G protein-coupled receptor kinase 2 (GRK2) by Src tyrosine kinase. *The Journal of biological chemistry* **274**, 34411-34416 (1999).

153. P. Penela, A. Elorza, S. Sarnago, F. Mayor, Jr., Beta-arrestin- and c-Src-dependent degradation of G-protein-coupled receptor kinase 2. *The EMBO journal* **20**, 5129-5138 (2001).

154. M. Cong, S. J. Perry, F. T. Lin, I. D. Fraser, L. A. Hu, W. Chen, J. A. Pitcher, J. D. Scott, R. J. Lefkowitz, Regulation of membrane targeting of the G protein-coupled receptor kinase 2 by protein kinase A and its anchoring protein AKAP79. *The Journal of biological chemistry* **276**, 15192-15199 (2001).

155. A. Elorza, S. Sarnago, F. Mayor, Jr., Agonist-dependent modulation of G protein-coupled receptor kinase 2 by mitogen-activated protein kinases. *Molecular pharmacology* **57**, 778-783 (2000).

156. R. Winstel, S. Freund, C. Krasel, E. Hoppe, M. J. Lohse, Protein kinase cross-talk: membrane targeting of the beta-adrenergic receptor kinase by protein kinase C. *Proceedings of the National Academy of Sciences of the United States of America* **93**, 2105-2109 (1996).

157. C. Krasel, S. Dammeier, R. Winstel, J. Brockmann, H. Mischak, M. J. Lohse, Phosphorylation of GRK2 by protein kinase C abolishes its inhibition by calmodulin. *The Journal of biological chemistry* **276**, 1911-1915 (2001).

158. J. I. Gold, J. S. Martini, J. Hullmann, E. Gao, J. K. Chuprun, L. Lee, D. G. Tilley, J. E. Rabinowitz, J. Bossuyt, D. M. Bers, W. J. Koch, Nuclear translocation of cardiac G protein-Coupled Receptor kinase 5 downstream of select Gq-activating hypertrophic ligands is a calmodulin-dependent process. *PloS one* **8**, e57324 (2013).

159. A. N. Pronin, C. V. Carman, J. L. Benovic, Structure-function analysis of G protein-coupled receptor kinase-5. Role of the carboxyl terminus in kinase regulation. *The Journal of biological chemistry* **273**, 31510-31518 (1998).

160. A. N. Pronin, J. L. Benovic, Regulation of the G protein-coupled receptor kinase GRK5 by protein kinase C. *The Journal of biological chemistry* **272**, 3806-3812 (1997).

161. A. N. Pronin, D. K. Satpaev, V. Z. Slepak, J. L. Benovic, Regulation of G protein-coupled receptor kinases by calmodulin and localization of the calmodulin binding domain. *The Journal of biological chemistry* **272**, 18273-18280 (1997).

162. P. Kunapuli, V. V. Gurevich, J. L. Benovic, Phospholipid-stimulated autophosphorylation activates the G protein-coupled receptor kinase GRK5. *The Journal of biological chemistry* **269**, 10209-10212 (1994).

163. A. Lymperopoulos, G. Rengo, W. J. Koch, Adrenergic nervous system in heart failure: pathophysiology and therapy. *Circulation research* **113**, 739-753 (2013).

164. A. Lymperopoulos, A. Bathgate, Arrestins in the cardiovascular system. *Prog Mol Biol Transl Sci* **118**, 297-334 (2013).

165. M. R. Bristow, R. Ginsburg, V. Umans, M. Fowler, W. Minobe, R. Rasmussen, P. Zera, R. Menlove, P. Shah, S. Jamieson, et al., Beta 1- and beta 2-adrenergic-receptor subpopulations in nonfailing and failing human ventricular myocardium: coupling of both receptor subtypes to muscle contraction and selective beta 1-receptor down-regulation in heart failure. *Circulation research* **59**, 297-309 (1986).

166. M. Ungerer, M. Bohm, J. S. Elce, E. Erdmann, M. J. Lohse, Altered expression of beta-adrenergic receptor kinase and beta 1-adrenergic receptors in the failing human heart. *Circulation* **87**, 454-463 (1993).

167. M. Ungerer, G. Parruti, M. Bohm, M. Puzicha, A. DeBlasi, E. Erdmann, M. J. Lohse, Expression of beta-arrestins and beta-adrenergic receptor kinases in the failing human heart. *Circulation research* **74**, 206-213 (1994).

168. W. J. Koch, H. A. Rockman, P. Samama, R. A. Hamilton, R. A. Bond, C. A. Milano, R. J. Lefkowitz, Cardiac function in mice overexpressing the beta-adrenergic receptor kinase or a beta ARK inhibitor. *Science* **268**, 1350-1353 (1995).

169. E. P. Chen, H. B. Bittner, S. A. Akhter, W. J. Koch, R. D. Davis, Myocardial recovery after ischemia and reperfusion injury is significantly impaired in hearts with transgenic overexpression of beta-adrenergic receptor kinase. *Circulation* **98**, II249-253; discussion II253-244 (1998).

170. H. Brinks, M. Boucher, E. Gao, J. K. Chuprun, S. Pesant, P. W. Raake, Z. M. Huang, X. Wang, G. Qiu, A. Gumpert, D. M. Harris, A. D. Eckhart, P. Most, W. J. Koch, Level of G protein-coupled receptor kinase-2 determines myocardial ischemia/reperfusion injury via pro- and anti-apoptotic mechanisms. *Circulation research* **107**, 1140-1149 (2010).

171. X. P. Yi, J. Zhou, J. Baker, X. Wang, A. M. Gerdes, F. Li, Myocardial expression and redistribution of GRKs in hypertensive hypertrophy and failure. *Anat Rec A Discov Mol Cell Evol Biol* **282**, 13-23 (2005).

172. N. Dzimiri, P. Muiya, E. Andres, Z. Al-Halees, Differential functional expression of human myocardial G protein receptor kinases in left ventricular cardiac diseases. *Eur J Pharmacol* **489**, 167-177 (2004).

173. F. Monto, E. Oliver, D. Vicente, J. Rueda, J. Aguero, L. Almenar, M. D. Ivorra, D. Barettino, P. D'Ocon, Different expression of adrenoceptors and GRKs in the human myocardium depends on heart failure etiology and correlates to clinical variables. *Am J Physiol Heart Circ Physiol* **303**, H368-376 (2012).

174. H. A. Rockman, D. J. Choi, N. U. Rahman, S. A. Akhter, R. J. Lefkowitz, W. J. Koch, Receptor-specific in vivo desensitization by the G protein-coupled receptor kinase-5 in transgenic mice. *Proceedings of the National Academy of Sciences of the United States of America* **93**, 9954-9959 (1996).

175. M. R. Bristow, R. E. Hershberger, J. D. Port, W. Minobe, R. Rasmussen, Beta 1- and beta 2-adrenergic receptor-mediated adenylate cyclase stimulation in nonfailing and failing human ventricular myocardium. *Molecular pharmacology* **35**, 295-303 (1989).

176. M. R. Bristow, R. Ginsburg, W. Minobe, R. S. Cubicciotti, W. S. Sageman, K. Lurie, M. E. Billingham, D. C. Harrison, E. B. Stinson, Decreased catecholamine sensitivity and beta-adrenergic-receptor density in failing human hearts. *N Engl J Med* **307**, 205-211 (1982).

177. A. Lymperopoulos, G. Rengo, H. Funakoshi, A. D. Eckhart, W. J. Koch, Adrenal GRK2 upregulation mediates sympathetic overdrive in heart failure. *Nat Med* **13**, 315-323 (2007).

178. A. Lymperopoulos, G. Rengo, E. Gao, S. N. Ebert, G. W. Dorn, 2nd, W. J. Koch, Reduction of sympathetic activity via adrenal-targeted GRK2 gene deletion attenuates heart failure progression and improves cardiac function after myocardial infarction. *The Journal of biological chemistry* **285**, 16378-16386 (2010).

179. A. Lymperopoulos, G. Rengo, C. Zincarelli, S. Soltys, W. J. Koch, Modulation of adrenal catecholamine secretion by in vivo gene transfer and manipulation of G protein-coupled receptor kinase-2 activity. *Mol Ther* **16**, 302-307 (2008).

180. G. Rengo, D. Leosco, C. Zincarelli, M. Marchese, G. Corbi, D. Liccardo, A. Filippelli, N. Ferrara, M. P. Lisanti, W. J. Koch, A. Lymperopoulos, Adrenal GRK2 lowering is an underlying mechanism for the beneficial sympathetic effects of exercise training in heart failure. *Am J Physiol Heart Circ Physiol* **298**, H2032-2038 (2010).

181. G. Rengo, A. Lymperopoulos, C. Zincarelli, G. Femminella, D. Liccardo, G. Pagano, C. de Lucia, A. Cannavo, P. Gargiulo, N. Ferrara, P. Perrone Filardi, W. Koch, D. Leosco, Blockade of beta-adrenoceptors restores the GRK2-mediated adrenal alpha(2) -adrenoceptor-catecholamine production axis in heart failure. *Br J Pharmacol* **166**, 2430-2440 (2012).

182. A. Fusco, G. Santulli, D. Sorriento, E. Cipolletta, C. Garbi, G. W. Dorn, 2nd, B. Trimarco, A. Feliciello, G. Iaccarino, Mitochondrial localization unveils a novel role for GRK2 in organelle biogenesis. *Cell Signal* **24**, 468-475 (2012).

183. M. E. Obrenovich, H. H. Palacios, E. Gasimov, J. Leszek, G. Aliev, The GRK2 Overexpression Is a Primary Hallmark of Mitochondrial Lesions during Early Alzheimer Disease. *Cardiovasc Psychiatry Neurol* **2009**, 327360 (2009).

184. M. Chen, P. Y. Sato, J. K. Chuprun, R. J. Peroutka, N. J. Otis, J. Ibetti, S. Pan, S. S. Sheu, E. Gao, W. J. Koch, Prodeath signaling of G protein-coupled receptor kinase 2 in cardiac myocytes after ischemic stress occurs via extracellular signal-regulated kinase-dependent heat shock protein 90-mediated mitochondrial targeting. *Circulation research* **112**, 1121-1134 (2013).

185. J. Luo, J. L. Benovic, G protein-coupled receptor kinase interaction with Hsp90 mediates kinase maturation. *The Journal of biological chemistry* **278**, 50908-50914 (2003).

186. M. Jaber, W. J. Koch, H. Rockman, B. Smith, R. A. Bond, K. K. Sulik, J. Ross, Jr., R. J. Lefkowitz, M. G. Caron, B. Giros, Essential role of beta-adrenergic receptor kinase 1 in cardiac development and function. *Proceedings of the National Academy of Sciences of the United States of America* **93**, 12974-12979 (1996).

187. H. A. Rockman, K. R. Chien, D. J. Choi, G. Iaccarino, J. J. Hunter, J. Ross, Jr., R. J. Lefkowitz, W. J. Koch, Expression of a beta-adrenergic receptor kinase 1 inhibitor prevents the development of myocardial failure in gene-targeted mice. *Proceedings of the National Academy of Sciences of the United States of America* **95**, 7000-7005 (1998).

188. J. Abd Alla, M. Graemer, X. Fu, U. Quitterer, Inhibition of G-protein-coupled Receptor Kinase 2 Prevents the Dysfunctional Cardiac Substrate Metabolism in Fatty Acid Synthase Transgenic Mice. *The Journal of biological chemistry* **291**, 2583-2600 (2016).

189. R. Gros, C. M. Tan, J. Chorazyczewski, D. J. Kelvin, J. L. Benovic, R. D. Feldman, G-protein-coupled receptor kinase expression in hypertension. *Clin Pharmacol Ther* **65**, 545-551 (1999).

190. R. Gros, J. L. Benovic, C. M. Tan, R. D. Feldman, G-protein-coupled receptor kinase activity is increased in hypertension. *J Clin Invest* **99**, 2087-2093 (1997).

191. A. D. Eckhart, T. Ozaki, H. Tevaearai, H. A. Rockman, W. J. Koch, Vascular-targeted overexpression of G protein-coupled receptor kinase-2 in transgenic mice attenuates beta-adrenergic receptor signaling and increases resting blood pressure. *Molecular pharmacology* **61**, 749-758 (2002).

192. S. Liu, R. T. Premont, C. D. Kontos, S. Zhu, D. C. Rockey, A crucial role for GRK2 in regulation of endothelial cell nitric oxide synthase function in portal hypertension. *Nat Med* **11**, 952-958 (2005).

193. E. P. Chen, H. B. Bittner, S. A. Akhter, W. J. Koch, R. D. Davis, Myocardial function in hearts with transgenic overexpression of the G protein-coupled receptor kinase 5. *The Annals of thoracic surgery* **71**, 1320-1324 (2001).

194. J. I. Gold, E. Gao, X. Shang, R. T. Premont, W. J. Koch, Determining the absolute requirement of G protein-coupled receptor kinase 5 for pathological cardiac hypertrophy: short communication. *Circulation research* **111**, 1048-1053 (2012).

195. J. L. Freeman, E. M. De La Cruz, T. D. Pollard, R. J. Lefkowitz, J. A. Pitcher, Regulation of G protein-coupled receptor kinase 5 (GRK5) by actin. *The Journal of biological chemistry* **273**, 20653-20657 (1998).

196. J. E. Hullmann, L. A. Grisanti, C. A. Makarewich, E. Gao, J. I. Gold, J. K. Chuprun, D. G. Tilley, S. R. Houser, W. J. Koch, GRK5-mediated exacerbation of pathological cardiac hypertrophy involves facilitation of nuclear NFAT activity. *Circulation research* **115**, 976-985 (2014).

197. K. N. Islam, J. W. Bae, E. Gao, W. J. Koch, Regulation of nuclear factor kappaB (NF-kappaB) in the nucleus of cardiomyocytes by G protein-coupled receptor kinase 5 (GRK5). *The Journal of biological chemistry* **288**, 35683-35689 (2013).

198. S. Patial, S. Shahi, Y. Saini, T. Lee, N. Packiriswamy, D. M. Appledorn, J. J. Lapres, A. Amalfitano, N. Parameswaran, G-protein coupled receptor kinase 5 mediates lipopolysaccharide-induced NFkappaB activation in primary macrophages and modulates inflammation in vivo in mice. *J Cell Physiol* **226**, 1323-1333 (2011).

199. N. Parameswaran, C. S. Pao, K. S. Leonhard, D. S. Kang, M. Kratz, S. C. Ley, J. L. Benovic, Arrestin-2 and G protein-coupled receptor kinase 5 interact with NFkappaB1 p105 and negatively regulate lipopolysaccharide-stimulated ERK1/2 activation in macrophages. *The Journal of biological chemistry* **281**, 34159-34170 (2006).

200. D. Sorriento, M. Ciccarelli, G. Santulli, A. Campanile, G. G. Altobelli, V. Cimini, G. Galasso, D. Astone, F. Piscione, L. Pastore, B. Trimarco, G. Iaccarino, The G-protein-coupled receptor kinase 5 inhibits NFkappaB transcriptional activity by inducing nuclear accumulation of IkappaB alpha. *Proceedings of the National Academy of Sciences of the United States of America* **105**, 17818-17823 (2008).

201. Y. Zhang, S. J. Matkovich, X. Duan, J. I. Gold, W. J. Koch, G. W. Dorn, 2nd, Nuclear effects of G-protein receptor kinase 5 on histone deacetylase 5-regulated gene transcription in heart failure. *Circulation. Heart failure* **4**, 659-668 (2011).

202. S. B. Liggett, S. Cresci, R. J. Kelly, F. M. Syed, S. J. Matkovich, H. S. Hahn, A. Diwan, J. S. Martini, L. Sparks, R. R. Parekh, J. A. Spertus, W. J. Koch, S. L. Kardia, G. W. Dorn, 2nd, A GRK5 polymorphism that inhibits beta-adrenergic receptor signaling is protective in heart failure. *Nat Med* **14**, 510-517 (2008).

203. S. Cresci, G. W. Dorn, 2nd, P. G. Jones, A. L. Beitelshees, A. Y. Li, P. A. Lenzini, M. A. Province, J. A. Spertus, D. E. Lanfear, Adrenergic-pathway gene variants influence beta-blocker-related outcomes after acute coronary syndrome in a race-specific manner. *J Am Coll Cardiol* **60**, 898-907 (2012).

204. L. Spinelli, V. Trimarco, S. Di Marino, M. Marino, G. Iaccarino, B. Trimarco, L41Q polymorphism of the G protein coupled receptor kinase 5 is associated with left ventricular apical ballooning syndrome. *Eur J Heart Fail* **12**, 13-16 (2010).

205. N. Ishizaka, R. W. Alexander, J. B. Laursen, H. Kai, T. Fukui, M. Oppermann, R. J. Lefkowitz, P. R. Lyons, K. K. Griendling, G protein-coupled receptor kinase 5 in cultured vascular smooth muscle cells and rat aorta. Regulation by angiotensin II and hypertension. *The Journal of biological chemistry* **272**, 32482-32488 (1997).

206. J. R. Keys, R. H. Zhou, D. M. Harris, C. A. Druckman, A. D. Eckhart, Vascular smooth muscle overexpression of G protein-coupled receptor kinase 5 elevates blood pressure, which segregates with sex and is dependent on Gi-mediated signaling. *Circulation* **112**, 1145-1153 (2005).

207. S. B. Biddinger, C. R. Kahn, From mice to men: insights into the insulin resistance syndromes. *Annu Rev Physiol* **68**, 123-158 (2006).

208. Y. Anis, O. Leshem, H. Reuveni, I. Wexler, R. Ben Sasson, B. Yahalom, M. Laster, I. Raz, S. Ben Sasson, E. Shafrir, E. Ziv, Antidiabetic effect of novel modulating peptides of G-protein-coupled kinase in experimental models of diabetes. *Diabetologia* **47**, 1232-1244 (2004).

209. L. Garcia-Guerra, I. Nieto-Vazquez, R. Vila-Bedmar, M. Jurado-Pueyo, G. Zalba, J. Diez, C. Murga, S. Fernandez-Veledo, F. Mayor, Jr., M. Lorenzo, G protein-coupled receptor kinase 2 plays a relevant role in insulin resistance and obesity. *Diabetes* **59**, 2407-2417 (2010).

210. R. Vila-Bedmar, M. Cruces-Sande, E. Lucas, H. L. Willemen, C. J. Heijnen, A. Kavelaars, F. Mayor, Jr., C. Murga, Reversal of diet-induced obesity and insulin resistance by inducible genetic ablation of GRK2. *Sci Signal* **8**, ra73 (2015).

211. E. Cipolletta, A. Campanile, G. Santulli, E. Sanzari, D. Leosco, P. Campiglia, B. Trimarco, G. Iaccarino, The G protein coupled receptor kinase 2 plays an essential role in beta-adrenergic receptor-induced insulin resistance. *Cardiovasc Res* **84**, 407-415 (2009).

212. K. Taguchi, M. Hida, M. Hasegawa, H. Narimatsu, T. Matsumoto, T. Kobayashi, Suppression of GRK2 expression reduces endothelial dysfunction by restoring glucose homeostasis. *Scientific reports* **7**, 8436 (2017).

213. L. Wang, M. Shen, F. Wang, L. Ma, GRK5 ablation contributes to insulin resistance. *Biochem Biophys Res Commun* **429**, 99-104 (2012).

214. M. U. Falcenberg, A.; Kinases as targets for anti-diabetic therapy. US20130336986A1, (2013)

215. F. Wang, L. Wang, M. Shen, L. Ma, GRK5 deficiency decreases diet-induced obesity and adipogenesis. *Biochem Biophys Res Commun* **421**, 312-317 (2012).

216. L. Nogues, J. Palacios-Garcia, C. Reglero, V. Rivas, M. Neves, C. Ribas, P. Penela, F. Mayor, Jr., G protein-coupled receptor kinases (GRKs) in tumorigenesis and cancer progression: GPCR regulators and signaling hubs. *Semin Cancer Biol* **48**, 78-90 (2018).

217. L. Nogues, C. Reglero, V. Rivas, A. Salcedo, V. Lafarga, M. Neves, P. Ramos, M. Mendiola, A. Berjon, K. Stamatakis, X. Z. Zhou, K. P. Lu, D. Hardisson, F. Mayor, Jr., P. Penela, G Protein-coupled Receptor Kinase 2 (GRK2) Promotes Breast Tumorigenesis Through a HDAC6-Pin1 Axis. *EBioMedicine* **13**, 132-145 (2016).

218. T. Metaye, P. Levillain, J. L. Kraimps, R. Perdrisot, Immunohistochemical detection, regulation and antiproliferative function of G-protein-coupled receptor kinase 2 in thyroid carcinomas. *J Endocrinol* **198**, 101-110 (2008).

219. Z. Wei, R. Hurtt, M. Ciccarelli, W. J. Koch, C. Doria, Growth inhibition of human hepatocellular carcinoma cells by overexpression of G-protein-coupled receptor kinase 2. *J Cell Physiol* **227**, 2371-2377 (2012).

220. X. Fu, S. Koller, J. Abd Alla, U. Quitterer, Inhibition of G-protein-coupled receptor kinase 2 (GRK2) triggers the growth-promoting mitogen-activated protein kinase (MAPK) pathway. *The Journal of biological chemistry* **288**, 7738-7755 (2013).

221. T. Metaye, E. Menet, J. Guilhot, J. L. Kraimps, Expression and activity of g protein-coupled receptor kinases in differentiated thyroid carcinoma. *J Clin Endocrinol Metab* **87**, 3279-3286 (2002).

222. F. M. Tsai, C. C. Wu, R. Y. Shyu, C. H. Wang, S. Y. Jiang, Tazarotene-induced gene 1 inhibits prostaglandin E2-stimulated HCT116 colon cancer cell growth. *J Biomed Sci* **18**, 88 (2011).

223. C. C. Wu, F. M. Tsai, R. Y. Shyu, Y. M. Tsai, C. H. Wang, S. Y. Jiang, G protein-coupled receptor kinase 5 mediates Tazarotene-induced gene 1-induced growth suppression of human colon cancer cells. *BMC Cancer* **11**, 175 (2011).

224. X. Chen, H. Zhu, M. Yuan, J. Fu, Y. Zhou, L. Ma, G-protein-coupled receptor kinase 5 phosphorylates p53 and inhibits DNA damage-induced apoptosis. *The Journal of biological chemistry* **285**, 12823-12830 (2010).

225. A. J. Levine, p53, the cellular gatekeeper for growth and division. *Cell* **88**, 323-331 (1997).

226. D. Leosco, F. Fortunato, G. Rengo, G. Iaccarino, E. Sanzari, L. Golino, C. Zincarelli, V. Canonico, M. Marchese, W. J. Koch, F. Rengo, Lymphocyte G-protein-coupled receptor kinase-2 is upregulated in patients with Alzheimer's disease. *Neurosci Lett* **415**, 279-282 (2007).

227. Z. Suo, M. Wu, B. A. Citron, G. T. Wong, B. W. Festoff, Abnormality of G-protein-coupled receptor kinases at prodromal and early stages of Alzheimer's disease: an association with early beta-amyloid accumulation. *J Neurosci* **24**, 3444-3452 (2004).

228. Z. Suo, A. A. Cox, N. Bartelli, I. Rasul, B. W. Festoff, R. T. Premont, G. W. Arendash, GRK5 deficiency leads to early Alzheimer-like pathology and working memory impairment. *Neurobiol Aging* **28**, 1873-1888 (2007).

229. L. Li, I. Rasul, J. Liu, B. Zhao, R. Tang, R. T. Premont, W. Z. Suo, Augmented axonal defects and synaptic degenerative changes in female GRK5 deficient mice. *Brain Res Bull* **78**, 145-151 (2009).

230. S. Cheng, L. Li, S. He, J. Liu, Y. Sun, M. He, K. Grasing, R. T. Premont, W. Z. Suo, GRK5 deficiency accelerates {beta}-amyloid accumulation in Tg2576 mice via impaired cholinergic activity. *The Journal of biological chemistry* **285**, 41541-41548 (2010).

231. L. Li, J. Liu, W. Z. Suo, GRK5 deficiency exaggerates inflammatory changes in TgAPPsw mice. *J Neuroinflammation* **5**, 24 (2008).

232. E. R. Bychkov, V. V. Gurevich, J. N. Joyce, J. L. Benovic, E. V. Gurevich, Arrestins and two receptor kinases are upregulated in Parkinson's disease with dementia. *Neurobiol Aging* **29**, 379-396 (2008).

233. S. Arawaka, M. Wada, S. Goto, H. Karube, M. Sakamoto, C. H. Ren, S. Koyama, H. Nagasawa, H. Kimura, T. Kawanami, K. Kurita, K. Tajima, M. Daimon, M. Baba, T. Kido *et al.*, The role of G-protein-coupled receptor kinase 5 in pathogenesis of sporadic Parkinson's disease. *J Neurosci* **26**, 9227-9238 (2006).

234. M. Takahashi, H. Uchikado, D. Caprotti, K. M. Weidenheim, D. W. Dickson, H. Ksiezak-Reding, G. M. Pasinetti, Identification of G-protein coupled receptor kinase 2 in paired helical filaments and neurofibrillary tangles. *J Neuropathol Exp Neurol* **65**, 1157-1169 (2006).

235. P. Tarantino, E. V. De Marco, G. Annesi, F. E. Rocca, F. Annesi, D. Civitelli, G. Provenzano, V. Scornaienchi, V. Greco, C. Colica, G. Nicoletti, A. Quattrone, Lack of association between G-protein coupled receptor kinase 5 gene and Parkinson's disease. *Am J Med Genet B Neuropsychiatr Genet* **156B**, 104-107 (2011).

236. G. B. D. Disease, I. Injury, C. Prevalence, Global, regional, and national incidence, prevalence, and years lived with disability for 310 diseases and injuries, 1990-2015: a systematic analysis for the Global Burden of Disease Study 2015. *Lancet* **388**, 1545-1602 (2016).

237. P. A. Heidenreich, N. M. Albert, L. A. Allen, D. A. Bluemke, J. Butler, G. C. Fonarow, J. S. Ikonomidis, O. Khavjou, M. A. Konstam, T. M. Maddox, G. Nichol, M. Pham, I. L. Pina, J. G. Trogdon, C. American Heart Association Advocacy Coordinating *et al.*, Forecasting the impact of heart failure in the United States: a policy statement from the American Heart Association. *Circulation. Heart failure* **6**, 606-619 (2013).

238. S. Khatibzadeh, F. Farzadfar, J. Oliver, M. Ezzati, A. Moran, Worldwide risk factors for heart failure: a systematic review and pooled analysis. *Int J Cardiol* **168**, 1186-1194 (2013).

239. P. Ponikowski, A. A. Voors, S. D. Anker, H. Bueno, J. G. Cleland, A. J. Coats, V. Falk, J. R. Gonzalez-Juanatey, V. P. Harjola, E. A. Jankowska, M. Jessup, C. Linde, P. Nihoyannopoulos, J. T. Parissis, B. Pieske *et al.*, 2016 ESC Guidelines for the diagnosis and treatment of acute and chronic heart failure: The Task Force for the diagnosis and treatment of acute and chronic heart failure of the European Society of Cardiology (ESC). Developed with the special contribution of the Heart Failure Association (HFA) of the ESC. *Eur J Heart Fail* **18**, 891-975 (2016).

240. M. Writing Group, D. Mozaffarian, E. J. Benjamin, A. S. Go, D. K. Arnett, M. J. Blaha, M. Cushman, S. R. Das, S. de Ferranti, J. P. Despres, H. J. Fullerton, V. J. Howard, M. D. Huffman, C. R. Isasi, M. C. Jimenez *et al.*, Heart Disease and Stroke Statistics-2016 Update: A Report From the American Heart Association. *Circulation* **133**, e38-360 (2016).

241. K. Lorenz, M. J. Lohse, U. Quitterer, Protein kinase C switches the Raf kinase inhibitor from Raf-1 to GRK-2. *Nature* **426**, 574-579 (2003).

242. K. Yeung, T. Seitz, S. Li, P. Janosch, B. McFerran, C. Kaiser, F. Fee, K. D. Katsanakis, D. W. Rose, H. Mischak, J. M. Sedivy, W. Kolch, Suppression of Raf-1 kinase activity and MAP kinase signalling by RKIP. *Nature* **401**, 173-177 (1999).

243. K. Yeung, P. Janosch, B. McFerran, D. W. Rose, H. Mischak, J. M. Sedivy, W. Kolch, Mechanism of suppression of the Raf/MEK/extracellular signal-regulated kinase pathway by the raf kinase inhibitor protein. *Molecular and cellular biology* **20**, 3079-3085 (2000).

244. K. Deiss, C. Kisker, M. J. Lohse, K. Lorenz, Raf kinase inhibitor protein (RKIP) dimer formation controls its target switch from Raf1 to G protein-coupled receptor kinase (GRK) 2. *The Journal of biological chemistry* **287**, 23407-23417 (2012).

245. E. Schmid, S. Neef, C. Berlin, A. Tomasovic, K. Kahlert, P. Nordbeck, K. Deiss, S. Denzinger, S. Herrmann, E. Wettwer, M. Weidendorfer, D. Becker, F. Schafer, N. Wagner, S. Ergun *et al.*, Cardiac RKIP induces a beneficial beta-adrenoceptor-dependent positive inotropy. *Nat Med* **21**, 1298-1306 (2015).

246. V. B. Harding, L. R. Jones, R. J. Lefkowitz, W. J. Koch, H. A. Rockman, Cardiac beta ARK1 inhibition prolongs survival and augments beta blocker therapy in a mouse model of severe heart failure. *Proceedings of the National Academy of Sciences of the United States of America* **98**, 5809-5814 (2001).

247. S. A. Akhter, A. D. Eckhart, H. A. Rockman, K. Shotwell, R. J. Lefkowitz, W. J. Koch, In vivo inhibition of elevated myocardial beta-adrenergic receptor kinase activity in hybrid transgenic mice restores normal beta-adrenergic signaling and function. *Circulation* **100**, 648-653 (1999).

248. M. Volkers, C. Weidenhammer, N. Herzog, G. Qiu, K. Spaich, F. V. Wegner, K. Peppel, O. J. Muller, S. Schinkel, J. E. Rabinowitz, H. J. Hippe, H. Brinks, H. A. Katus, W. J. Koch, A. D. Eckhart *et al.*, The inotropic peptide betaARKct improves betaAR responsiveness in normal and failing cardiomyocytes through G(betagamma)-mediated L-type calcium current disinhibition. *Circulation research* **108**, 27-39 (2011).

249. P. W. Raake, P. Schlegel, J. Ksienzyk, J. Reinkober, J. Barthelmes, S. Schinkel, S. Pleger, W. Mier, U. Haberkorn, W. J. Koch, H. A. Katus, P. Most, O. J. Muller, AAV6.betaARKct cardiac gene therapy ameliorates cardiac function and normalizes the catecholaminergic axis in a clinically relevant large animal heart failure model. *Eur Heart J* **34**, 1437-1447 (2013).

250. J. L. Benovic, J. Onorato, M. J. Lohse, H. G. Dohlman, C. Staniszewski, M. G. Caron, R. J. Lefkowitz, Synthetic peptides of the hamster beta 2-adrenoceptor as substrates and inhibitors of the beta-adrenoceptor kinase. *Br J Clin Pharmacol* **30 Suppl 1**, 3S-12S (1990).

251. R. Winstel, H. G. Ihlenfeldt, G. Jung, C. Krasel, M. J. Lohse, Peptide inhibitors of G protein-coupled receptor kinases. *Biochemical pharmacology* **70**, 1001-1008 (2005).

252. R. H. Lee, B. S. Lieberman, R. N. Lolley, A novel complex from bovine visual cells of a 33,000-dalton phosphoprotein with beta- and gamma-transducin: purification and subunit structure. *Biochemistry* **26**, 3983-3990 (1987).

253. J. A. Reig, L. Yu, D. C. Klein, Pineal transduction. Adrenergic----cyclic AMP-dependent phosphorylation of cytoplasmic 33-kDa protein (MEKA) which binds beta gamma-complex of transducin. *The Journal of biological chemistry* **265**, 5816-5824 (1990).

254. K. Bluml, W. Schnepp, S. Schroder, M. Beyermann, M. Macias, H. Oschkinat, M. J. Lohse, A small region in phosducin inhibits G-protein betagamma-subunit function. *The EMBO journal* **16**, 4908-4915 (1997).

255. J. L. Benovic, W. C. Stone, M. G. Caron, R. J. Lefkowitz, Inhibition of the beta-adrenergic receptor kinase by polyanions. *The Journal of biological chemistry* **264**, 6707-6710 (1989).

256. J. Setyawan, K. Koide, T. C. Diller, M. E. Bunnage, S. S. Taylor, K. C. Nicolaou, L. L. Brunton, Inhibition of protein kinases by balanol: specificity within the serine/threonine protein kinase subfamily. *Molecular pharmacology* **56**, 370-376 (1999).

257. D. M. Thal, R. Y. Yeow, C. Schoenau, J. Huber, J. J. Tesmer, Molecular mechanism of selectivity among G protein-coupled receptor kinase 2 inhibitors. *Molecular pharmacology* **80**, 294-303 (2011).

258. G. Manning, D. B. Whyte, R. Martinez, T. Hunter, S. Sudarsanam, The protein kinase complement of the human genome. *Science* **298**, 1912-1934 (2002).

259. S. Ikeda, M. Keneko, S. Fujiwara, inventors; Takeda Pharmaceutical Company Ltd. *Ikeda S, Keneko M, and Fujiwara S, assignees. Cardiotonic agent comprising GRK inhibitor. World patent WO2007034846*, (2007).

260. T. Okawa, Y. Aramaki, M. Yamamoto, T. Kobayashi, S. Fukumoto, Y. Toyoda, T. Henta, A. Hata, S. Ikeda, M. Kaneko, I. D. Hoffman, B. C. Sang, H. Zou, T. Kawamoto, Design, Synthesis, and Evaluation of the Highly Selective and Potent G-Protein-Coupled Receptor Kinase 2 (GRK2) Inhibitor for the Potential Treatment of Heart Failure. *J Med Chem* **60**, 6942-6990 (2017).

261. D. M. Thal, K. T. Homan, J. Chen, E. K. Wu, P. M. Hinkle, Z. M. Huang, J. K. Chuprun, J. Song, E. Gao, J. Y. Cheung, L. A. Sklar, W. J. Koch, J. J. Tesmer, Paroxetine is a direct inhibitor of g protein-coupled receptor kinase 2 and increases myocardial contractility. *ACS chemical biology* **7**, 1830-1839 (2012).

262. S. M. Schumacher, E. Gao, W. Zhu, X. Chen, J. K. Chuprun, A. M. Feldman, J. J. Tesmer, W. J. Koch, Paroxetine-mediated GRK2 inhibition reverses cardiac dysfunction and remodeling after myocardial infarction. *Sci Transl Med* **7**, 277ra231 (2015).

263. H. V. Waldschmidt, K. T. Homan, M. C. Cato, O. Cruz-Rodriguez, A. Cannavo, M. W. Wilson, J. Song, J. Y. Cheung, W. J. Koch, J. J. Tesmer, S. D. Larsen, Structure-Based Design of Highly Selective and Potent G Protein-Coupled Receptor Kinase 2 Inhibitors Based on Paroxetine. *J Med Chem* **60**, 3052-3069 (2017).

264. G. Mayer, B. Wulffen, C. Huber, J. Brockmann, B. Flicke, L. Neumann, D. Hafenbradl, B. M. Klebl, M. J. Lohse, C. Krasel, M. Blind, An RNA molecule that specifically inhibits G-protein-coupled receptor kinase 2 in vitro. *RNA* **14**, 524-534 (2008).

265. V. M. Tesmer, S. Lennarz, G. Mayer, J. J. Tesmer, Molecular mechanism for inhibition of g protein-coupled receptor kinase 2 by a selective RNA aptamer. *Structure* **20**, 1300-1309 (2012).

266. M. Hafner, A. Schmitz, I. Grune, S. G. Srivatsan, B. Paul, W. Kolanus, T. Quast, E. Kremmer, I. Bauer, M. Famulok, Inhibition of cytohesins by SecinH3 leads to hepatic insulin resistance. *Nature* **444**, 941-944 (2006).

267. A. H. Rosenberg, B. N. Lade, D. S. Chui, S. W. Lin, J. J. Dunn, F. W. Studier, Vectors for selective expression of cloned DNAs by T7 RNA polymerase. *Gene* **56**, 125-135 (1987).

268. F. W. Studier, A. H. Rosenberg, J. J. Dunn, J. W. Dubendorff, Use of T7 RNA polymerase to direct expression of cloned genes. *Methods in enzymology* **185**, 60-89 (1990).

269. J. W. Dubendorff, F. W. Studier, Controlling basal expression in an inducible T7 expression system by blocking the target T7 promoter with lac repressor. *J Mol Biol* **219**, 45-59 (1991).

270. J. L. Vaughn, R. H. Goodwin, G. J. Tompkins, P. McCawley, The establishment of two cell lines from the insect Spodoptera frugiperda (Lepidoptera; Noctuidae). *In Vitro* **13**, 213-217 (1977).

271. V. C. Ciccarone, D. A. Polayes, V. A. Luckow, Generation of Recombinant Baculovirus DNA in E.coli Using a Baculovirus Shuttle Vector. *Methods Mol Med* **13**, 213-235 (1998).

272. V. A. Luckow, S. C. Lee, G. F. Barry, P. O. Olins, Efficient generation of infectious recombinant baculoviruses by site-specific transposon-mediated insertion of foreign genes into a baculovirus genome propagated in Escherichia coli. *J Virol* **67**, 4566-4579 (1993).

273. G. F. Barry, A broad-host-range shuttle system for gene insertion into the chromosomes of gram-negative bacteria. *Gene* **71**, 75-84 (1988).

274. D. Anderson, R. Harris, D. Polayes, V. Ciccarone, R. Donahue, G. Gerard, J. Jessee, *Rapid generation of recombinant baculovirus and expression of foreign genes using the BAC-to-BAC Baculovirus expression system*. (1995), vol. 17.

275. V. A. Luckow, M. D. Summers, Signals important for high-level expression of foreign genes in Autographa californica nuclear polyhedrosis virus expression vectors. *Virology* **167**, 56-71 (1988).

276. M. M. Bradford, A rapid and sensitive method for the quantitation of microgram quantities of protein utilizing the principle of protein-dye binding. *Analytical biochemistry* **72**, 248-254 (1976).

277. L. M. Ittner, J. Gotz, Pronuclear injection for the production of transgenic mice. *Nature protocols* **2**, 1206-1215 (2007).

278. M. Boshart, F. Weber, G. Jahn, K. Dorsch-Hasler, B. Fleckenstein, W. Schaffner, A very strong enhancer is located upstream of an immediate early gene of human cytomegalovirus. *Cell* **41**, 521-530 (1985).

279. J. A. Nelson, C. Reynolds-Kohler, B. A. Smith, Negative and positive regulation by a short segment in the 5'-flanking region of the human cytomegalovirus major immediate-early gene. *Molecular and cellular biology* **7**, 4125-4129 (1987).

280. J. Folch, M. Lees, G. H. Sloane Stanley, A simple method for the isolation and purification of total lipides from animal tissues. *The Journal of biological chemistry* **226**, 497-509 (1957).

281. L. Liu, C. M. Trent, X. Fang, N. H. Son, H. Jiang, W. S. Blaner, Y. Hu, Y. X. Yin, R. V. Farese, Jr., S. Homma, A. V. Turnbull, J. W. Eriksson, S. L. Hu, H. N. Ginsberg, L. S. Huang *et al.*,

Cardiomyocyte-specific loss of diacylglycerol acyltransferase 1 (DGAT1) reproduces the abnormalities in lipids found in severe heart failure. *The Journal of Biological Chemistry* **289**, 29881-29891 (2014).

282. J. H. Wu, J. Hagaman, S. Kim, R. L. Reddick, N. Maeda, Aortic constriction exacerbates atherosclerosis and induces cardiac dysfunction in mice lacking apolipoprotein E. *Arterioscler Thromb Vasc Biol* **22**, 469-475 (2002).

283. S. Abdalla, X. Fu, S. S. Elzahwy, K. Klaetschke, T. Streichert, U. Quitterer, Up-regulation of the cardiac lipid metabolism at the onset of heart failure. *Cardiovasc Hematol Agents Med Chem* **9**, 190-206 (2011).

284. J. Abd Alla, S. Wolf, U. Quitterer; Cell-protective compounds and their use. WO2018130537, (2018)

285. G. Kong, R. Penn, J. L. Benovic, A beta-adrenergic receptor kinase dominant negative mutant attenuates desensitization of the beta 2-adrenergic receptor. *The Journal of biological chemistry* **269**, 13084-13087 (1994).

286. J. Gulick, A. Subramaniam, J. Neumann, J. Robbins, Isolation and characterization of the mouse cardiac myosin heavy chain genes. *The Journal of biological chemistry* **266**, 9180-9185 (1991).

287. J. H. Choi, A. S. Banks, J. L. Estall, S. Kajimura, P. Bostrom, D. Laznik, J. L. Ruas, M. J. Chalmers, T. M. Kamenecka, M. Bluher, P. R. Griffin, B. M. Spiegelman, Anti-diabetic drugs inhibit obesity-linked phosphorylation of PPARgamma by Cdk5. *Nature* **466**, 451-456 (2010).

288. E. Burgermeister, R. Seger, MAPK kinases as nucleo-cytoplasmic shuttles for PPARgamma. *Cell cycle* **6**, 1539-1548 (2007).

289. A. S. Banks, F. E. McAllister, J. P. Camporez, P. J. Zushin, M. J. Jurczak, D. Laznik-Bogoslavski, G. I. Shulman, S. P. Gygi, B. M. Spiegelman, An ERK/Cdk5 axis controls the diabetogenic actions of PPARgamma. *Nature* **517**, 391-395 (2015).

290. E. Hu, J. B. Kim, P. Sarraf, B. M. Spiegelman, Inhibition of adipogenesis through MAP kinase-mediated phosphorylation of PPARgamma. *Science* **274**, 2100-2103 (1996).

291. P. A. Furth, L. Hennighausen, C. Baker, B. Beatty, R. Woychick, The variability in activity of the universally expressed human cytomegalovirus immediate early gene 1 enhancer/promoter in transgenic mice. *Nucleic Acids Res* **19**, 6205-6208 (1991).

292. N. C. Salazar, X. Vallejos, A. Siryk, G. Rengo, A. Cannavo, D. Liccardo, C. De Lucia, E. Gao, D. Leosco, W. J. Koch, A. Lymperopoulos, GRK2 blockade with beta ARKct is essential for cardiac beta(2)-adrenergic receptor signaling towards increased contractility. *Cell Commun Signal* **11**, (2013).

293. J. L. Benovic, R. H. Strasser, M. G. Caron, R. J. Lefkowitz, Beta-adrenergic receptor kinase: identification of a novel protein kinase that phosphorylates the agonist-occupied form of the receptor. *Proceedings of the National Academy of Sciences of the United States of America* **83**, 2797-2801 (1986).

294. P. H. Bauer, S. Muller, M. Puzicha, S. Pippig, B. Obermaier, E. J. Helmreich, M. J. Lohse, Phosducin is a protein kinase A-regulated G-protein regulator. *Nature* **358**, 73-76 (1992).

295. Z. Li, K. L. Laugwitz, K. Pinkernell, I. Pragst, C. Baumgartner, E. Hoffmann, K. Rosport, G. Munch, A. Moretti, J. Humrich, M. J. Lohse, M. Ungerer, Effects of two Gbetagamma-binding proteins--N-

terminally truncated phosducin and beta-adrenergic receptor kinase C terminus (betaARKct)--in heart failure. *Gene Ther* **10**, 1354-1361 (2003).

296. S. Danner, M. J. Lohse, Phosducin is a ubiquitous G-protein regulator. *Proceedings of the National Academy of Sciences of the United States of America* **93**, 10145-10150 (1996).

297. P. Zuo, J. L. Manley, Functional domains of the human splicing factor ASF/SF2. *The EMBO journal* **12**, 4727-4737 (1993).

298. J. C. Hagopian, C. T. Ma, B. R. Meade, C. P. Albuquerque, J. C. Ngo, G. Ghosh, P. A. Jennings, X. D. Fu, J. A. Adams, Adaptable molecular interactions guide phosphorylation of the SR protein ASF/SF2 by SRPK1. *J Mol Biol* **382**, 894-909 (2008).

299. J. C. Ngo, K. Giang, S. Chakrabarti, C. T. Ma, N. Huynh, J. C. Hagopian, P. C. Dorrestein, X. D. Fu, J. A. Adams, G. Ghosh, A sliding docking interaction is essential for sequential and processive phosphorylation of an SR protein by SRPK1. *Mol Cell* **29**, 563-576 (2008).

300. J. C. Ngo, S. Chakrabarti, J. H. Ding, A. Velazquez-Dones, B. Nolen, B. E. Aubol, J. A. Adams, X. D. Fu, G. Ghosh, Interplay between SRPK and Clk/Sty kinases in phosphorylation of the splicing factor ASF/SF2 is regulated by a docking motif in ASF/SF2. *Mol Cell* **20**, 77-89 (2005).

301. W. Cao, S. F. Jamison, M. A. Garcia-Blanco, Both phosphorylation and dephosphorylation of ASF/SF2 are required for pre-mRNA splicing in vitro. *RNA* **3**, 1456-1467 (1997).

302. T. Kim, J. O. Kim, J. G. Oh, S. E. Hong, D. H. Kim, Pressure-overload cardiac hypertrophy is associated with distinct alternative splicing due to altered expression of splicing factors. *Mol Cells* **37**, 81-87 (2014).

303. X. Xu, D. Yang, J. H. Ding, W. Wang, P. H. Chu, N. D. Dalton, H. Y. Wang, J. R. Bermingham, Jr., Z. Ye, F. Liu, M. G. Rosenfeld, J. L. Manley, J. Ross, Jr., J. Chen, R. P. Xiao *et al.*, ASF/SF2-regulated CaMKIIdelta alternative splicing temporally reprograms excitation-contraction coupling in cardiac muscle. *Cell* **120**, 59-72 (2005).

304. Q. Gu, N. Jin, H. Sheng, X. Yin, J. Zhu, Cyclic AMP-dependent protein kinase A regulates the alternative splicing of CaMKIIdelta. *PloS one* **6**, e25745 (2011).

305. B. Hoch, R. Meyer, R. Hetzer, E. G. Krause, P. Karczewski, Identification and expression of delta-isoforms of the multifunctional Ca2+/calmodulin-dependent protein kinase in failing and nonfailing human myocardium. *Circulation research* **84**, 713-721 (1999).

306. U. Kirchhefer, W. Schmitz, H. Scholz, J. Neumann, Activity of cAMP-dependent protein kinase and Ca2+/calmodulin-dependent protein kinase in failing and nonfailing human hearts. *Cardiovasc Res* **42**, 254-261 (1999).

307. J. M. Colomer, L. Mao, H. A. Rockman, A. R. Means, Pressure overload selectively up-regulates Ca2+/calmodulin-dependent protein kinase II in vivo. *Mol Endocrinol* **17**, 183-192 (2003).

308. X. Ai, J. W. Curran, T. R. Shannon, D. M. Bers, S. M. Pogwizd, Ca2+/calmodulin-dependent protein kinase modulates cardiac ryanodine receptor phosphorylation and sarcoplasmic reticulum Ca2+ leak in heart failure. *Circulation research* **97**, 1314-1322 (2005).

309. J. N. Cohn, G. R. Johnson, R. Shabetai, H. Loeb, F. Tristani, T. Rector, R. Smith, R. Fletcher, Ejection fraction, peak exercise oxygen consumption, cardiothoracic ratio, ventricular arrhythmias, and plasma norepinephrine as determinants of prognosis in heart failure. The V-HeFT VA Cooperative Studies Group. *Circulation* **87**, VI5-16 (1993).

310. X. Zhang, C. Szeto, E. Gao, M. Tang, J. Jin, Q. Fu, C. Makarewich, X. Ai, Y. Li, A. Tang, J. Wang, H. Gao, F. Wang, X. J. Ge, S. P. Kunapuli *et al.*, Cardiotoxic and cardioprotective features of chronic beta-adrenergic signaling. *Circ Res* **112**, 498-509 (2013).

311. T. Eschenhagen, Beta-adrenergic signaling in heart failure-adapt or die. *Nat Med* **14**, 485-487 (2008).

312. H. A. Rockman, W. J. Koch, R. J. Lefkowitz, Seven-transmembrane-spanning receptors and heart function. *Nature* **415**, 206-212 (2002).

313. M. Sallese, L. Iacovelli, A. Cumashi, L. Capobianco, L. Cuomo, A. De Blasi, Regulation of G protein-coupled receptor kinase subtypes by calcium sensor proteins. *Biochimica et Biophysica Acta* **1498**, 112-121 (2000).

314. G. W. Dorn, 2nd, T. Force, Protein kinase cascades in the regulation of cardiac hypertrophy. *J Clin Invest* **115**, 527-537 (2005).

315. D. D. D'Angelo, Y. Sakata, J. N. Lorenz, G. P. Boivin, R. A. Walsh, S. B. Liggett, G. W. Dorn, 2nd, Transgenic Galphaq overexpression induces cardiac contractile failure in mice. *Proceedings of the National Academy of Sciences of the United States of America* **94**, 8121-8126 (1997).

316. G. W. Dorn, 2nd, N. M. Tepe, J. N. Lorenz, W. J. Koch, S. B. Liggett, Low- and high-level transgenic expression of beta2-adrenergic receptors differentially affect cardiac hypertrophy and function in Galphaq-overexpressing mice. *Proceedings of the National Academy of Sciences of the United States of America* **96**, 6400-6405 (1999).

317. J. W. Adams, Y. Sakata, M. G. Davis, V. P. Sah, Y. Wang, S. B. Liggett, K. R. Chien, J. H. Brown, G. W. Dorn, 2nd, Enhanced Galphaq signaling: a common pathway mediates cardiac hypertrophy and apoptotic heart failure. *Proceedings of the National Academy of Sciences of the United States of America* **95**, 10140-10145 (1998).

318. S. M. Schumacher, E. Gao, M. Cohen, M. Lieu, J. K. Chuprun, W. J. Koch, A peptide of the RGS domain of GRK2 binds and inhibits Galpha(q) to suppress pathological cardiac hypertrophy and dysfunction. *Sci Signal* **9**, ra30 (2016).

319. R. Lappano, M. Maggiolini, G protein-coupled receptors: novel targets for drug discovery in cancer. *Nat Rev Drug Discov* **10**, 47-60 (2011).

320. A. Tohgo, K. L. Pierce, E. W. Choy, R. J. Lefkowitz, L. M. Luttrell, beta-Arrestin scaffolding of the ERK cascade enhances cytosolic ERK activity but inhibits ERK-mediated transcription following angiotensin AT1a receptor stimulation. *The Journal of biological chemistry* **277**, 9429-9436 (2002).

321. K. A. DeFea, J. Zalevsky, M. S. Thoma, O. Dery, R. D. Mullins, N. W. Bunnett, beta-arrestin-dependent endocytosis of proteinase-activated receptor 2 is required for intracellular targeting of activated ERK1/2. *J Cell Biol* **148**, 1267-1281 (2000).

322. D. G. Tilley, I. M. Kim, P. A. Patel, J. D. Violin, H. A. Rockman, beta-Arrestin mediates beta1-adrenergic receptor-epidermal growth factor receptor interaction and downstream signaling. *The Journal of biological chemistry* **284**, 20375-20386 (2009).

323. I. Kehat, J. D. Molkentin, Extracellular signal-regulated kinase 1/2 (ERK1/2) signaling in cardiac hypertrophy. *Ann N Y Acad Sci* **1188**, 96-102 (2010).

324. M. Maillet, N. H. Purcell, M. A. Sargent, A. J. York, O. F. Bueno, J. D. Molkentin, DUSP6 (MKP3) null mice show enhanced ERK1/2 phosphorylation at baseline and increased myocyte proliferation in the heart affecting disease susceptibility. *The Journal of biological chemistry* **283**, 31246-31255 (2008).

325. N. H. Purcell, B. J. Wilkins, A. York, M. K. Saba-El-Leil, S. Meloche, J. Robbins, J. D. Molkentin, Genetic inhibition of cardiac ERK1/2 promotes stress-induced apoptosis and heart failure but has no effect on hypertrophy in vivo. *Proceedings of the National Academy of Sciences of the United States of America* **104**, 14074-14079 (2007).

326. O. Yamaguchi, T. Watanabe, K. Nishida, K. Kashiwase, Y. Higuchi, T. Takeda, S. Hikoso, S. Hirotani, M. Asahi, M. Taniike, A. Nakai, I. Tsujimoto, Y. Matsumura, J. Miyazaki, K. R. Chien *et al.*, Cardiac-specific disruption of the c-raf-1 gene induces cardiac dysfunction and apoptosis. *J Clin Invest* **114**, 937-943 (2004).

327. H. Cheng, G. Kari, A. P. Dicker, U. Rodeck, W. J. Koch, T. Force, A novel preclinical strategy for identifying cardiotoxic kinase inhibitors and mechanisms of cardiotoxicity. *Circulation research* **109**, 1401-1409 (2011).

328. D. J. Lips, O. F. Bueno, B. J. Wilkins, N. H. Purcell, R. A. Kaiser, J. N. Lorenz, L. Voisin, M. K. Saba-El-Leil, S. Meloche, J. Pouyssegur, G. Pages, L. J. De Windt, P. A. Doevendans, J. D. Molkentin, MEK1-ERK2 signaling pathway protects myocardium from ischemic injury in vivo. *Circulation* **109**, 1938-1941 (2004).

329. E. Lucas, M. Jurado-Pueyo, M. A. Fortuno, S. Fernandez-Veledo, R. Vila-Bedmar, L. J. Jimenez-Borreguero, J. J. Lazcano, E. Gao, J. Gomez-Ambrosi, G. Fruhbeck, W. J. Koch, J. Diez, F. Mayor, Jr., C. Murga, Downregulation of G protein-coupled receptor kinase 2 levels enhances cardiac insulin sensitivity and switches on cardioprotective gene expression patterns. *Biochim Biophys Acta* **1842**, 2448-2456 (2014).

330. S. Z. Duan, C. Y. Ivashchenko, M. W. Russell, D. S. Milstone, R. M. Mortensen, Cardiomyocyte-specific knockout and agonist of peroxisome proliferator-activated receptor-gamma both induce cardiac hypertrophy in mice. *Circulation research* **97**, 372-379 (2005).

331. N. H. Son, T. S. Park, H. Yamashita, M. Yokoyama, L. A. Huggins, K. Okajima, S. Homma, M. J. Szabolcs, L. S. Huang, I. J. Goldberg, Cardiomyocyte expression of PPARgamma leads to cardiac dysfunction in mice. *J Clin Invest* **117**, 2791-2801 (2007).

332. N. H. Son, S. Yu, J. Tuinei, K. Arai, H. Hamai, S. Homma, G. I. Shulman, E. D. Abel, I. J. Goldberg, PPARgamma-induced cardiolipotoxicity in mice is ameliorated by PPARalpha deficiency despite increases in fatty acid oxidation. *J Clin Invest* **120**, 3443-3454 (2010).

333. B. Razani, H. Zhang, P. C. Schulze, J. D. Schilling, J. Verbsky, I. J. Lodhi, V. K. Topkara, C. Feng, T. Coleman, A. Kovacs, D. P. Kelly, J. E. Saffitz, G. W. Dorn, 2nd, C. G. Nichols, C. F. Semenkovich, Fatty acid synthase modulates homeostatic responses to myocardial stress. *The Journal of biological chemistry* **286**, 30949-30961 (2011).

334. N. Maeda, M. Takahashi, T. Funahashi, S. Kihara, H. Nishizawa, K. Kishida, H. Nagaretani, M. Matsuda, R. Komuro, N. Ouchi, H. Kuriyama, K. Hotta, T. Nakamura, I. Shimomura, Y. Matsuzawa, PPARgamma ligands increase expression and plasma concentrations of adiponectin, an adipose-derived protein. *Diabetes* **50**, 2094-2099 (2001).

335. T. Tomaru, D. J. Steger, M. I. Lefterova, M. Schupp, M. A. Lazar, Adipocyte-specific expression of murine resistin is mediated by synergism between peroxisome proliferator-activated receptor

gamma and CCAAT/enhancer-binding proteins. *The Journal of biological chemistry* **284**, 6116-6125 (2009).

336. M. Murholm, K. Dixen, J. B. Hansen, Ras signalling regulates differentiation and UCP1 expression in models of brown adipogenesis. *Biochim Biophys Acta* **1800**, 619-627 (2010).

337. S. Neubauer, The failing heart--an engine out of fuel. *N Engl J Med* **356**, 1140-1151 (2007).

338. N. Li, J. Wang, F. Gao, Y. Tian, R. Song, S. J. Zhu, The role of uncoupling protein 2 in the apoptosis induced by free fatty acid in rat cardiomyocytes. *J Cardiovasc Pharmacol* **55**, 161-167 (2010).

339. N. Bodyak, D. L. Rigor, Y. S. Chen, Y. Han, E. Bisping, W. T. Pu, P. M. Kang, Uncoupling protein 2 modulates cell viability in adult rat cardiomyocytes. *Am J Physiol Heart Circ Physiol* **293**, H829-835 (2007).

340. J. S. Flier, K. S. Cook, P. Usher, B. M. Spiegelman, Severely impaired adipsin expression in genetic and acquired obesity. *Science* **237**, 405-408 (1987).

341. N. Shahini, A. E. Michelsen, P. H. Nilsson, K. Ekholt, L. Gullestad, K. Broch, C. P. Dahl, P. Aukrust, T. Ueland, T. E. Mollnes, A. Yndestad, M. C. Louwe, The alternative complement pathway is dysregulated in patients with chronic heart failure. *Scientific reports* **7**, 42532 (2017).

342. B. J. Goldstein, R. G. Scalia, X. L. Ma, Protective vascular and myocardial effects of adiponectin. *Nat Clin Pract Cardiovasc Med* **6**, 27-35 (2009).

343. T. Pischon, C. J. Girman, G. S. Hotamisligil, N. Rifai, F. B. Hu, E. B. Rimm, Plasma adiponectin levels and risk of myocardial infarction in men. *JAMA* **291**, 1730-1737 (2004).

344. R. Shibata, Y. Numaguchi, K. Matsushita, T. Sone, R. Kubota, T. Ohashi, M. Ishii, S. Kihara, K. Walsh, N. Ouchi, T. Murohara, Usefulness of adiponectin to predict myocardial salvage following successful reperfusion in patients with acute myocardial infarction. *Am J Cardiol* **101**, 1712-1715 (2008).

345. J. George, S. Patal, D. Wexler, Y. Sharabi, E. Peleg, Y. Kamari, E. Grossman, D. Sheps, G. Keren, A. Roth, Circulating adiponectin concentrations in patients with congestive heart failure. *Heart* **92**, 1420-1424 (2006).

346. I. D. Laoutaris, I. K. Vasiliadis, A. Dritsas, S. Mavrogeni, M. S. Kallistratos, A. Manginas, A. Chaidaroglou, D. Degiannis, D. B. Panagiotakos, D. V. Cokkinos, High plasma adiponectin is related to low functional capacity in patients with chronic heart failure. *Int J Cardiol* **144**, 230-231 (2010).

347. T. Nakamura, H. Funayama, N. Kubo, T. Yasu, M. Kawakami, M. Saito, S. Momomura, S. E. Ishikawa, Association of hyperadiponectinemia with severity of ventricular dysfunction in congestive heart failure. *Circ J* **70**, 1557-1562 (2006).

348. C. M. Steppan, S. T. Bailey, S. Bhat, E. J. Brown, R. R. Banerjee, C. M. Wright, H. R. Patel, R. S. Ahima, M. A. Lazar, The hormone resistin links obesity to diabetes. *Nature* **409**, 307-312 (2001).

349. M. S. Burnett, C. W. Lee, T. D. Kinnaird, E. Stabile, S. Durrani, M. K. Dullum, J. M. Devaney, C. Fishman, S. Stamou, D. Canos, S. Zbinden, L. C. Clavijo, G. J. Jang, J. A. Andrews, J. Zhu *et al.*, The potential role of resistin in atherogenesis. *Atherosclerosis* **182**, 241-248 (2005).

350. B. W. Wang, H. F. Hung, H. Chang, P. Kuan, K. G. Shyu, Mechanical stretch enhances the expression of resistin gene in cultured cardiomyocytes via tumor necrosis factor-alpha. *Am J Physiol Heart Circ Physiol* **293**, H2305-2312 (2007).

351. M. Kim, J. K. Oh, S. Sakata, I. Liang, W. Park, R. J. Hajjar, D. Lebeche, Role of resistin in cardiac contractility and hypertrophy. *J Mol Cell Cardiol* **45**, 270-280 (2008).

352. D. S. Frankel, R. S. Vasan, R. B. D'Agostino, Sr., E. J. Benjamin, D. Levy, T. J. Wang, J. B. Meigs, Resistin, adiponectin, and risk of heart failure the Framingham offspring study. *J Am Coll Cardiol* **53**, 754-762 (2009).

353. L. W. Stanton, P. A. Ponte, R. T. Coleman, M. A. Snyder, Expression of CA III in rodent models of obesity. *Mol Endocrinol* **5**, 860-866 (1991).

354. D. L. Brasaemle, Thematic review series: adipocyte biology. The perilipin family of structural lipid droplet proteins: stabilization of lipid droplets and control of lipolysis. *J Lipid Res* **48**, 2547-2559 (2007).

355. Y. Nakachi, K. Yagi, I. Nikaido, H. Bono, M. Tonouchi, C. Schonbach, Y. Okazaki, Identification of novel PPARgamma target genes by integrated analysis of ChIP-on-chip and microarray expression data during adipocyte differentiation. *Biochem Biophys Res Commun* **372**, 362-366 (2008).

356. I. Holme, A. H. Aastveit, N. Hammar, I. Jungner, G. Walldius, Haptoglobin and risk of myocardial infarction, stroke, and congestive heart failure in 342,125 men and women in the Apolipoprotein MOrtality RISk study (AMORIS). *Ann Med* **41**, 522-532 (2009).

357. M. P. Mayer, B. Bukau, Hsp70 chaperones: cellular functions and molecular mechanism. *Cell Mol Life Sci* **62**, 670-684 (2005).

358. Z. M. Jenei, T. Gombos, Z. Forhecz, Z. Pozsonyi, I. Karadi, L. Janoskuti, Z. Prohaszka, Elevated extracellular HSP70 (HSPA1A) level as an independent prognostic marker of mortality in patients with heart failure. *Cell Stress Chaperones* **18**, 809-813 (2013).

359. P. Deng, Y. Chen, N. Ji, Y. Lin, Q. Yuan, L. Ye, Q. Chen, Cysteine dioxygenase type 1 promotes adipogenesis via interaction with peroxisome proliferator-activated receptor gamma. *Biochem Biophys Res Commun* **458**, 123-127 (2015).

360. K. Carvajal, R. Moreno-Sanchez, Heart metabolic disturbances in cardiovascular diseases. *Arch Med Res* **34**, 89-99 (2003).

361. T. S. Park, I. J. Goldberg, Sphingolipids, lipotoxic cardiomyopathy, and cardiac failure. *Heart Fail Clin* **8**, 633-641 (2012).

362. C. Christoffersen, E. Bollano, M. L. Lindegaard, E. D. Bartels, J. P. Goetze, C. B. Andersen, L. B. Nielsen, Cardiac lipid accumulation associated with diastolic dysfunction in obese mice. *Endocrinology* **144**, 3483-3490 (2003).

363. Y. A. Hannun, L. M. Obeid, Many ceramides. *The Journal of biological chemistry* **286**, 27855-27862 (2011).

364. D. Dyntar, M. Eppenberger-Eberhardt, K. Maedler, M. Pruschy, H. M. Eppenberger, G. A. Spinas, M. Y. Donath, Glucose and palmitic acid induce degeneration of myofibrils and modulate apoptosis in rat adult cardiomyocytes. *Diabetes* **50**, 2105-2113 (2001).

365. J. Yu, W. Pan, R. Shi, T. Yang, Y. Li, G. Yu, Y. Bai, E. H. Schuchman, X. He, G. Zhang, Ceramide is upregulated and associated with mortality in patients with chronic heart failure. *Can J Cardiol* **31**, 357-363 (2015).

366. D. Mochly-Rosen, K. Das, K. V. Grimes, Protein kinase C, an elusive therapeutic target? *Nat Rev Drug Discov* **11**, 937-957 (2012).

367. Q. Liu, J. D. Molkentin, Protein kinase Calpha as a heart failure therapeutic target. *J Mol Cell Cardiol* **51**, 474-478 (2011).

368. Y. T. Zhou, P. Grayburn, A. Karim, M. Shimabukuro, M. Higa, D. Baetens, L. Orci, R. H. Unger, Lipotoxic heart disease in obese rats: implications for human obesity. *Proceedings of the National Academy of Sciences of the United States of America* **97**, 1784-1789 (2000).

369. J. E. de Vries, M. M. Vork, T. H. Roemen, Y. F. de Jong, J. P. Cleutjens, G. J. van der Vusse, M. van Bilsen, Saturated but not mono-unsaturated fatty acids induce apoptotic cell death in neonatal rat ventricular myocytes. *J Lipid Res* **38**, 1384-1394 (1997).

370. G. C. Sparagna, D. L. Hickson-Bick, L. M. Buja, J. B. McMillin, A metabolic role for mitochondria in palmitate-induced cardiac myocyte apoptosis. *Am J Physiol Heart Circ Physiol* **279**, H2124-2132 (2000).

371. L. L. Listenberger, J. E. Schaffer, Mechanisms of lipoapoptosis: implications for human heart disease. *Trends Cardiovasc Med* **12**, 134-138 (2002).

372. J. E. Kim, M. W. Ahn, S. H. Baek, I. K. Lee, Y. W. Kim, J. Y. Kim, J. M. Dan, S. Y. Park, AMPK activator, AICAR, inhibits palmitate-induced apoptosis in osteoblast. *Bone* **43**, 394-404 (2008).

373. S. J. Matkovich, A. Diwan, J. L. Klanke, D. J. Hammer, Y. Marreez, A. M. Odley, E. W. Brunskill, W. J. Koch, R. J. Schwartz, G. W. Dorn, 2nd, Cardiac-specific ablation of G-protein receptor kinase 2 redefines its roles in heart development and beta-adrenergic signaling. *Circulation research* **99**, 996-1003 (2006).

374. M. Purgato, D. Papola, C. Gastaldon, C. Trespidi, L. R. Magni, C. Rizzo, T. A. Furukawa, N. Watanabe, A. Cipriani, C. Barbui, Paroxetine versus other anti-depressive agents for depression. *Cochrane Database Syst Rev*, CD006531 (2014).

375. K. E. Wurst, C. Poole, S. A. Ephross, A. F. Olshan, First trimester paroxetine use and the prevalence of congenital, specifically cardiac, defects: a meta-analysis of epidemiological studies. *Birth Defects Res A Clin Mol Teratol* **88**, 159-170 (2010).

376. K. Lorenz; Rkip agonism in the treatment and prevention of heart failure. US201615555725 20160307, (2016)

377. W. J. Koch, Genetic and phenotypic targeting of beta-adrenergic signaling in heart failure. *Mol Cell Biochem* **263**, 5-9 (2004).

378. R. R. Gainetdinov, L. M. Bohn, J. K. Walker, S. A. Laporte, A. D. Macrae, M. G. Caron, R. J. Lefkowitz, R. T. Premont, Muscarinic supersensitivity and impaired receptor desensitization in G protein-coupled receptor kinase 5-deficient mice. *Neuron* **24**, 1029-1036 (1999).

379. N. Oyama, K. Urasawa, S. Kaneta, H. Sakai, T. Saito, C. Takagi, I. Yoshida, A. Kitabatake, H. Tsutsui, Angiotensin converting enzyme inhibitors attenuated the expression of G-protein coupled receptor kinases in heart failure patients. *Circ J* **70**, 362-363 (2006).

13. Appendix

13.1. Sequencing of pFastBac6HisTEVADRBK1

Sequencing pFastBac6HisTEVADRBK1 clone 1

GTC GAC: SalI restriction site

ATG: Startcodon orf

XXX: 6x Histidin tag

XXX: TEV protease cleavage site

TGA: Stopcodon orf

AAG CTT: HindIII restriction site

6xHisTEVADRBK1	**4079 - 6217**
1_FastBacGRK2_54 FastBac-for	4010 - 5135
2_FastBacGRK2_54 GKR2seq34	5025 - 5505
3_FastBacGRK2_54 FastBac-rev	5207 - 6272

Sequencing 17.5.2015
Primer from Mircosynth Primer List:
FastBac-for TACTGTTTTCGTAACAGTTTTG

1_FastBacGRK2_54 FastBac-for
ATACCGTCCCACCATCGGGCGCGGATCCCGGTCCGAAGCGCGCGGAATTCAAAGGCCTACGTCGACACCATGTCGTACTACCATCAC
CATCACCATCACGATTACGATATCCCAACGACCGAAAACCTGTATTTTCAGGGCGCGGACCTGGAGGCGGTGCTGGCCGACGTGAGC
TACCTGATGGCCATGGAGAAGAGCAAGGCCACGCCGGCCGCGCGCGCCAGCAAGAAGATACTGCTGCCCGAGCCCAGCATCCGCAGT
GTCATGCAGAAGTACCTGGAGGACCGGGGCGAGGTGACCTTTGAGAAGATCTTTTCCCAGAAGCTGGGGTACCTGCTCTTCCGAGAC
TTCTGCCTGAACCACCTGGAGGAGGCCAGGCCCTTGGTGGAATTCTATGAGGAGATCAAGAAGTACGAGAAGCTGGAGACGGAGGAG
GAGCGTGTGGCCCGCAGCCGGGAGATCTTCGACTCATACATCATGAAGGAGCTGCTGGCCTGCTCGCATCCCTTCTCGAAGAGTGCC
ACTGAGCATGTCCAAGGCCACCTGGGGAAGAAGCAGGTGCCTCCGGATCTCTTCCAGCCATACATCGAAGAGATTTGTCAAAACCTC
CGAGGGGACGTGTTCCAGAAATTCATTGAGAGCGATAAGTTCACACGGTTTTGCCAGTGGAAGAATGTGGAGCTCAACATCCACCTG
ACCATGAATGACTTCAGCGTGCATCGCATCATTGGGCGCGGGGGCTTTGGCGAGGTCTATGGGTGCCGGAAGGCTGACACAGGCAAG
ATGTACGCCATGAAGTGCCTGGACAAAAAGCGCATCAAGATGAAGCAGGGGGAGACCCTGGCCCTGAACGAGCGCATCATGCTCTCG
CTCGTCAGCACTGGGGACTGCCCATTCATTGTCTGCATGTCATACGCGTTCCACACGCCAGACAAGCTCAGCTTCATCCTGGACCTC
ATGAACGGTGGGGACCTGCACTACCACCTCTCCCAGCACGGGGTCTTCTCAGAGGCTGACATGCGCTTCTATGCGGCCGAGATCATC
CTGGGCCTGGAGCACATGCACAACCGCTTCGTGGTCTACCGGGACCTGAAGCCAGCCAACATCCTTCTGGACGAGCATGGCCMCGTG
CGGATYTCGGACCTGGGCCTGGCCTGKGACTTY

Alignment statistics for match #1

Score	Expect	Identities	Gaps	Strand
2132 bits(1154)	0.0	1159/1163(99%)	0/1163(0%)	Plus/Plus

```
Query  4010  ATACCGTCCCACCATCGGGCGCGGATCCCGGTCCGAAGCGCGCGGAATTCAAAGGCCTAC  4069
              ||||||||||||||||||||||||||||||||||||||||||||||||||||||||||||
Sbjct  1     ATACCGTCCCACCATCGGGCGCGGATCCCGGTCCGAAGCGCGCGGAATTCAAAGGCCTAC  60

Query  4070  GTCGACACCATGTCGTACTACCATCACCATCACCATCACGATTACGATATCCCAACGACC  4129
              ||||||||||||||||||||||||||||||||||||||||||||||||||||||||||||
Sbjct  61    GTCGACACCATGTCGTACTACCATCACCATCACCATCACGATTACGATATCCCAACGACC  120

Query  4130  GAAAACCTGTATTTTCAGGGCGCGGACCTGGAGGCGGTGCTGGCCGACGTGAGCTACCTG  4189
              ||||||||||||||||||||||||||||||||||||||||||||||||||||||||||||
Sbjct  121   GAAAACCTGTATTTTCAGGGCGCGGACCTGGAGGCGGTGCTGGCCGACGTGAGCTACCTG  180

Query  4190  ATGGCCATGGAGAAGAGCAAGGCCACGCCGGCCGCGCGCGCCAGCAAGAAGATCCTGCTG  4249
              ||||||||||||||||||||||||||||||||||||||||||||||||||||||||||||
Sbjct  181   ATGGCCATGGAGAAGAGCAAGGCCACGCCGGCCGCGCGCGCCAGCAAGAAGATCCTGCTG  240

Query  4250  CCCGAGCCCAGCATCCGCAGTGTCATGCAGAAGTACCTGGAGGACCGGGGCGAGGTGACC  4309
              ||||||||||||||||||||||||||||||||||||||||||||||||||||||||||||
Sbjct  241   CCCGAGCCCAGCATCCGCAGTGTCATGCAGAAGTACCTGGAGGACCGGGGCGAGGTGACC  300

Query  4310  TTTGAGAAGATCTTTTCCCAGAAGCTGGGGTACCTGCTCTTCCGAGACTTCTGCCTGAAC  4369
              ||||||||||||||||||||||||||||||||||||||||||||||||||||||||||||
Sbjct  301   TTTGAGAAGATCTTTTCCCAGAAGCTGGGGTACCTGCTCTTCCGAGACTTCTGCCTGAAC  360

Query  4370  CACCTGGAGGAGGCCAGGCCCTTGGTGGAATTCTATGAGGAGATCAAGAAGTACGAGAAG  4429
              ||||||||||||||||||||||||||||||||||||||||||||||||||||||||||||
Sbjct  361   CACCTGGAGGAGGCCAGGCCCTTGGTGGAATTCTATGAGGAGATCAAGAAGTACGAGAAG  420

Query  4430  CTGGAGACGGAGGAGGAGCGTGTGGCCCGCAGCCGGGAGATCTTCGACTCATACATCATG  4489
              ||||||||||||||||||||||||||||||||||||||||||||||||||||||||||||
Sbjct  421   CTGGAGACGGAGGAGGAGCGTGTGGCCCGCAGCCGGGAGATCTTCGACTCATACATCATG  480

Query  4490  AAGGAGCTGCTGGCCTGCTCGCATCCCTTCTCGAAGAGTGCCACTGAGCATGTCCAAGGC  4549
              ||||||||||||||||||||||||||||||||||||||||||||||||||||||||||||
Sbjct  481   AAGGAGCTGCTGGCCTGCTCGCATCCCTTCTCGAAGAGTGCCACTGAGCATGTCCAAGGC  540

Query  4550  CACCTGGGGAAGAAGCAGGTGCCTCCGGATCTCTTCCAGCCATACATCGAAGAGATTTGT  4609
              ||||||||||||||||||||||||||||||||||||||||||||||||||||||||||||
Sbjct  541   CACCTGGGGAAGAAGCAGGTGCCTCCGGATCTCTTCCAGCCATACATCGAAGAGATTTGT  600
```

```
Query  4610  CAAAACCTCCGAGGGGACGTGTTCCAGAAATTCATTGAGAGCGATAAGTTCACACGGTTT  4669
             ||||||||||||||||||||||||||||||||||||||||||||||||||||||||||||
Sbjct  601   CAAAACCTCCGAGGGGACGTGTTCCAGAAATTCATTGAGAGCGATAAGTTCACACGGTTT  660

Query  4670  TGCCAGTGGAAGAATGTGGAGCTCAACATCCACCTGACCATGAATGACTTCAGCGTGCAT  4729
             ||||||||||||||||||||||||||||||||||||||||||||||||||||||||||||
Sbjct  661   TGCCAGTGGAAGAATGTGGAGCTCAACATCCACCTGACCATGAATGACTTCAGCGTGCAT  720

Query  4730  CGCATCATTGGGCGCGGGGGCTTTGGCGAGGTCTATGGGTGCCGGAAGGCTGACACAGGC  4789
             ||||||||||||||||||||||||||||||||||||||||||||||||||||||||||||
Sbjct  721   CGCATCATTGGGCGCGGGGGCTTTGGCGAGGTCTATGGGTGCCGGAAGGCTGACACAGGC  780

Query  4790  AAGATGTACGCCATGAAGTGCCTGGACAAAAAGCGCATCAAGATGAAGCAGGGGGAGACC  4849
             ||||||||||||||||||||||||||||||||||||||||||||||||||||||||||||
Sbjct  781   AAGATGTACGCCATGAAGTGCCTGGACAAAAAGCGCATCAAGATGAAGCAGGGGGAGACC  840

Query  4850  CTGGCCCTGAACGAGCGCATCATGCTCTCGCTCGTCAGCACTGGGGACTGCCCATTCATT  4909
             ||||||||||||||||||||||||||||||||||||||||||||||||||||||||||||
Sbjct  841   CTGGCCCTGAACGAGCGCATCATGCTCTCGCTCGTCAGCACTGGGGACTGCCCATTCATT  900

Query  4910  GTCTGCATGTCATACGCGTTCCACACGCCAGACAAGCTCAGCTTCATCCTGGACCTCATG  4969
             ||||||||||||||||||||||||||||||||||||||||||||||||||||||||||||
Sbjct  901   GTCTGCATGTCATACGCGTTCCACACGCCAGACAAGCTCAGCTTCATCCTGGACCTCATG  960

Query  4970  AACGGTGGGGACCTGCACTACCACCTCTCCCAGCACGGGGTCTTCTCAGAGGCTGACATG  5029
             ||||||||||||||||||||||||||||||||||||||||||||||||||||||||||||
Sbjct  961   AACGGTGGGGACCTGCACTACCACCTCTCCCAGCACGGGGTCTTCTCAGAGGCTGACATG  1020

Query  5030  CGCTTCTATGCGGCCGAGATCATCCTGGGCCTGGAGCACATGCACAACCGCTTCGTGGTC  5089
             ||||||||||||||||||||||||||||||||||||||||||||||||||||||||||||
Sbjct  1021  CGCTTCTATGCGGCCGAGATCATCCTGGGCCTGGAGCACATGCACAACCGCTTCGTGGTC  1080

Query  5090  TACCGGGACCTGAAGCCAGCCAACATCCTTCTGGACGAGCATGGCCACGTGCGGATCTCG  5149
             |||||||||||||||||||||||||||||||||||||||||||| ||||||||| |||
Sbjct  1081  TACCGGGACCTGAAGCCAGCCAACATCCTTCTGGACGAGCATGGCCMCGTGCGGATYTCG  1140

Query  5150  GACCTGGGCCTGGCCTGTGACTT  5172
             |||||||||||||||| |||||
Sbjct  1141  GACCTGGGCCTGGCCTGKGACTT  1163
```

Sequencing 17.5.2015
Primer GRK2seq34

2_FastBacGRK2_54 GKR2seq34
AGGCAAGATGTACGCCATGAAGTGCCTGGACAAAAAGCGCATCARGATGAAGCAGGGGGAGACCCTGGCCCTGAACGAGCGCATCAN
GCTCTCGCTCGTCAGCACTGGGGACTGCCCATTCATTGTCTGCATGTCATACGCGTTCCACACGCCAGACAAGCTCAGCTTCATCCT
GGACCTCATGAACGGNGGGGACCTGCACTACCACCTCTCCCAGCACGGGGTCTTCTCAGAGGCTGACATGCGCTTCTATGCGGCCGA
GATCATCCTGGGCCTGGAGCACATGCACAACCGCTTCGTGGTCTACCGGGACCTGAAGCCAGCCAACATCCTTCTGGACGAGCATGG
CCACGTGCGGATCTCGGACCTGGGCCTGGCCTGTGACTTCTCCAAGAAGAAGCCCCATGCCAGCGTGGGCACCCACGGGTACATGGC
TCCGGAGGTCCTGCAGAAGGGCGTGGCCTACGACAGCAGTGCCGACTGGTTCTCTCTGGGGTGCATGCTCTTCAAGTTGCTGCGGGG
GCACAGCCCCTTCCGGCAGCACAAGACCAAAGACAAGCATGAGATCGACCGCATGACGCTGACGATGGCCGTGGAGCTGCCCGACTC
CTTCTCCCCTGAACTACGCTCCCTGCTGGAGGGGTTGCTGCAGAGGGATGTCAACCGGAGATTGGGCTGCCTGGGCCGAGGGGCTCA
GGAGGTGAAAGAGAGCCCCTTTTTCCGCTCCCTGGACTGGCAGATGGTCTTCTTGCAAAAGTACCCTCCCCCGCTGATCCCCCCACG
AGGGGAGGTGAACGCGGCCGACGCCTTCGACATTGGCTCCTTCGATGAGGAGGACACAAAAGGAATCAAGTTACTGGACAGTGATCA
GGAGCTCTACCGCAACTTCCCCCTCACCATCTCGGAGCGGTGGCAGCAKGAGGTGGCAGAGACTGTCTTCGACACCATCAACGGTTG
AGACAGACCCGGCTGGAAGGCTCGCAAGAAAGCCAAGAACAAGCCAGCTGGGCCCATGAGGAAAAACTACCCCCCTGGGGCAAGGAC
TGGCATCATGGCATGGGCTACATGTTCCAARATGGGGCAACCCCCTTCCTGGACCCAATGGGCAGSCGGCGGTTACCTTCTACCTTG
TTCCCCAAACCGGCCTCGGAGTGGGCGGGGGCGAAGGGCCAAGGCCC

```
Query  4786  AGGCAAGATGTACGCCATGAAGTGCCTGGACAAAAAGCGCATCAAGATGAAGCAGGGGGA  4845
              |||||||||||||||||||||||||||||||||||||||||||||| ||||||||||||||||
Sbjct  1      AGGCAAGATGTACGCCATGAAGTGCCTGGACAAAAAGCGCATCARGATGAAGCAGGGGGA  60

Query  4846  GACCCTGGCCCTGAACGAGCGCATCATGCTCTCGCTCGTCAGCACTGGGGACTGCCCATT  4905
              |||||||||||||||||||||||||| ||||||||||||||||||||||||||||||||||
Sbjct  61    GACCCTGGCCCTGAACGAGCGCATCANGCTCTCGCTCGTCAGCACTGGGGACTGCCCATT  120

Query  4906  CATTGTCTGCATGTCATACGCGTTCCACACGCCAGACAAGCTCAGCTTCATCCTGGACCT  4965
              ||||||||||||||||||||||||||||||||||||||||||||||||||||||||||||||
Sbjct  121   CATTGTCTGCATGTCATACGCGTTCCACACGCCAGACAAGCTCAGCTTCATCCTGGACCT  180

Query  4966  CATGAACGGTGGGGACCTGCACTACCACCTCTCCCAGCACGGGGTCTTCTCAGAGGCTGA  5025
              ||||||||| ||||||||||||||||||||||||||||||||||||||||||||||||||||
Sbjct  181   CATGAACGGNGGGGACCTGCACTACCACCTCTCCCAGCACGGGGTCTTCTCAGAGGCTGA  240

Query  5026  CATGCGCTTCTATGCGGCCGAGATCATCCTGGGCCTGGAGCACATGCACAACCGCTTCGT  5085
              ||||||||||||||||||||||||||||||||||||||||||||||||||||||||||||||
Sbjct  241   CATGCGCTTCTATGCGGCCGAGATCATCCTGGGCCTGGAGCACATGCACAACCGCTTCGT  300

Query  5086  GGTCTACCGGGACCTGAAGCCAGCCAACATCCTTCTGGACGAGCATGGCCACGTGCGGAT  5145
              ||||||||||||||||||||||||||||||||||||||||||||||||||||||||||||||
Sbjct  301   GGTCTACCGGGACCTGAAGCCAGCCAACATCCTTCTGGACGAGCATGGCCACGTGCGGAT  360

Query  5146  CTCGGACCTGGGCCTGGCCTGTGACTTCTCCAAGAAGAAGCCCCATGCCAGCGTGGGCAC  5205
              ||||||||||||||||||||||||||||||||||||||||||||||||||||||||||||||
Sbjct  361   CTCGGACCTGGGCCTGGCCTGTGACTTCTCCAAGAAGAAGCCCCATGCCAGCGTGGGCAC  420

Query  5206  CCACGGGTACATGGCTCCGGAGGTCCTGCAGAAGGGCGTGGCCTACGACAGCAGTGCCGA  5265
              ||||||||||||||||||||||||||||||||||||||||||||||||||||||||||||||
Sbjct  421   CCACGGGTACATGGCTCCGGAGGTCCTGCAGAAGGGCGTGGCCTACGACAGCAGTGCCGA  480

Query  5266  CTGGTTCTCTCTGGGGTGCATGCTCTTCAAGTTGCTGCGGGGGCACAGCCCCTTCCGGCA  5325
              ||||||||||||||||||||||||||||||||||||||||||||||||||||||||||||||
Sbjct  481   CTGGTTCTCTCTGGGGTGCATGCTCTTCAAGTTGCTGCGGGGGCACAGCCCCTTCCGGCA  540

Query  5326  GCACAAGACCAAAGACAAGCATGAGATCGACCGCATGACGCTGACGATGGCCGTGGAGCT  5385
              ||||||||||||||||||||||||||||||||||||||||||||||||||||||||||||||
Sbjct  541   GCACAAGACCAAAGACAAGCATGAGATCGACCGCATGACGCTGACGATGGCCGTGGAGCT  600
```

```
Query  5386  GCCCGACTCCTTCTCCCCTGAACTACGCTCCCTGCTGGAGGGGTTGCTGCAGAGGGATGT  5445
             ||||||||||||||||||||||||||||||||||||||||||||||||||||||||||||
Sbjct  601   GCCCGACTCCTTCTCCCCTGAACTACGCTCCCTGCTGGAGGGGTTGCTGCAGAGGGATGT  660

Query  5446  CAACCGGAGATTGGGCTGCCTGGGCCGAGGGGCTCAGGAGGTGAAAGAGAGCCCCTTTTT  5505
             ||||||||||||||||||||||||||||||||||||||||||||||||||||||||||||
Sbjct  661   CAACCGGAGATTGGGCTGCCTGGGCCGAGGGGCTCAGGAGGTGAAAGAGAGCCCCTTTTT  720

Query  5506  CCGCTCCCTGGACTGGCAGATGGTCTTCTTGCAGAAGTACCCTCCCCCGCTGATCCCCCC  5565
             |||||||||||||||||||||||||||||||| ||||||||||||||||||||||||||
Sbjct  721   CCGCTCCCTGGACTGGCAGATGGTCTTCTTGCAAAAGTACCCTCCCCCGCTGATCCCCCC  780

Query  5566  ACGAGGGGAGGTGAACGCGGCCGACGCCTTCGACATTGGCTCCTTCGATGAGGAGGACAC  5625
             ||||||||||||||||||||||||||||||||||||||||||||||||||||||||||||
Sbjct  781   ACGAGGGGAGGTGAACGCGGCCGACGCCTTCGACATTGGCTCCTTCGATGAGGAGGACAC  840

Query  5626  AAAAGGAATCAAGTTACTGGACAGTGATCAGGAGCTCTACCGCAACTTCCCCCTCACCAT  5685
             ||||||||||||||||||||||||||||||||||||||||||||||||||||||||||||
Sbjct  841   AAAAGGAATCAAGTTACTGGACAGTGATCAGGAGCTCTACCGCAACTTCCCCCTCACCAT  900

Query  5686  CTCGGAGCGGTGGCAGCAGGAGGTGGCAGAGACTGTCTTCGACACCATCAACGCT-GAGA  5744
             |||||||||||||||| |||||||||||||||||||||||||||||| | ||||
Sbjct  901   CTCGGAGCGGTGGCAGCAKGAGGTGGCAGAGACTGTCTTCGACACCATCAACGGTTGAGA  960

Query  5745  CAGACC-GGCTGG-AGGCTCGCAAGAAAGCCAAGAACAAGC-AGCTGGGCC-ATGAGGAA  5800
             |||||| |||||| |||||||||||||||||||||||||| ||||||||| ||||||||
Sbjct  961   CAGACCCGGCTGGAAGGCTCGCAAGAAAGCCAAGAACAAGCCAGCTGGGCCCATGAGGAA  1020

Query  5801  GA-CTACGCCC-TGGG-CAAGGACTG-CATCATG-CATGG-CTACATGT-CCAAGATGGG  5853
              | |||| ||| |||| ||||||||| ||||||| ||||| |||||||| |||| |||||
Sbjct  1021  AAACTACCCCCCTGGGGCAAGGACTGGCATCATGGCATGGGCTACATGTTCCAARATGGG  1080

Query  5854  -CAACCCC-TTCCTG-ACCCAGTGG-CAG-CGGCGGT-AC-TTCTACCT-GTTCCCCAA-  5904
              ||||||| |||||| ||||| ||| ||| ||||||| || |||||||| |||||||||
Sbjct  1081  GCAACCCCCTTCCTGGACCCAATGGGCAGSCGGCGGTTACCTTCTACCTTGTTCCCCAAA  1140

Query  5905  CCG-CCTCG-AGTGG-CGGGG-CGA-GGGCGA-GGCCC  5936
             ||| ||||| ||||| ||||| ||| |||| | |||||
Sbjct  1141  CCGGCCTCGGAGTGGGCGGGGGCGAAGGGCCAAGGCCC  1178
```

Sequencing 17.5.2015
Primer from Mircosynth Primer List:
FastBac-rev CATTTTATGTTTCAGGTTCAGG

3_FastBacGRK2_54 FastBac-rev
CCTCTACAAATGTGGTATGGCTGATTATGATCCTCTAGTACTTCTCGACAAGCTTTCAGAGGCCGTTGGCACTGCCGCGCTGGACCA
GCGGCACCTTGCTCAGCTCCACCACGGGCGAGCGCGGCTTGTTCTTCATCTTGGGCACCCGCTGCACCAGCTGCTGGGCCTCGCGGT
AGGCGTCGCGCAGCTCCTTCTTCCACTGCACCAGCTCAGGGTCGCTATCGCACTGCAAAATGAACTGTTTCCCACCGCGGATCTTGA
GGAGCAGGCACTTGCGCTCCTTGATCTGCGTCTCCTCCACCGACTGGATCTCCTCCATGGTCAGCAGGCTCTGCGGGGCCTCGCCCT
CGCCCCGCCACTCGAGGCGGTTGGGGAACAGGTAGAAGTACCGCCGCTGCCACTGGGTCAGGAAGGGGTTGCCCATCTTGGACATGT
AGCCATGCATGATGCAGTCCTTGCCCAGGGCGTAGTCTTCCTCATGGCCCAGCTGCTTGTTCTTGGCTTTCTTGCGAGCCTCCAGCC
GGTCTGTCTCAGCGTTGATGGTGTCGAAGACAGTCTCTGCCACCTCCTGCTGCCACCGCTCCGAGATGGTGAGGGGGAAGTTGCGGT
AGAGCTCCTGATCACTGTCCAGTAACTTGATTCCTTTTGTGTCCTCCTCATCGAAGGAGCCAATGTCGAAGGCGTCGGCCGCGTTCA
CCTCCCCTCGTGGGGGGATCAGCGGGGGAGGGTACTTCTGCAAGAAGACCATCTGCCAGTCCAGGGAGCGGAAAAAGGGGCTCTCTT
TCACCTCCTGAGCCCCTCGGCCCAGGCAGCCCAATCTCCGGTTGACATCCCTCTGCAGCAACCCCTCCAGCAGGGAGCGTAGTTCAG
GGGAGAAGGAGTCGGGCAGCTCCACGGCCATCGTCAGCGTCATGCGGTCGATCTCATGCTTGTCTTTGGTCTTGTGCTGCCGGAAGG
GGCTGTGCCCCCGCAGCAACTTGAAGAGCATGCACCCCAGAGAGAACCAGTCGGCACTGCTGTCGTAGGCCACGCCCTTCTGCAGGA
CCTCCGGAGCCATGTACCCGTGGGTGCCCACGCTGGCATGGGGCTTCTTCTTGGAAAAGTCACAGGCCAGGCCCAGGTCCGARATCC
GCACGTGGCCATGCTCGTCCARAAAGGATGTTGGCTGGGTTTCAGGTCCCGGTAA

Score	Expect	Identities	Gaps	Strand
2158 bits(1168)	0.0	1179/1185(99%)	2/1185(0%)	Plus/Minus

```
Query  5090  TACCGGGACCTGAA-GCCAGCCAACATCCTT-CTGGACGAGCATGGCCACGTGCGGATCT  5147
              ||||||||||||||  ||||||||||||||  |||||||||||||||||||||||||| |
Sbjct  1185  TACCGGGACCTGAAACCCAGCCAACATCCTTTYTGGACGAGCATGGCCACGTGCGGATYT  1126

Query  5148  CGGACCTGGGCCTGGCCTGTGACTTCTCCAAGAAGAAGCCCCATGCCAGCGTGGGCACCC  5207
              ||||||||||||||||||||||||| ||||||||||||||||||||||||||||||||||
Sbjct  1125  CGGACCTGGGCCTGGCCTGTGACTTTTCCAAGAAGAAGCCCCATGCCAGCGTGGGCACCC  1066

Query  5208  ACGGGTACATGGCTCCGGAGGTCCTGCAGAAGGGCGTGGCCTACGACAGCAGTGCCGACT  5267
              ||||||||||||||||||||||||||||||||||||||||||||||||||||||||||||
Sbjct  1065  ACGGGTACATGGCTCCGGAGGTCCTGCAGAAGGGCGTGGCCTACGACAGCAGTGCCGACT  1006

Query  5268  GGTTCTCTCTGGGGTGCATGCTCTTCAAGTTGCTGCGGGGGCACAGCCCCTTCCGGCAGC  5327
              ||||||||||||||||||||||||||||||||||||||||||||||||||||||||||||
Sbjct  1005  GGTTCTCTCTGGGGTGCATGCTCTTCAAGTTGCTGCGGGGGCACAGCCCCTTCCGGCAGC  946

Query  5328  ACAAGACCAAAGACAAGCATGAGATCGACCGCATGACGCTGACGATGGCCGTGGAGCTGC  5387
              ||||||||||||||||||||||||||||||||||||||||||||||||||||||||||||
Sbjct  945   ACAAGACCAAAGACAAGCATGAGATCGACCGCATGACGCTGACGATGGCCGTGGAGCTGC  886

Query  5388  CCGACTCCTTCTCCCCTGAACTACGCTCCCTGCTGGAGGGGTTGCTGCAGAGGGATGTCA  5447
              ||||||||||||||||||||||||||||||||||||||||||||||||||||||||||||
Sbjct  885   CCGACTCCTTCTCCCCTGAACTACGCTCCCTGCTGGAGGGGTTGCTGCAGAGGGATGTCA  826

Query  5448  ACCGGAGATTGGGCTGCCTGGGCCGAGGGGCTCAGGAGGTGAAAGAGAGCCCCTTTTTCC  5507
              ||||||||||||||||||||||||||||||||||||||||||||||||||||||||||||
Sbjct  825   ACCGGAGATTGGGCTGCCTGGGCCGAGGGGCTCAGGAGGTGAAAGAGAGCCCCTTTTTCC  766

Query  5508  GCTCCCTGGACTGGCAGATGGTCTTCTTGCAGAAGTACCCTCCCCCGCTGATCCCCCCAC  5567
              ||||||||||||||||||||||||||||||||||||||||||||||||||||||||||||
Sbjct  765   GCTCCCTGGACTGGCAGATGGTCTTCTTGCAGAAGTACCCTCCCCCGCTGATCCCCCCAC  706

Query  5568  GAGGGGAGGTGAACGCGGCCGACGCCTTCGACATTGGCTCCTTCGATGAGGAGGACACAA  5627
              ||||||||||||||||||||||||||||||||||||||||||||||||||||||||||||
Sbjct  705   GAGGGGAGGTGAACGCGGCCGACGCCTTCGACATTGGCTCCTTCGATGAGGAGGACACAA  646

Query  5628  AAGGAATCAAGTTACTGGACAGTGATCAGGAGCTCTACCGCAACTTCCCCCTCACCATCT  5687
              ||||||||||||||||||||||||||||||||||||||||||||||||||||||||||||
Sbjct  645   AAGGAATCAAGTTACTGGACAGTGATCAGGAGCTCTACCGCAACTTCCCCCTCACCATCT  586
```

```
Query  5688  CGGAGCGGTGGCAGCAGGAGGTGGCAGAGACTGTCTTCGACACCATCAACGCTGAGACAG  5747
             ||||||||||||||||||||||||||||||||||||||||||||||||||||||||||||
Sbjct  585   CGGAGCGGTGGCAGCAGGAGGTGGCAGAGACTGTCTTCGACACCATCAACGCTGAGACAG  526

Query  5748  ACCGGCTGGAGGCTCGCAAGAAAGCCAAGAACAAGCAGCTGGGCCATGAGGAAGACTACG  5807
             ||||||||||||||||||||||||||||||||||||||||||||||||||||||||||||
Sbjct  525   ACCGGCTGGAGGCTCGCAAGAAAGCCAAGAACAAGCAGCTGGGCCATGAGGAAGACTACG  466

Query  5808  CCCTGGGCAAGGACTGCATCATGCATGGCTACATGTCCAAGATGGGCAACCCCTTCCTGA  5867
             ||||||||||||||||||||||||||||||||||||||||||||||||||||||||||||
Sbjct  465   CCCTGGGCAAGGACTGCATCATGCATGGCTACATGTCCAAGATGGGCAACCCCTTCCTGA  406

Query  5868  CCCAGTGGCAGCGGCGGTACTTCTACCTGTTCCCCAACCGCCTCGAGTGGCGGGGCGAGG  5927
             ||||||||||||||||||||||||||||||||||||||||||||||||||||||||||||
Sbjct  405   CCCAGTGGCAGCGGCGGTACTTCTACCTGTTCCCCAACCGCCTCGAGTGGCGGGGCGAGG  346

Query  5928  GCGAGGCCCCGCAGAGCCTGCTGACCATGGAGGAGATCCAGTCGGTGGAGGAGACGCAGA  5987
             ||||||||||||||||||||||||||||||||||||||||||||||||||||||||||||
Sbjct  345   GCGAGGCCCCGCAGAGCCTGCTGACCATGGAGGAGATCCAGTCGGTGGAGGAGACGCAGA  286

Query  5988  TCAAGGAGCGCAAGTGCCTGCTCCTCAAGATCCGCGGTGGGAAACAGTTCATTTTGCAGT  6047
             ||||||||||||||||||||||||||||||||||||||||||||||||||||||||||||
Sbjct  285   TCAAGGAGCGCAAGTGCCTGCTCCTCAAGATCCGCGGTGGGAAACAGTTCATTTTGCAGT  226

Query  6048  GCGATAGCGACCCTGAGCTGGTGCAGTGGAAGAAGGAGCTGCGCGACGCCTACCGCGAGG  6107
             ||||||||||||||||||||||||||||||||||||||||||||||||||||||||||||
Sbjct  225   GCGATAGCGACCCTGAGCTGGTGCAGTGGAAGAAGGAGCTGCGCGACGCCTACCGCGAGG  166

Query  6108  CCCAGCAGCTGGTGCAGCGGGTGCCCAAGATGAAGAACAAGCCGCGCTCGCCCGTGGTGG  6167
             ||||||||||||||||||||||||||||||||||||||||||||||||||||||||||||
Sbjct  165   CCCAGCAGCTGGTGCAGCGGGTGCCCAAGATGAAGAACAAGCCGCGCTCGCCCGTGGTGG  106

Query  6168  AGCTGAGCAAGGTGCCGCTGGTCCAGCGCGGCAGTGCCAACGGCCTCTGAAAGCTTGTCG  6227
             ||||||||||||||||||||||||||||||||||||||||||||||||||||||||||||
Sbjct  105   AGCTGAGCAAGGTGCCGCTGGTCCAGCGCGGCAGTGCCAACGGCCTCTGAAAGCTTGTCG  46

Query  6228  AGAAGTACTAGAGGATCATAATCAGCCATACCACATTTGTAGAGG  6272
             |||||||||||||||||||||||||||||||||||||||||||||
Sbjct  45    AGAAGTACTAGAGGATCATAATCAGCCATACCACATTTGTAGAGG  1
```